# Ring-Opening Metathesis Polymerization with Tungsten Based Catalysts : Kinetics, Thermodynamics and Mechanism

Thesis by

Jérôme Claverie

In Partial Fulfillment of the Requirements

for the Degree of

Doctor of Philosophy

*California Institute of Technology*

*Pasadena, California*

1996

(Defended on June 13, 1995)

Pour Titouno, Marie Christmas et

Patache

and For Thuy

## Acknowledgments

This thesis work has been effected in the laboratory of Bob Grubbs. To prepare a Ph.D. at Caltech is a very enriching experience in all regards: the stimulating enthusiasm, the cultural melting pot and the workaholic dedication that realms over Caltech (from time to time) appealed to me. Thanks to Bob for creating such an exceptional place. Bob favors new ideas and scientific journeys over academic performances, and scientific curiosity over pure productivity. It took me many years to begin to understand Bob, and to appreciate him for his true value; thanks, Bob, for granting me your patient trust.

There are many people who have participated in one way or another to the elaboration of this work. Randy Lee, has hooked me on metathesis, polyacetylenes and the joy of margaritas and greasy pizzas at 3 am by the NMR. I wish I could pay him back in some way for all he has taught me, and thank him as well for his beneficial and peaceful cheerfulness. The insightful Alto Benedicto brought me the thrills of scientific rigor and logic, as well as the pleasure of being in contact with his unleashed imagination and unorthodox culture.

Zhong-Ren Chen (alias John Graine) has been an impressive and cheerful collaborator in the cyclics project, who has also taught me a lot about calculations as well as engineering. I wish him the best of luck.

I could not have done anything without the generous spirits wandering in the lab, who have been kind enough to spend a long time teaching me: especially to Doug Gin (Look at Me!) and Phil Hampton, I am very indebted for all the lab knowledge they passed along to me. I have discovered the joys of organometallic chemistry through Javi De la

Mata and more recently Seth Brown. They have shared generously and willingly their knowledge and enthusiasm: what a treat! My proofreaders have also debugged the French text, and packaged it in English: thanks Geoff, Zhong-Ren, Seth, Marya and Amy for having worked so hard on such short notice!

So many people have helped me over the years I could not give a full account. A random drawing includes Zhe Wu, Jean-Pierre Shaller, Mark Mc Laughlin, Osamu Fujimura, Geoff Coates (and Sabine too), Eric Dias, Marcia France, Jan-Karel Buijink (as well as Christen), Eva Boumboum, Bob Kumpf, Amy Pangborn, Lin Pu, Babette Burns (and the Girls!), Delwin Elder, Tom Wilhelm, Glenn Sammis and Dian Buchness. Others, many others, have provided friendship and moral comfort: the list would be too long. To all, (friends and labmates and musicians), thank you for making my stay in the U.S. so good. However, how could I not express my gratitude to Yonchu and Toshi, the 348 club (Gary, Jack, Max and Hoa), Quita and Pascal, Stephanie and Fabien, Conrad, and my dear Thuy?

# ABSTRACT

Ring-opening metathesis polymerization (ROMP) is instrumental in the synthesis of a variety of polymers. Since the appearance of well defined metathesis catalysts, the synthesis and characterization of ROMP polymers has been greatly improved.

In the **first chapter**, the kinetics and the thermodynamics of such polymerizations are presented. When a living ROMP polymerization is effected in the presence of a chain transfer-agent, the molecular weight distribution is governed by the **kinetics** of the polymerization. The molecular weight distribution has been evaluated numerically, and the numerical results have been compared to experimental ones. The living polymerization of norbornene by Mo(=CHR)(=N-1,3-*i*-Pr-$C_6H_3$)(O-*t*-Bu)$_2$ (R = -*t*-Bu, -$C(CH_3)_2$Ph) in the presence of neohexene and styrene has been used as a model experiment. When the ROMP catalyst is too active, chain transfer to the polymer occurs, and the molecular weight distribution is dependent upon the **thermodynamics** of the polymerization. The theoretical thermodynamic product distribution has been predicted, and compared to experimental results for the polymerization of 1,5-cyclooctadiene (COD) and cyclooctene. The results have been applied to the synthesis of short polyacetylene oligomers by ROMP of *sec*-butyl-cyclooctatetraene.

In the **second chapter**, the synthesis of monodisperse substituted polyacetylenes is described. For this synthesis, one has to use very active ROMP catalysts which appreciably initiate the polymerization. The new class of tungsten vinyl alkylidenes allows such a polymerization.

Synthesis, characterization and catalytic properties of tungsten imido and oxo vinyl alkylidenes is described.

In the **third chapter**, reactivity of tertiary alcohols with tungsten vinyl alkylidenes and neopentylidenes is examined. These alcohols are found in trace amounts in all the samples of these tungsten carbenes. The role of the alcohols in ROMP is studied for polynorbornene, polycyclooctadiene and polyacetylene. Activation of these catalysts has been observed, even by trace amounts of alcohol, and has important consequences in the microstructure of the resulting polymer. Mechanistic implications toward a general scheme of acid activation of the well defined tungsten carbenes is proposed.

# TABLE OF CONTENTS



## CHAPTER 1

## CHAPTER 2

## CHAPTER 3

# TABLE OF FIGURES

## CHAPTER 1

## CHAPTER 2

## CHAPTER 3

# TABLE OF TABLES

## CHAPTER 1



## CHAPTER 2

## CHAPTER 3

*I like France,*
*where everybody thinks he is Napoleon*

F. Scott Fitzgerald
Tender is the Night, 1931.

*De la France, les Americains n'y ont retenu*
*que leurs préjugés*

Marjorie Le Cève
Je me Fous de Vous, 1968.

# CHAPTER 1

# KINETICS AND THERMODYNAMICS OF POLYMERIZATION: THEORY AND EXPERIMENTS

## I. Classification of ROMP polymerizations

### 1. Introduction

The most general scheme of Ring-Opening Metathesis Polymerization (ROMP) consists of five different reactions (Figure 1).[1] The reactions of initiation (a) and propagation (b) are necessary steps required for the synthesis of a polymer. Generally, metathesis catalysts do not completely discriminate between cyclic double bonds of the monomer, and acyclic double bonds of the polymer, or any acyclic olefin present in the reaction medium. Therefore, along with polymerization, transfer reactions are usually observed either with an intentionally added chain transfer agent (CTA, Figure 1 c), or with the polymer (Figure 1, d and e). Transfer to the polymer can be intermolecular (Figure 1, d) or intramolecular (backbiting reaction, Figure 1, e), hence giving rise to cyclic oligomers. Finally, termination reactions, whereby the metallic carbene is deactivated, are usually present.

This large number of reactions usually hampers the prediction of the behavior of the polymerization. In this chapter, we intend to show that under certain circumstances, the polymerization scheme can be simplified to two limiting cases. For poorly active catalysts, a kinetic control of the polymerization is observed, whereas a thermodynamic control is observed for very active catalysts. The features of these two polymerizations is vastly different, and both theoretical and experimental results will be presented for them.

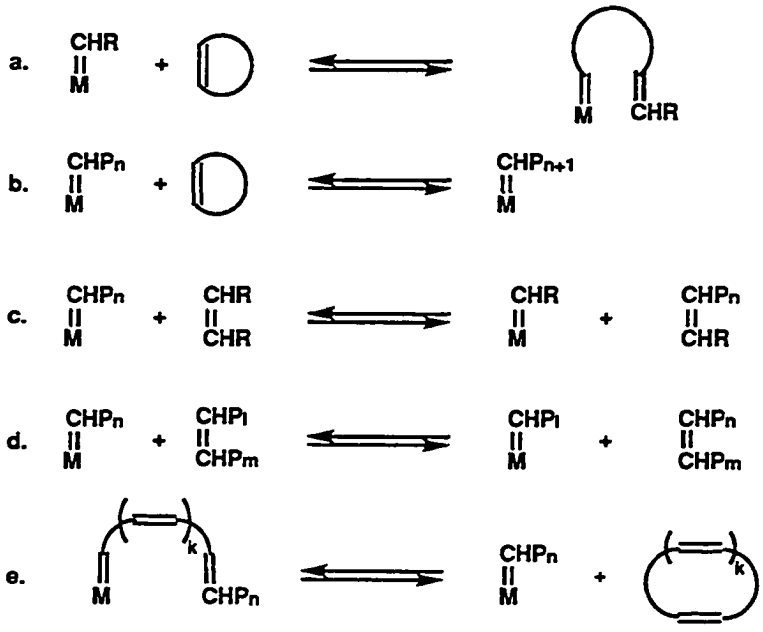


**Figure 1.** Scheme of ROMP polymerization. a. initiation, b. propagation, c. transfer to a chain transfer agent (CTA), d. intermolecular chain transfer, e. intramolecular chain transfer.

## 2. Living polymerizations

A polymerization is living *if, and only if,* the reactions of initiation (a) and propagation (b) are the only reactions observed. No transfer and no deactivation reaction is present in a living polymerization. Consequently, one metathesis catalyst is attached to one polymer chain, so the metathesis catalyst is indeed a polymerization initiator. It should be noticed that the backward reactions a and b (depolymerization reactions) are in fact intramolecular transfer reactions to the polymer; therefore, in a living polymerization, the reactions a and b are irreversible.

For a living ROMP polymerization to occur, the initiator must be tuned so that it reacts selectively with the double bonds of the monomer. Therefore, the reactivity of the monomer should be much larger than the one of the double bonds of the polymer, and this condition is fulfilled when the

monomer is very strained, and the catalyst is relatively inactive. This limitation is such that only a small number of living polymerizations are known in ROMP (Figure 2). In simplifying terms, living polymerizations are feasible for norbornene, cyclobutenes and their derivatives.

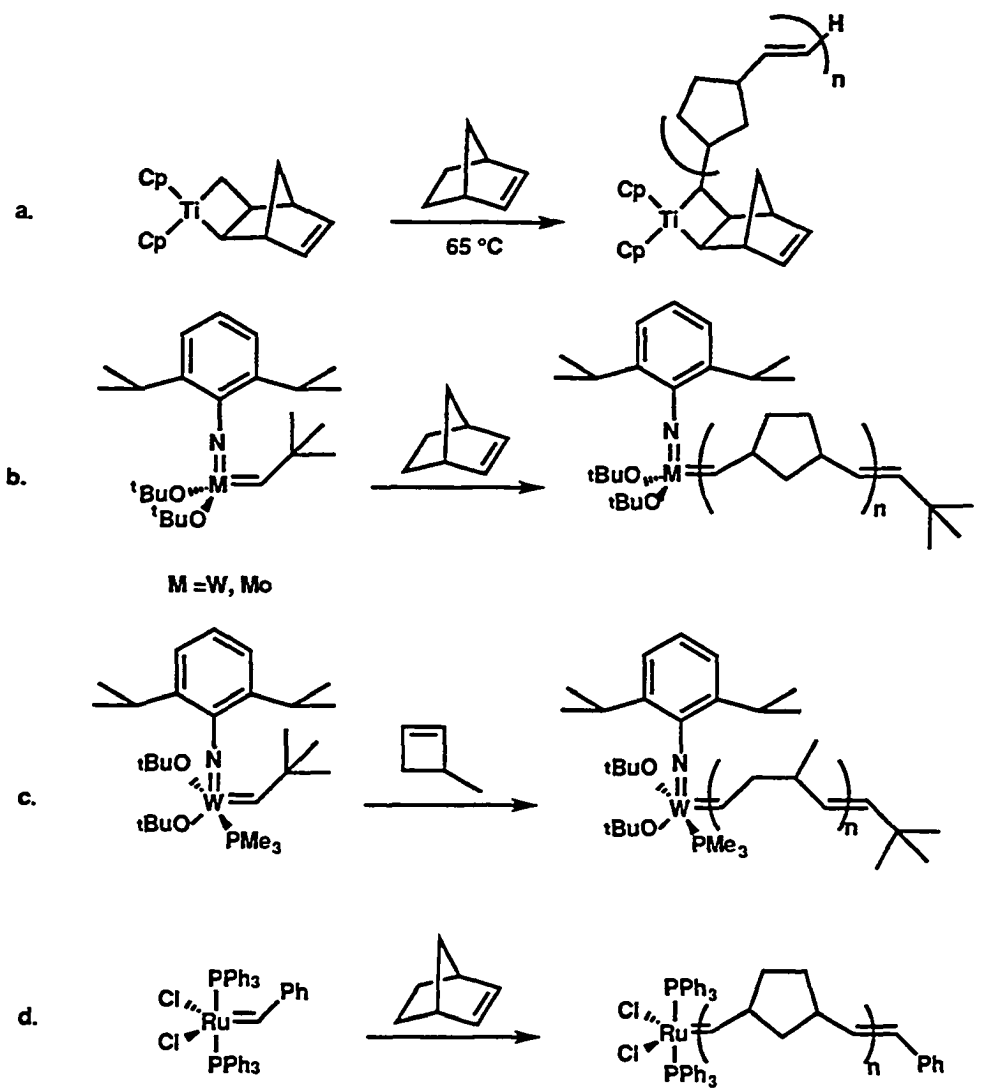


**Figure 2.** Examples of ROMP living polymerizations. a. See reference 2, b. reference 3, c. reference 4, d. reference 5. Other norbornene and cyclobutene derivatives have recently been polymerized in a living fashion with this ruthenium catalyst.[6,7]

The molecular weight distribution and the polydispersity index (PDI) for a living polymerization has been calculated analytically or numerically as a function of the kinetic rate constants of the initiation ($k_i$) and propagation ($k_p$) reactions.

When the initiation is faster than the propagation ($k_i \geq k_p$), the mean degree of polymerization, $\bar{X}_n$, is exactly the ratio of the feeds of monomer to catalyst (equation 1), and the distribution is of the Poisson type (equation 2).[8,9] The resulting PDI, given in equation 3, is very close to 1 as long as chains longer than 10 units are made.

$$\bar{X}_n = \frac{[MON]}{[INIT]} \tag{1}$$

$$P_n = [INIT] \frac{1}{(n-1)!} \left(\bar{X}_n\right)^{n-1} e^{-\bar{X}_n} \tag{2}$$

$$PDI = 1 + \frac{1}{\bar{X}_n} \tag{3}$$

In equations (1) to (3), [MON] and [INIT] are respectively the initial concentrations of monomer and initiator, and $P_n$ is the concentration of polymer chains of length n.

When $k_i < k_p$, the mean degree of polymerization and the PDI cannot be easily written under an analytical form. If the reactions of initiation and propagation *are first order with respect to monomer, initiator and propagating species concentrations*, then a numerical solution to this problem has been provided by L. Gold.[10,11] For a large range of $k_i$ and $k_p$, the PDI is comprised between 1.01 and 1.3. Furthermore, the amount of initiator consumed (which is directly related to the mean degree of polymerization, equation 4) can be

written as a function of $k_i$ and $k_p$. Inversely, the ratio $k_p/k_i$ can be written as a function of the initiator consumed (equation 5). The use of this equation[1] has allowed us to obtain the ratio $k_p/k_i$ by measuring (by $^1H$ NMR, e.g.) the amount of initiator left, $[INIT]_{t=\infty}$.

$$\overline{X}_n = \frac{[MON]}{[INIT]-[INIT]_{t=\infty}} \tag{4}$$

$$\frac{k_p}{k_i} = \frac{1 - \frac{[MON]}{[INIT]} - \frac{[INIT]_{t=\infty}}{[INIT]}}{\ln\left(\frac{[INIT]_{t=\infty}}{[INIT]}\right) + 1 - \frac{[INIT]_{t=\infty}}{[INIT]}} \tag{5}$$

3. Non-living polymerizations

Because the definition of a living polymerization is very restrictive, a ROMP polymerization can be non-living for a wealth of reasons. For example, the polymerization can be non-living because, along with reactions a and b, fast irreversible termination reactions are observed. In this case, the polymerization obeys the classical chain-polymerization scheme, typical of radical polymerizations. In ROMP, an example of this type of polymerization is obtained with poorly-defined catalysts such as $WCl_6/SnMe_4$. Polymerizations can also be non-living because one has intentionally added a chain transfer agent (Figure 1, reaction c). If the reaction c is reversible, then a pseudo-living polymerization scheme is taking place, as in an immortal polymerization.[12] To our knowledge, such a behavior has not yet been observed in ROMP. On the other hand, the chain

---

[1] From now on, this equation will be referred as Gold equation.

transfer reaction could be irreversible, and a novel type of polymerization scheme occurs. The product distribution is governed by the kinetics of initiation, propagation and transfer. We will analyze this case in detail below.

**Table 1.** Different types of polymerization schemes

| Polym. Type | Reactions | Ex[1] | Catalyst Activity | Remarks |
|---|---|---|---|---|
| living | a + b | yes | poor | |
| pseudo-living | a + b + c | no | unknown | the reaction c is reversible |
| kinetic case | a + b + c | yes | poor | see below |
| chain-type | a + b + termination | yes | indif | "steady state" polymerization |
| chain type with transfer | a + b + c + termination | no | poor | transfer obeys Mayo relationship |
| thermo-dynamic | a + b + c + d + e | yes | large | termination reactions can be present as long as thermodynamic equilibrium is reached |
| intermediate | a + b + c + d + e + termination | yes | indif[2] | termination occurs before equilibrium is reached |

1. Examples in ROMP
2. Indifferent.

Until now, only cases where transfer reactions to the polymer are absent have been considered (low activity catalyst). When chain transfer to the polymer occurs (Figure 1, d and e), and when no termination is present, a state of thermodynamic equilibrium is eventually reached, regardless of the kinetic rates. The product distribution is also independent of the catalyst choice. This case will also be analyzed in detail below.

When termination reactions prevail, an intermediate case (between the kinetic distribution and the thermodynamic one) is obtained: reactions a

to e are all observed, but the lifetime of the catalyst (or duration of the reaction) is too small for the thermodynamic equilibrium to be reached. ROMP polymerizations in this last category result in products distributions which are different from the two limiting cases. Table 1 summarizes the different possibilities for a ROMP polymerization.

## 4. Simplification to kinetic and thermodynamic polymerizations

For intermediate cases, the knowledge of precise experimental and theoretical results is an outrageously difficult task, because of the complexity of the kinetic scheme. The work presented here is done with so called "well-defined" catalysts. When polymerizing *simple* cyclic olefins with this class of catalysts, the set of reactions a to e occur in a time scale which is much faster than termination reactions. For example, typical polymerization of 1,5-cyclooctadiene (COD) by very active tungsten and molybdenum catalysts is over in less than one minute. Transfer reactions occur in a slower time scale (of the order of a few hours, see below). However, metathesis activity is retained after a few days. We can therefore conclude that termination reactions are usually slow enough not to interfere with the work presented here.

Because the termination reactions are quite slow, the polymerization of most simple olefins can be adequately treated as either a kinetic or a thermodynamic type of polymerization. Yet, it has to be realized that this simplification is only valid under optimal conditions. Nevertheless, these limiting cases are rich of information, and permit to better comprehend the mechanism of polymerization.

## II. Kinetically controlled polymerizations

### 1. Motivations and goal

In this chapter, we are interested to a living polymerization where one has purposely added a chain transfer agent (CTA). A CTA is supposed to be different from a monomer and a polymer, and a transfer reaction is supposed to generate an active site, and a *dead* polymer chain.[2] There are many reasons for adding a CTA to a living polymerization:

- In a living polymerization, the initiator is often a reactive and fragile chemical species, which can be in very low concentration or poorly defined. By using a CTA, the initiator role is indeed transformed in catalyst and the CTA plays the role of initiator. A catalytic cycle can be written for the catalyst (CAT), whereas in living polymerization, stoichiometric amounts of intiator are necessary. However, despite the presence of a catalytic cycle, the product distribution, as shown below, is *dependent* on the amount of catalyst used.

- In a living polymerization (without CTA), the chain ends are dependent on the chemical nature of the initiator. The use of CTA allows the introduction of tailored chain ends. To our knowledge, this technique has not yet been used in kinetically controlled ROMP, but it has been used in the thermodynamic controlled polymerization for the synthesis of telechelic polymers (see below). This method should be contrasted with the more traditional way of synthesizing telechelic polymers, whereby an endcapping reagent is added at the end of the polymerization to cleave the living chains.

---

[2] A dormant polymer chain will be obtained after transfer if the catalyst can react again with the chain. This case is not treated here.

Besides being economically unfavorable, only one chain end is functionalized by this method.

In this chapter, we will analyze the behavior of $\bar{X}_n$ and PDI of a living polymerization where CTAs have been added. It is first clear that $\bar{X}_n$ is not equal to MON / (CAT + CTA), because not all the chain transfer agent is always consumed. However, in such an experiment, the monomer will be used up, because of the irreversibility of the propagation reaction (reaction b, Figure 1).

Theoretical analysis of this problem has been effected in collaboration with A. Benedicto. Most detailed theoretical results can be found in his Ph.D. thesis[11] and in a joint publication.[13] Only a summary of the theoretical results will be presented here. On the other hand, experimental results will be described, and compared to theoretical calculations.

## 2. Theoretical results

The polymerization scheme is constituted of three different equations: initiation (6), propagation (7) and transfer (8).

$$W_0 + M \xrightarrow{k_i} W_1 \qquad (6)$$

$$W_n + M \xrightarrow{k_p} W_{n+1}\ , \qquad n \geq 1 \qquad (7)$$

$$W_n + P_0 \xrightarrow{k_{tr}} W_0 + P_n\ , \qquad n \geq 1 \qquad (8)$$

[CAT], [MON] and [CTA] are respectively the *initial* concentrations of catalyst, monomer and transfer agent, whereas $W_0$, M and $P_0$ are respectively the concentrations of catalyst, monomer and transfer agent at time t. $W_n$ and $P_n$ are respectively the concentrations of living and dead n-

unit long chains at time t. A living (dead) chain containing 0 unit is effectively a catalyst (chain transfer agent) molecule, which explains the notation $W_0$ ($P_0$) for catalyst (chain transfer agent).

The equations 6 to 8 have been solved numerically on a SPARCserver (670 MiPs), using Mathematica 2.0 software. An approached analytical solution has been found using a steady state approximation. This steady state approximation is valid when $k_{tr} < k_p$ and a large quantity of CTA is used. In this case, the average degree of polymerization can be written as:

$$\overline{X}_n = \frac{[MON]}{[CTA]} \frac{1}{1-\left[1+\left(\frac{k_p}{k_{tr}}-1\right)\frac{[MON]}{[CTA]}\right]^{-\frac{1}{\frac{k_p}{k_{tr}}-1}}} \qquad (9)$$

Very good agreement has been found between numerical results and equation 9. Unfortunately, this equation is only valid when the two conditions

$$\begin{aligned} k_{tr} &< k_p \\ [CAT] &<< [CTA] \end{aligned} \qquad (10)$$

are fulfilled. In all other cases, the steady state condition does not apply, and only a numerical resolution of the problem can be effected.

## 3. Interpretation of the theoretical results

Three different polymerization regimes have been found, depending on the efficiency of the chain transfer agent relative to the propagation.

a. Case ktr/kp « 1

If the transfer is very poor, the polymerization can be thought to be a living polymerization which is slightly perturbed. Indeed, we found that no transfer occurs during the 95%[3] of the polymerization, until the propagation is slow enough (because of monomer depletion) for transfer to compete. For the first 95%, the polymerization is living: the molecular weight grows linearly with the conversion, and the PDI is very low. When transfer begins to prevail, very little monomer is left, so only short chains are created. As a result, the average molecular weight decreases, and the PDI increases drastically.

b. Case ktr/kp » 1

In this case, transfer occurs as soon as a few monomer units are inserted. Therefore, there is a rapid build-up of very short chains in the system, until all CTA is consumed. Then, the left-over monomer is consumed by the catalyst, to give long living chains. The resulting size distribution is bimodal: very short oligomers created by transfer, and long living monodisperse chains, created after CTA depletion.

c. Case ktr/kp ≈ 1

This case is the most complex because of a competition between propagation and transfer. Different behaviors are observed, depending not only on the kinetic rate constants, but also on the concentrations of reagents. However, only in this region the transfer may be very efficient, that is to say that the following conditions are fulfilled:

---

[3] This value is indicative only

- The size distribution is monomodal

- The yield of the reaction is very high: most of the CTA is consumed at the end of the reaction

- $\bar{X}_n$ can be varied with by changing the ratio CTA/ MON

## 4. Experimental results

In order to illustrate the theoretical results, we have used the polymerization of norbornene by molybdenum catalysts **1** and **2**. Neohexene and styrene have been chosen as chain transfer agents. We have experimentally found the rate constants $k_i$, $k_p$ and $k_{tr}$. Polymerizations have been carried out in the presence of various amounts of chain transfer agents, and the polymers have been analyzed by GPC. It is then possible to compare the experimental results with the molecular weights found theoretically by entering the exact values of $k_i$, $k_p$ and $k_{tr}$ in the numerical evaluation.

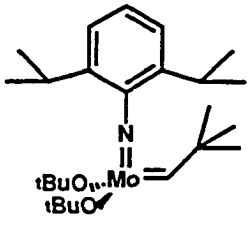


1

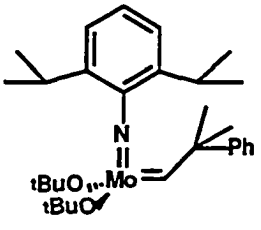


2

The polymerization of norbornene by catalysts **1** and **2** has been shown to be living in at least two occasions.[3,14] Both of these catalysts present very different kinetic properties as the amount of protic impurities in the sample varies (see chapter 3). All the results described here are obtained with the *same* batch of catalyst **1** and **2**. In addition, careful air and moisture

free conditions have been used. Therefore, only residual amount of *tert*-butanol is present, warranting the reproducibility of our results.

With neohexene as a chain transfer agent, we can write a catalytic cycle (Figure 3) which is kinetically identical to equations 6 to 8. It should be mentionned, that, as reported by Schrock,[15] we also found that neohexene does not react with **2** over a range of three days, which is much longer than the polymerization time (2 hours).

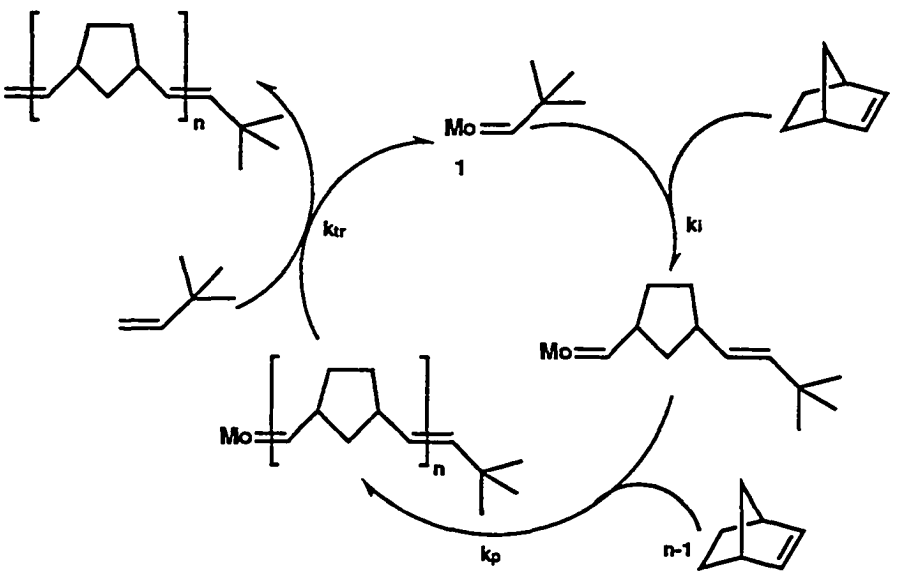


Figure 3. Chain-transfer by neohexene

When styrene is used as a CTA, the reinitiating carbene obtained after transfer $W_0$ is different from the initial carbene, $V_0$ (equations 11-14)

$$V_0 + M \xrightarrow{k_0} W_1 \qquad (11)$$

$$W_n + M \xrightarrow{k_p} W_{n+1} \qquad n \geq 1 \quad (12)$$

$$W_n + P_0 \xrightarrow{k_{tr}} W_0 + P_n \quad n \geq 1 \qquad (13)$$

$$W_0 + M \xrightarrow{k_i} W_1 \qquad (14)$$

In this case, the calculations are slightly more complex than the one described in reference 13 and they are described in appendix 1 following this chapter. The corresponding catalytic cycle is represented in Figure 4.

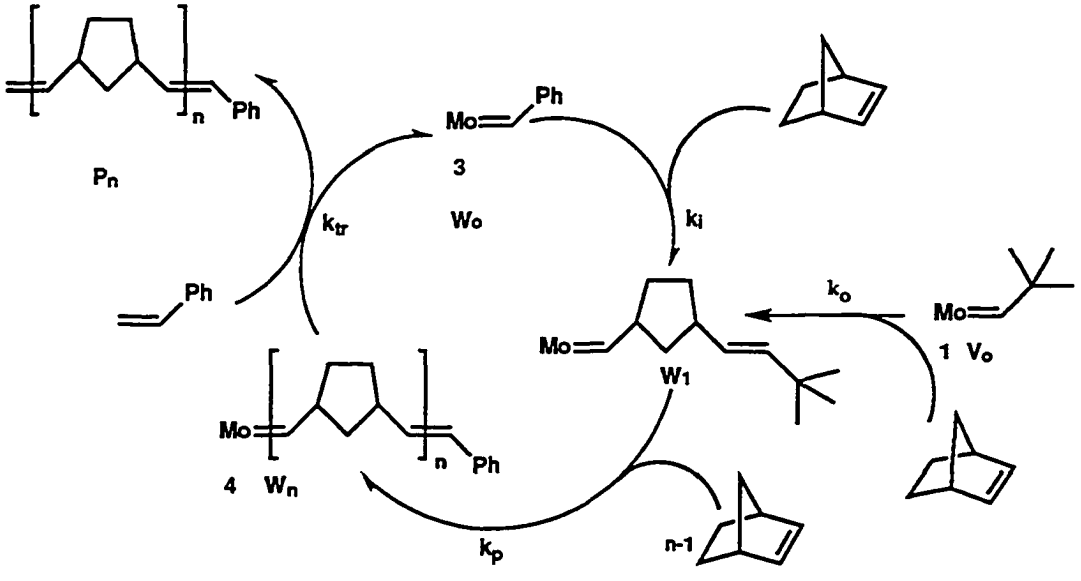


Figure 4. Chain-transfer with styrene.

1 and 2 react only very slowly with styrene to give carbene 3. For example, a 2 $10^{-2}$ mol/l solution of 2 reacts with 17 equivalents of styrene in benzene in 18 hours, affording only 18% of 3, and untouched starting materials. However, over a period of 3 hours (typical polymerization time), no 3 could be detected. Therefore, direct reaction of 1 or 2 with styrene will be neglected in the polymerization scheme (equations 11 -14).

a. Measurement of kp

$k_p$ has been measured by following the kinetics of norbornene consumption by NMR or by GC. Detailed description of the measurement of kp has been reported by A. Benedicto in reference 13. $k_p$ is equal to 16l.mol$^{-1}$s$^{-1}$.

b. Measurement of ki

$k_i$ cannot be measured by following the build-up of the propagating carbene and the disappearance of the initial carbene, because of the rapidity of the polymerization. Consequently, $k_i$ has been measured indirectly, by the means of Gold equation. In a typical experiment, an aliquot of a very concentrated norbornene solution[4] is added to a $10^{-2}$ mol/l solution of **1** in deuterated benzene. When the polymerization is complete, integration of carbene peaks in $^1$H NMR allows the extraction of the ratio $k_p/k_i$ from Gold equation. This measurement presents a large number of difficulties.

Because the values $[INIT]_{t=\infty}$ / $[INIT]_{t=0}$ and (1 - $[INIT]_{t=\infty}$ / $[INIT]_{t=0}$) are needed for calculating $k_p/k_i$ in equation 5, one needs to find experimental conditions whereby approximately 50% of the initiator is consumed, lest one should divide a very small number by a large one or inversely. Consequently, if the catalyst initiates very poorly, then a large amount of monomer should be used, so that half of the initiator is used up. Yet, the amount of monomer may be so large, that it entails a large loss of sensitivity in the integration of the carbene signals. For catalysts which

---

[4] The use of a concentrated norbornene solution allows to check for the absence of polymer: if the norbornene is polymerized, then the solution should be viscous (see experimental part).

initiate very well, then a very small amount of monomer needs to be used (as little as 0.1 µl), creating large measurement uncertainties.

**Table 2** Uncertainty in the measurement of $k_p/k_i$ by Gold equation. The values for the unreacted initiator are given with a 5% uncertainty. The $k_p/k_i$ value, the range of $k_p/ki$ ($[k_p/k_i]min$ - $[k_p/k_i]max$) and the uncertainty values ($\Delta[k_p/k_i] / k_p/k_i$) are calculated by using Gold equation.

| MON / INIT | $[INIT]_{t=\infty} / [INIT]_{t=0}$ | $k_p/k_i$ | $[k_p/k_i]min$ - $[k_p/k_i]max$ | $\Delta[k_p/k_i] / k_p/k_i$ |
|---|---|---|---|---|
| 1 | 0.1 ± 0.05 | $7.1\ 10^{-2}$ | $2.4\ 10^{-2}$ - $1.4\ 10^{-1}$ | 160 % |
| 1 | 0.5 ± 0.05 | 2.6 | 1.8 - 3.7 | 73 % |
| 1 | 0.9 ± 0.05 | 168 | 68 - 730 | 400 % |
| 5 | 0.1 ± 0.05 | 2.8 | 1.9 - 3.7 | 64 % |
| 5 | 0.5 ± 0.05 | 18 | 14 - 23 | 50 % |
| 5 | 0.9 ± 0.05 | $5.8\ 10^{2}$ | $3.9\ 10^{2}$ - $3.8\ 10^{3}$ | 590 % |
| 10 | 0.1 ± 0.05 | 6.5 | 4.4 - 8.7 | 66 % |
| 10 | 0.5 ± 0.05 | 49 | 38 - 65 | 55 % |
| 10 | 0.9 ± 0.05 | $1.8\ 10^{3}$ | $7.8\ 10^{2}$ - $7.7\ 10^{3}$ | 390 % |

These technical problems could be overcome if a more sensitive analytical method than NMR was to be used. However, one should still be careful, because Gold equation amplifies uncertainties. This amplification phenomenon is illustrated in Table 2: uncertainties of 5% in the value of the initiator left is reflected by uncertainties as large as 590% for the calculated value $k_p/k_i$. Again it is observed that uncertainties are smaller when about 50% of the initiator is consumed.

Because of these difficulties, we have measured the ratio $k_p/k_i$ of **1** and **2** a large number of times (Table 3). These measurements have been done with different stock solutions of monomer and catalyst (but with the same batch of catalyst). To our surprise, we have found a good reproducibility in our results, and accurate average $k_i$ values have therefore been extracted.

**Table 3** Measurement of $k_p/k_i$ for catalyst **1** and **2**. Average for catalyst **1**: $k_p/k_i = 31 \pm 4.2$, average for catalyst **2**: $k_p/k_i = 16 \pm 2$.

| Catalyst | Trial | $k_p/k_i$ |
|---|---|---|
| **1** | 1 | 16.0[a] |
| **1** | 2 | 14.1 |
| **1** | 3 | 16.3 |
| **1** | 4 | 15.1 |
| **1** | 5 | 17.2 |
| **2** | 1 | 35.2 |
| **2** | 2 | 27.5 |
| **2** | 3 | 35.6 |
| **2** | 4 | 29.5 |
| **2** | 5 | 33.0 |
| **2** | 6 | 28.0 |
| **2** | 7 | 20.7[b] |

a. I am grateful to Amy Pangborn for providing this value.
b. This value has been discarded in the average.

The measurement of $k_i$ for catalyst **3** (that is to say the phenyl carbene in figure 4) cannot be made directly because this carbene is not available by synthetic methods. The generation of this carbene has to be made *in situ*, by preparing the polymeric carbene **4**, then adding styrene to cleave the polynorbornene chain and generate carbene **3**, which is stable for hours in solution (Figure 5). If too a small amount of norbornene is added (less than 30 equivalents), the propagating carbene **4** is contaminated by the initial carbene **1**. However, **1** does not react with styrene, and **3** reacts more than ten times faster than **1** with norbornene. Consequently, the presence of **1** is

not interfering with the $k_p/k_i$ measurement of 3. It should also be noted that 3 does not react at an appreciable rate with polynorbornene, proving the absence of chain transfer reactions to the polymer.

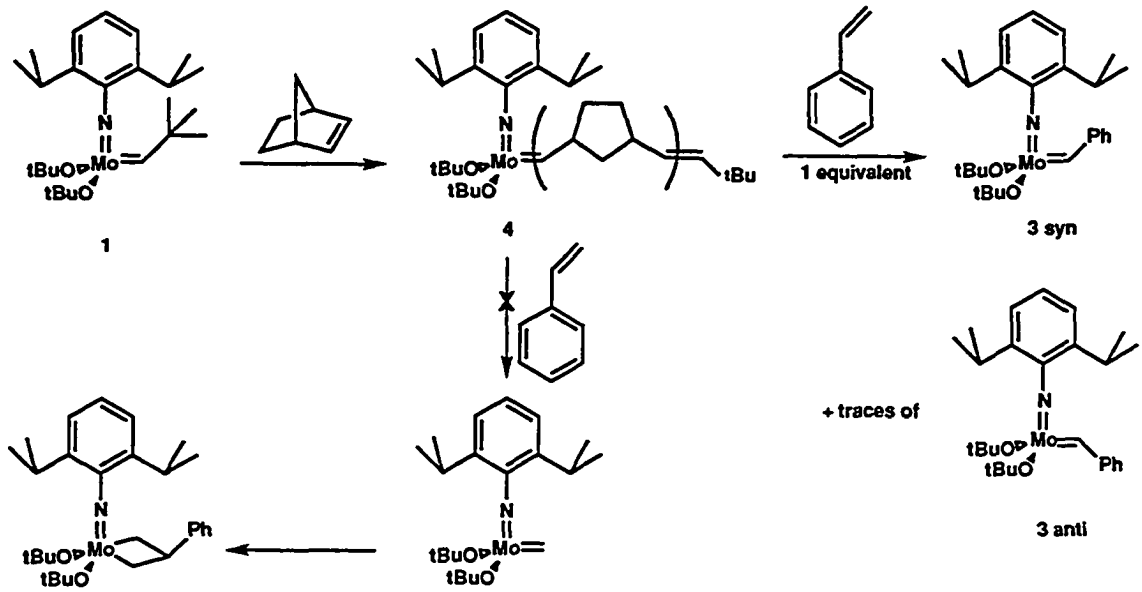


Figure 5. In situ preparation of carbene 3

We have found that the addition of *exactly one* equivalent of styrene is regioselective, and does not produce a methylidene carbene, or any resulting decomposition product from the methylidene carbene. The carbene 3 appears under the form of two rotamers, syn and anti. The ratio syn/anti has been found to be of 21/1. Addition of more than one equivalent of styrene to 4 induces slow decomposition of 3. Decomposition is also observed for reaction of styrene with the similar metathesis catalysts $M(=CH^tBu)(=NAr)(OC(CH_3)(CF_3)_2)_2$ (M = Mo or W, Ar = 2,6-diisopropyl-phenyl). This decomposition is believed to proceed via metallacycle formation (Figure 5).

The ratio $k_p/k_i$ for carbene 3 has been calculated twice, and gives an average $k_p/k_i$ of 1.5.

c. Measurement of ktr

The measurement of the styrene and neohexene $k_{tr}$ has been effected by following the decay of the propagating carbene 4 by NMR, after addition of chain transfer agent (Figure 6). The fit of the second order reaction (Figure 7) permits to obtain the transfer rate. Table 4 summarizes the set of rate constants for catalyst **1, 2** and for styrene and neohexene as chain transfer agents.

**Table 4.** Rate constants in $l \cdot mol^{-1} \cdot s^{-1}$ for catalysts **1** and **2**.[a]

| Catalyst | CTA | $k_O$ | $k_i$ | $k_p$ | $k_{tr}$ |
|---|---|---|---|---|---|
| **1** | Neohexene | 1.0 | 1.0 | 16 | $2.9\ 10^{-5}$ |
| **2** | Neohexene | 0.5 | 1.0 | 16 | $2.910^{-5}$ |
| **1** | Styrene | 1.0 | 10.6 | 16 | $1.2\ 10^{-2}$ |
| **2** | Styrene | 0.5 | 10.6 | 16 | $1.2\ 10^{-2}$ |

a. The constants were determined at 17 °C using standard NMR techniques.

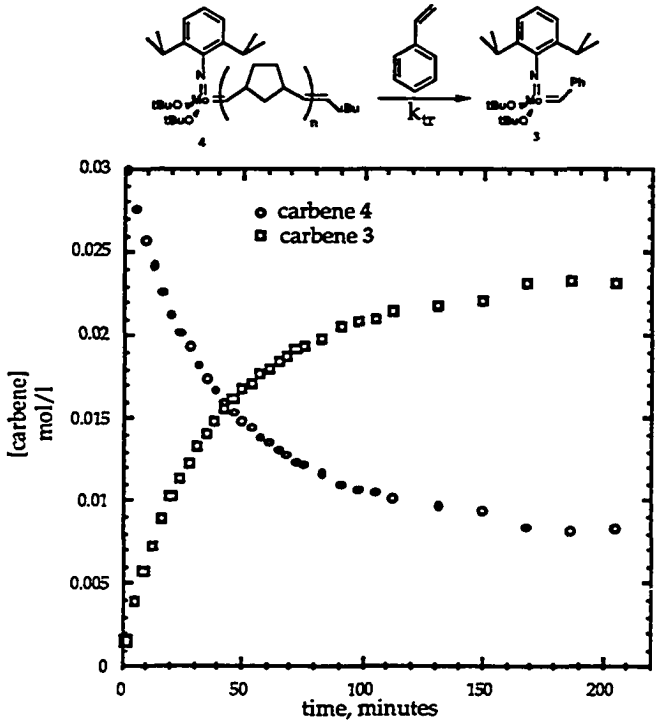


**Figure 6.** Kinetics of the cross metathesis between carbene 4 and styrene. $[4]_0$ = 3.54 $10^{-2}$ mol/l, $[styrene]_0$ = 2.71 $10^{-2}$ mol/l, in benzene at room temperature.

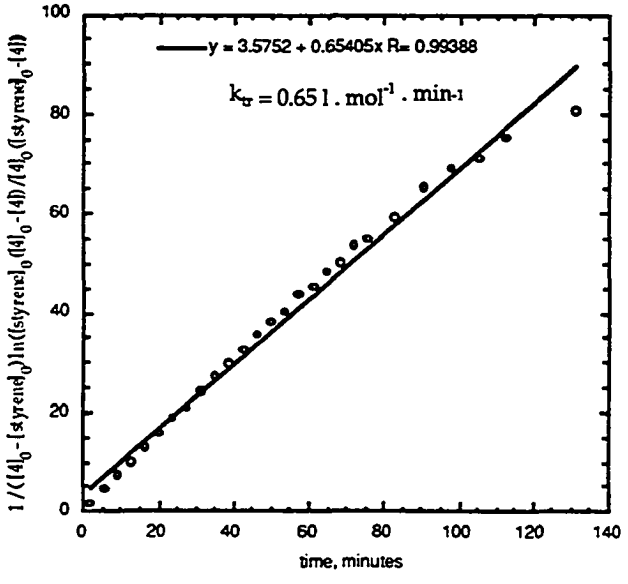


**Figure 7.** Linearization of the second order kinetics. The experimental conditions are given in Figure 6.

5. Polymerizations and Mayo plot

All polymerizations have been effected in benzene or toluene and analyzed by using size exclusion chromatography in toluene at 60 °C. The polymers have been precipitated from methanol and dried in vacuo before injection in the GPC instrument.

a. Experimental and theoretical molecular weight distribution

In a typical experiment, a series of samples have been prepared where monomer and catalyst concentrations are fixed, but where the CTA concentration varies from sample to sample. Experimental results can be compared to theoretical ones (Table 5 to 7), obtained by using the kinetic rate constants $k_i$, $k_p$, $k_0$ and $k_{tr}$.

**Table 5.** Variation of number-average degree of polymerization with [neohexene]/[norbornene][16a] at 22°C when [neohexene]/[1] = 152[a]

| [neohexene]/[norb] | $\overline{M}_n$[b] | $\overline{X}_n$, expt'l[c] | PDI, expt'l | $\overline{X}_n$, theor[d] | PDI, theor |
|---|---|---|---|---|---|
| 0 | 49700 | 152 | 1.06 | 152 | 1.04 |
| 26.51 | 47500 | 145 | 1.05 | 150 | 1.05 |
| 53.03 | 45500 | 139 | 1.08 | 147 | 1.07 |
| 79.54 | 40600 | 124 | 1.12 | 145 | 1.08 |
| 106.05 | 41900 | 128[e] | 1.14[e] | 143 | 1.09 |

[a] The volume of the solutions is kept constant by addition of appropriate amounts of toluene. For the last entry, the solution contains 14% toluene only. [b]Relative to polystyrene standard. [c]Factor of 3.5 is used to convert molecular weight referenced to polystyrene to that of polynorbornene.[16b] [d]As calculated from substituting the specific rates into the differential equations. [e] For this entry, the polymer has precipitated before the end of the polymerization, because of the very small mount of toluene.

We found that practically no transfer occurs when neohexene is used as a chain transfer agent (Table 5), resulting in a nearly constant molecular weight. However, a large molecular weight decrease is observed with

styrene as a chain transfer agent. We believe that styrene is a better transfer agent because of a combination of steric effects (styrene is less bulky than neohexene) and electronic effects (phenyl carbene is conjugated).

**Table 6.** Variation of number-average degree of polymerization with [styrene]/[norbornene]at 22°C when [norbornene]/[1] = 171[a]

| [styrene]/[norb] | $\overline{M}_n$[b] | $\overline{X}_n$, expt'l[c] | PDI, expt'l | $\overline{X}_n$, theor[d] | PDI, theor |
|---|---|---|---|---|---|
| 0 | 27600[e] | 173 | 1.3 | 171 | 1.05 |
| 0.21 | 23100 | 145 | 1.5 | 148 | 1.2 |
| 0.58 | 21500 | 134 | 1.8 | 120 | 1.4 |
| 1.94 | 11900 | 74 | 2.3 | 72 | 2.0 |
| 2.44 | 8450 | 53 | 2.7 | 51 | 2.4 |
| 10.2 | 3300 | 21 | 2.6 | 24 | 3.1 |

[a]The volume of the solutions is kept constant by addition of appropriate amounts of toluene. [b]Relative to polystyrene standard. [c]Factor of 1.7 is used to convert molecular weight referenced to polystyrene to that of polynorbornene.[16b] [d]As calculated from substituting the specific rates into the differential equations. [e]For this particular value, the distribution is bimodal. The MW of the major peak is reported. If the small shoulder of high molecular weight were included, the value should be 61110, giving an Xn of 382.

**Table 7.** Variation of number-average degree of polymerization with [styrene]/[norbornene] at 22°C when [norbornene]/[2] = 103[a]

| [styrene]/[norb] | $\overline{M}_n$[b] | $\overline{X}_n$, expt'l[c] | PDI, expt'l | $\overline{X}_n$, theor[d] | PDI, theor |
|---|---|---|---|---|---|
| 0 | 26000[e] | 102 | 1.4[e] | 103 | 1.05 |
| 0.32 | 23400 | 92 | 1.2 | 91 | 1.2 |
| 1.45 | 16400 | 64 | 1.7 | 66 | 1.5 |
| 2.72 | 11400 | 45 | 1.9 | 50 | 1.8 |
| 17.8 | 4000 | 16 | 2.4 | 15 | 2.9 |

[a-d]See table 6.-[e]For this particular value, the distribution is bimodal. The MW of the major peak is reported. If the small shoulder of high molecular weight were included, the value should be 31000, giving an Xn of 172.

Very good agreement is found between theoretical and experimental results, which indeed indicates the validity of our model. Therefore it is possible to analyze with confidence the temporal behavior of the polymerization using the model : these data are not accessible experimentally because the polymerization is very fast.

For sake of clarity, a primer experiment has been chosen, which corresponds to the fourth entry of Table 6 (CTA / MON = 1.94). In order to simplify, the calculations are customarily made with adimensional parameters and a time variable comprised between 0 and 1. In the primer case, one time unit corresponds to 92 seconds. Similarly, the concentrations are given in non-dimensional units: the concentration of the catalyst is chosen to be exactly 1. Thus, the concentrations of the monomer (171) and CTA (332) correspond to the number of equivalents relative to the catalyst.

The model indicates that the monomer is consumed very rapidly: in 0.4 x 92 seconds = 37 seconds, all the monomer is used up (Figure 8). However, nearly no chain transfer agent is consumed during that time period (Figure 9). For example, when 85% of the monomer is used, only 0.15% of the chain transfer agent is consumed, and the used amount of chain transfer agent does not reach 1% before 99.9% of the monomer is converted (Figure 10). Accordingly, the average degree of polymerization first increases steadily and then decreases because of transfer (Figure 11).

The behavior of the PDI for this polymerization is also interesting (Figure 12). The PDI first decreases with time, characteristic of a living polymerization where longer and longer chains are made (equation 3). Then, a clear change of polymerization regime occurs: the polymerization is no more living because the PDI increases steadily with time. This drastic change is due to the generation of short transferred chains, which broadens the polymer size distribution.

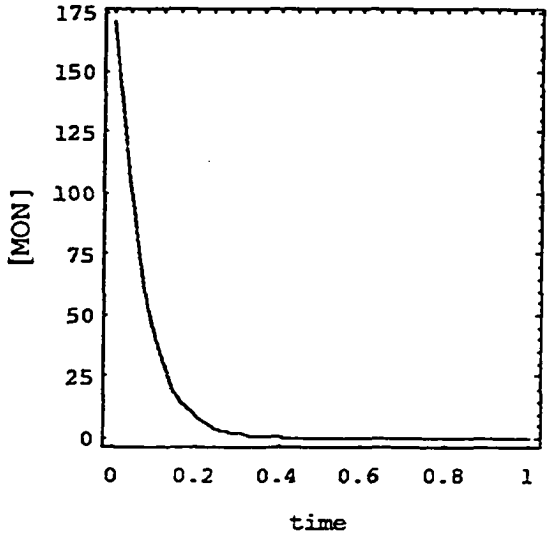


Figure 8. Variation of the monomer concentration versus time.

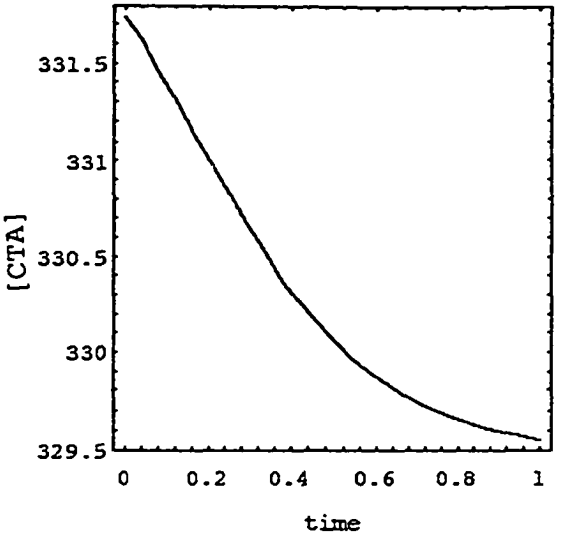


Figure 9. Variation of the chain transfer agent concentration versus time.

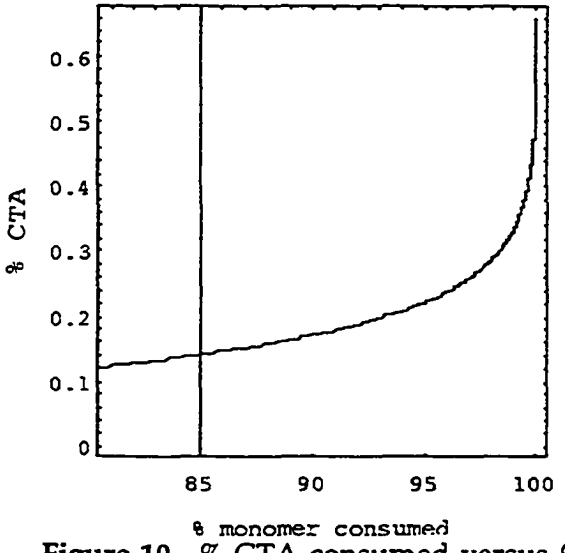


Figure 10. % CTA consumed versus % monomer consumed.

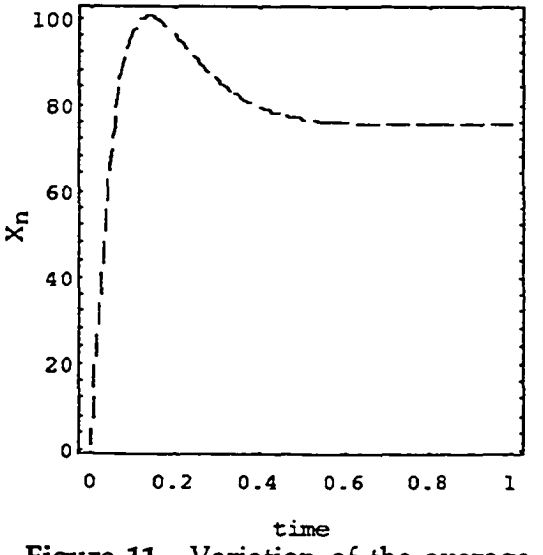


Figure 11. Variation of the average degree of polymerization versus time.

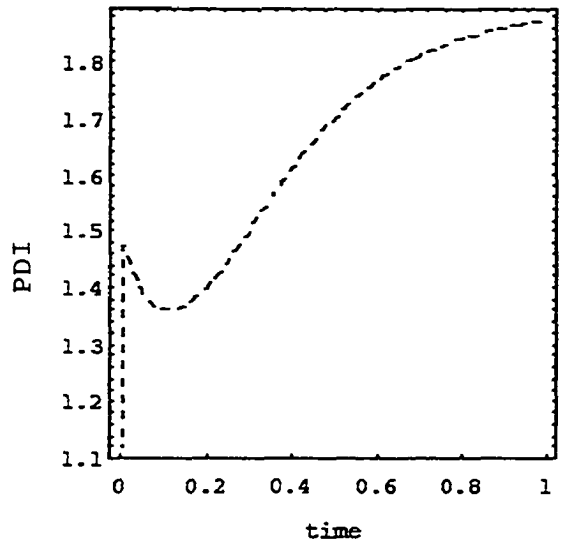


**Figure 12.** Variation of the PDI versus time.

b. Theoretical results on Mayo plot

When a polymerization is effected in the presence of added chain transfer agent, it is customary to plot the inverse of the molecular weight as a function of the ratio CTA /MON. This plot is usually called the Mayo plot. The use of the Mayo plot originates from classical studies in radical polymerization, where it can be shown that[17]

$$\left(\frac{1}{\overline{X}_n}\right)_{\text{with CTA}} = \left(\frac{1}{\overline{X}_n}\right)_{\text{without CTA}} + \frac{k_{tr}}{k_p}\left(\frac{\text{CTA}}{\text{MON}}\right) \qquad (15)$$

Consequently, in a radical polymerization, the slope of the Mayo plot is exactly the ratio $k_{tr}/k_p$.

In our case, theoretical calculations show that plotting $1/\overline{X}_n$ versus CTA/MON gives linear plots (Figure 13). However, the slope of this plot is not equal to the ratio $k_{tr}/k_p$.

Using the approximate equation 9, the slope $S_c$ is found to be:

$$S_c = \frac{d\left(\frac{1}{\overline{X}_n}\right)}{d\left(\frac{CTA}{MON}\right)} = 1 - \left(1 + \frac{1}{\frac{CTA}{MON} + \frac{k_p}{k_{tr}} - 1}\right)\left(1 + \frac{\frac{k_p}{k_{tr}} - 1}{\frac{CTA}{MON}}\right)^{-\frac{1}{\frac{k_p}{k_{tr}} - 1}} \quad (16)$$

This approximate solution does not depend on the initiation properties of the catalysts ($k_i$), nor does it depend on the amount of catalyst. However, exact numerical calculations show that this result is often wrong (except in the region where a steady state can be written, equation 10), and that the resulting polymer is in fact dependent on the amount of catalyst used.

Using the values of $k_i$, $k_0$, $k_p$ and $k_{tr}$ of the third entry of table 4, we have been able to generate a theoretical Mayo plot (Figure 13). On this plot, experimental values from Table 6 have been superimposed, and a good agreement between both plots has been found.

The slope of the Mayo plot as obtained experimentally is $3.9 \times 10^{-3}$, in good agreement with the theoretical value of $3.8 \times 10^{-3}$ predicted by our method. Again, it is important to note that the slope of the Mayo plot is not the same as the value of $k_{tr}/k_p$, which is $7.5 \times 10^{-4}$ (see Table 4), nearly one order of magnitude smaller.

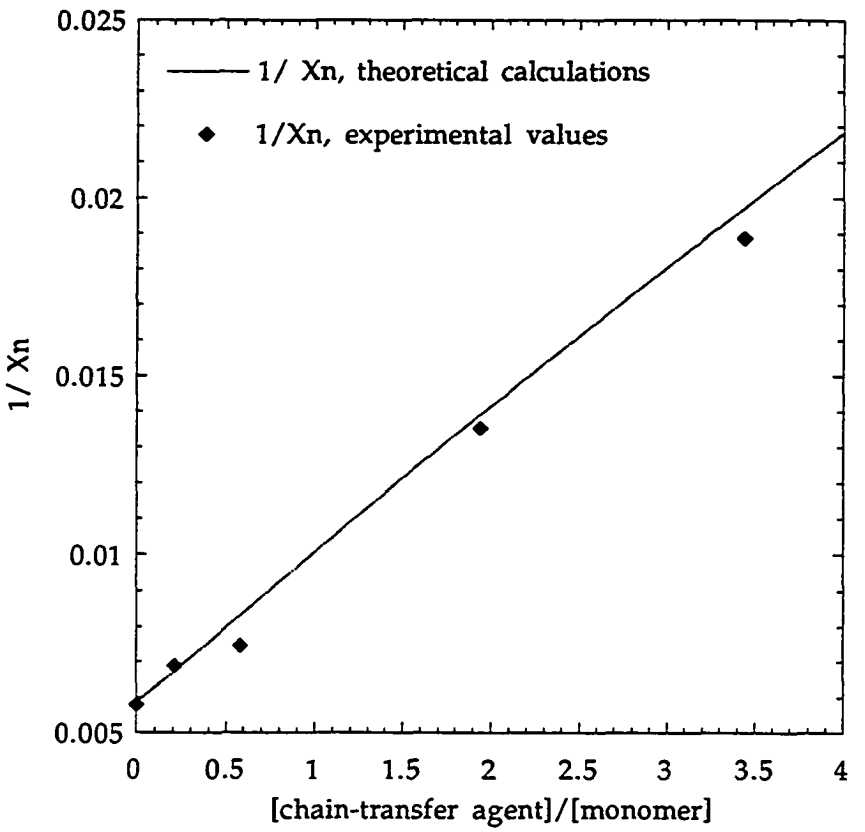


**Figure 13.** Mayo plot. The data points are obtained experimentally by size-exclusion chromatography. The line is the predicted behavior theoretically.

## III Thermodynamically controlled polymerizations

### 1. Introduction

In this part, we will treat the case of a polymerization where a thermodynamic equilibrium is established at the end of the reaction. All the reactions of the polymerization scheme described in Figure 1 are observed and reversible.

At equilibrium, the polymer distribution is bimodal : one distribution is formed of linear polymers, and the other one is made of cyclic oligomers, which originate from intramolecular transfer reactions (backbiting). Backbiting reactions are observed in numerous other chain polymerizations (cationic,[18] anionic[19,20]) and step polymerizations.[21] Evidently, the extent of this reaction is very much dependent on monomer concentration, as any typical cyclization reaction.

In 1950, Jacobson and Stockmayer developed a theory based on the existence of an equilibrium between cyclic and linear polymers (so called ring-chain theory).[22,23] This theory predicts the equilibrium constant between a cyclic polymer and its linear analog as a function of its size. In the case of ROMP, this theory needs to be slightly modified, because of the specifications of the reaction. For example, Jacobson and Stockmayer hypothesizes that cyclic compounds do not possess strain energy. This argument obviously falls short in ROMP, because ring strain is a neccessary criteria to ensure polymerizability. As well, small cyclics (< C18), observed in ROMP products have quite a bit of strain (see below).

The repercussions of the presence of strain energy are apparent at two different instances. First, the probability of cyclization for a strained chain is smaller than for a perfectly flexible chain. We will theoretically translate this phenomenon by ruling out the use of the freely jointed model for the polymer chain. Instead, the R.I.S. theory (rotational isomeric states), developed by Flory,[24-26] will be used. Notably, this theory has already been used in numerous occasions, to account for strain energy in cyclization reactions.[27] Second, it has been found that using RIS theory is not sufficient to describe accurately the size distribution in a ROMP polymer. Therefore an enthalpic contribution has been introduced in the cyclization equilibrium

constant, that precisely describes the difference of strain between cyclic and linear compounds. This enthalpic term has been evaluated by molecular mechanics calculations,[28] and this strategy proved to furnish good results, yet at the price of computer time.

Despite the numerous numerical difficulties encountered in this project, our objective, that is to say the prediction of the whole polymer distribution, has been reached, at least for simple ROMP polymers. Besides, numerous motivations exist for this project:

1. Although in standard polymerization conditions, the amount of cyclics rarely overreaches 5% in weight of the total polymer, the physical properties of the resulting polymer are largely affected by the presence of small amounts of cyclics.[29-32] For example, it has been shown that the viscosity of cyclic oligomers is smaller than linear analogs. In contrast, for longer chains, the situation is inverted. Technologically, this phenomenon is important because cyclic oligomers can potentially act as efficient plasticizers of the polymer.

2. When the polymerization is carried-out at high dilution, the cyclic oligomers become the major product, and this phenomenon has beeen taken advantage of by depolymerizing unsaturated polymers.[1] Poly(cyclopentene), an elastomer which is closely related to polybutadiene, can be totally depolymerized to cyclopentene at high temperature.[33] The application of this technique to the recycling of polymers is curently studied for polybutadiene, polyisoprene and copolymers.[34] Recently, it has been shown that a crosslinked matrix of polyisoprene can be partially digested, and that cyclic oligomers can be isolated.[35]

3. The metathesis reaction has been used in our group to elegantly synthesize cyclic molecules by the RCM method (Ring Closing

Metathesis).[36-40] The reaction products are obtained either by intramolecular cyclization, or by cyclodimerization. The prediction of size distribution of cyclic oligomers will allow one to distinguish between these two routes (see below).

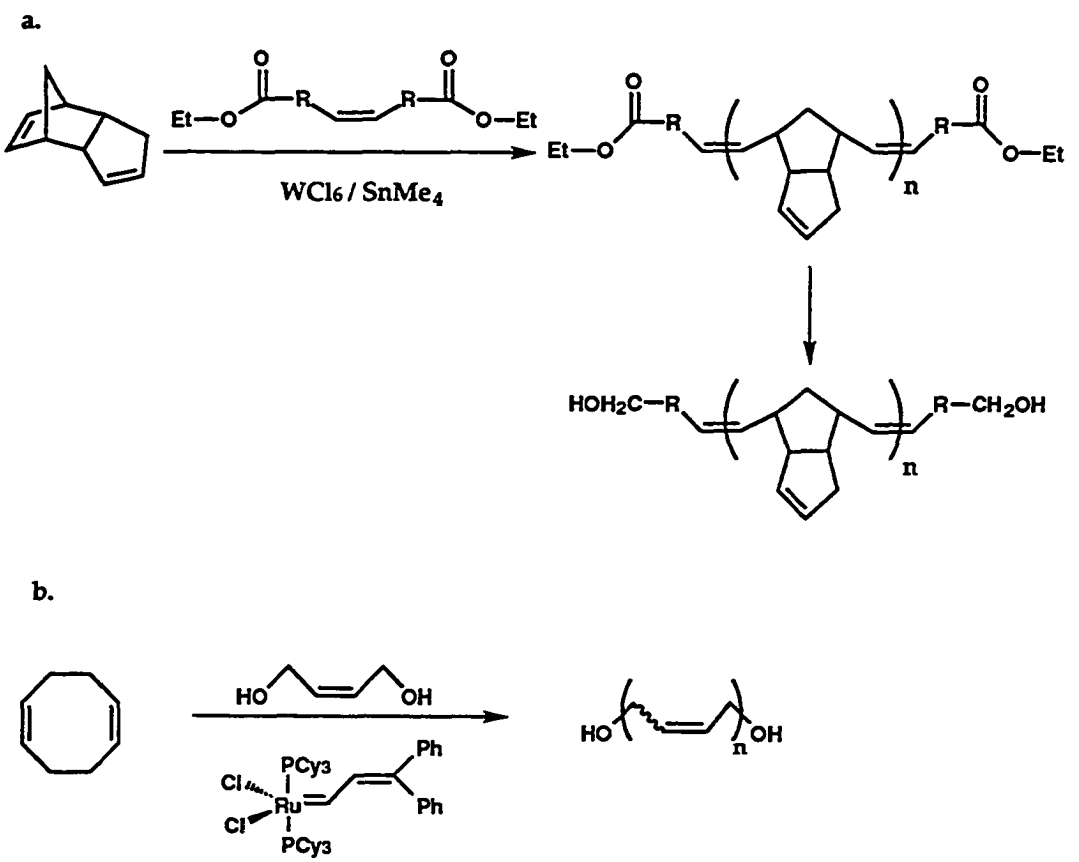


Figure 14. Application of the chain transfer technique in ROMP. (a) Synthesis of telechelic polydicyclopentadiene (b) Synthesis of hydroxytelechelic polybutadiene, a commercial polymer usually synthesized by radical polymerization.

4. The synthesis of telechelic polymers by ROMP has been effected in a thermodynamically controlled polymerization. This method leads to spectacular results, because, contrarily to the kinetically controlled regime, all the chain transfer and all the monomer is consumed. To date, two

examples have been furnished in literature,[41] to form highly interesting telechelic polymers (Figure 14). Nevertheless, the presence of unfunctionalized cyclic oligomers could hamper this process.

Our goal is to estimate the concentration of monomer, CTA, and cyclic and linear products at equilibrium. The theory will be presented here but calculations based on this theory and precise interpretation of numerical results, which are mainly the work of Zhong-Ren Chen, are describd in a printed publication.[42] Accordingly, only an outline of these results will be presented here. Finally, experimental results will be presented here and will be compared to theory.

## 2. Theory

### a. Flory distribution and step polymerization

At thermodynamic equilibrium, the total degree of polymerization is the average of the degree of polymerization of linear polymers (p) and of cyclic oligomers. Let $P_n$ and $C_n$ be respectively the concentrations of linear and cyclic polymers containing n units. Rigorously, one should take into account the living chains $W_n$ which are still attached to the catalyst, nevertheless, the distribution of these chains is identical to the distribution of the linear polymers $P_n$. At equilibrium, no linear chain can exist in the presence of unreacted chain transfer agent, therefore, the number of linear chains is exactly CTA + CAT. For these chains, the average degree of polymerization is

$$p = \frac{MON - M_c}{CTA + CAT} \qquad (17)$$

where MON is the initial concentration of monomer, and $M_c$ is a critical concentration of monomer. More precisely, $M_c$ is the concentration of monomers incorporated in cyclic oligomers, and (MON - $M_c$) / MON is the fraction of monomers incorporated in linear chains. Therefore, the mathematical definition of $M_c$ is:

$$M_c = \sum_1^\infty x\, C_x \qquad (18)$$

It is intuitive to say that the distribution of linear chains should obey the Flory distribution (most probable distribution), because at thermodynamic equilibrium, all the polymer units are equireactive (in reason of the intermolecular transfer reaction). Despite the presence of a well defined active site for the monomer addition, this polymerization is indeed a step polymerization, where all chains are equally probable.

By a short statistical argument, it is possible to retrieve rigorously the chain distribution. For example, let us consider a statistical "ensemble" made of linear products (distribution $P_n$) and of cyclic products (distribution $C_n$), and let us wonder under which conditions the thermodynamic equilibrium is reached. The statistical ensemble is submitted to three constraints:

$$MON = \sum_1^\infty n\, C_n + \sum_1^\infty n\, P_n \qquad (19)$$

$$CTA = \sum_1^\infty P_n \qquad (20)$$

$$C = \sum_1^\infty C_n \qquad (21)$$

For a given distribution, the total number of conformations is:

$$W(P_n, C_n) = \frac{CTA!}{\prod_n P_n!} \cdot \frac{C!}{\prod_n C_n!} \qquad (22)$$

Thermodynamic equilibrium is reached for the distribution which maximizes the function W.[43] This maximum can be found using the method of Lagrange multiplicators, affording for the equilibrium distribution:

$$P_x = \frac{CTA}{1+p}\left(\frac{p}{1+p}\right)^x \qquad (23)$$

$$C_x = K_x\left(\frac{p}{1+p}\right)^x \qquad (24)$$

The constant $K_x$ is explicitly given by Jacobson-Stockmayer theory. If this constant $K_x$ is known, and if the average degree of polymerization of linear chains (p) is known, then the distribution of cyclic and linear products can be deduced from equations 23 and 24.

b. Calculation of the constant Kx.

Jacobson and Stockmayer have considered the equilibrium of backbiting between a linear chain of degree of polymerization y, a cyclic product of size x and a smaller linear chain, of degree of polymerization y-x:

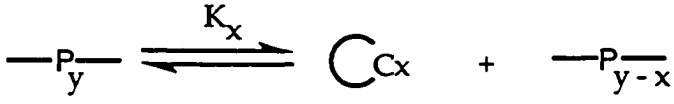


(25)

By replacing the concentration $C_x$, $C_y$ and $C_{y-x}$ by the values found in equations 23 and 24, one finds that the equilibrium constant of the reaction 25 is in fact $K_x$.

On the other hand, $K_X$ can be calculated by statistical arguments:[22,23]

$$K_X = \frac{1}{N_a \sigma_{R_X}} \left( \frac{3}{2\pi \langle r_x^2 \rangle} \right)^{3/2} \qquad (26)$$

$N_a$ is the Avogadro number, $\sigma_{Rx}$ is a statistical symmetry number which is equal to 2 x, and $\langle r_x^2 \rangle$ is the mean square end to end distance of the polymer. In early calculations, it was assumed that the chain was behaving as a random walk, for which $\langle r_x^2 \rangle = C \cdot x$ (C is a constant). For the reasons indicated in the introduction, this method has been discarded. $\langle r_x^2 \rangle$ is now evaluated by the R.I.S. theory, developed by Flory. This method, although simple in principle, is heavy in calculations (see appendix 2).

The Jacobson Stockmayer $K_X$ contains only an entropic contribution, which is derived from the intrinsic elasticity of the polymer chain in order to cyclize. We have added an enthalpic contribution to $K_X$ which chemically corresponds to the strain energy (S.E.) of the cyclic product:

$$K_X = e^{-\frac{\Delta H^0}{RT} + \frac{\Delta S^0}{R}} = \frac{1}{N_a \sigma_{R_X}} \left( \frac{3}{2\pi \langle r_x^2 \rangle} \right)^{3/2} e^{-\frac{S.E.}{RT}} \qquad (27)$$

Strain energies (S.E.) have been evaluated by molecular mechanics (MM3 field). Knowing the strain energy of a cyclic of size x, as well as the end to end distance $\langle r_x^2 \rangle$ of the linear polymer, the constant $K_X$ can be calculated by using equation 27. An example of such calculations is given in Appendix 2 of this chapter.

3. Overview of the numerical results

The model allows the prediction of the critical concentration $M_c$ as well as the behavior of the cyclic and linear distribution. At very low initial monomer concentration, most of the products are cyclic, and the critical concentration is equal to the monomer concentration (Figure 15). When the initial monomer concentration increases, some linear polymers are formed, and there is a partition between cyclic and linear chains. Increasing further the monomer concentration permits the generation of linear polymers, but no additional cyclics are formed: the critical concentration is constant. This value of critical concentration for high monomer concentrations has been found to be 0.21 mol/l for cyclooctene, 0.45 mol/l for cyclobutene, and 0.13 mol/l for cyclododecene. Therefore, when cyclooctene is polymerized neat (c = 7.9 mol/l), 0.21 / 7.9 = 2.7% of the monomer is incorporated in cyclic products. A more precise and detailed interpretation is given in reference 42.

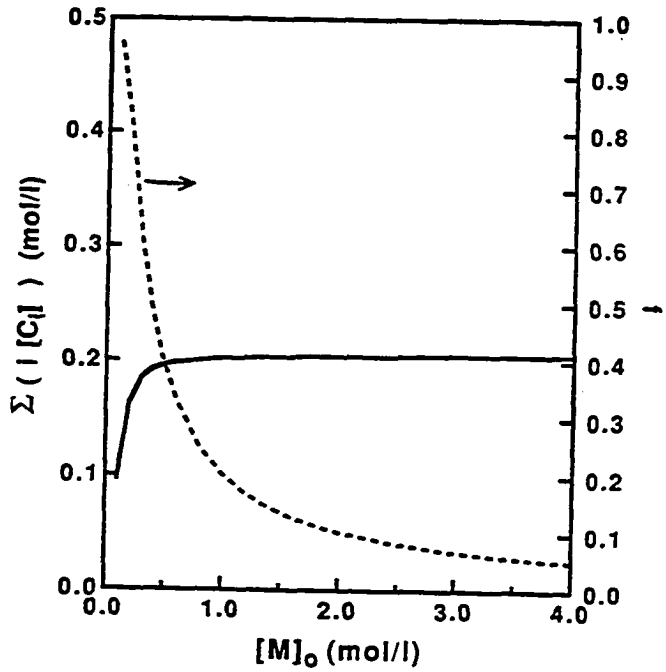


**Figure 15.** Fraction of cyclics (dashed curve, right axis) and total cyclics concentration (solid curve, left axis) as a function of initial cyclooctene concentration: calculated at 300 K in a θ solvent, with MON / CTA = 200.[44]

The model can also predict the influence of chain transfer agent concentrations, temperature and solvent quality. At high ratio MON / CTA (≥ 200), there is no influence of CTA concentration on the cyclic distribution. However, lowering the ration MON / CTA (that is to say increasing CTA concentration) produces higher amounts of short cyclics at the expense of bigger ones. The amount of cyclic products increases with the temperature, except for the polymerization of cyclohexene. Finally, the amount of cyclic products increase when the reaction is done in a poor solvent.

## 4. Experimental methods

A large number of works describe the equilibrium distribution of cyclic oligomers in ROMP. The majority of these works deal with the polymerization of 1,5-cyclooctadiene, COD,[45-49] and cyclopentene.[33, 50-51] The results vastly differ from author to author. With the exception of Hocker, who utilizes the concept of critical concentration as we defined it, all other researchers use the concept of ceiling concentration $M_e$, above which macromolecular products are observed.[52] This concentration is defined by

$$\ln[M]_e = \frac{\Delta H}{RT} - \frac{\Delta S}{R} \qquad (28)$$

where $\Delta H$ and $\Delta S$ are the enthalpy and entropy of the reaction of polymerization.

The range of values reported for $M_e$ is very large. For example, for COD polymerization, Chauvin proposes that $M_e$ = 0.65 mol/l, whereas for Ivin, $M_e$ = 0.002 mol/l. Two reasons can be invoked for explaining these large disparities. First, none of these authors have checked that the final product of their polymerization is actually a thermodynamic product. Although the catalysts used for this study are extremely active ($(CO)_5W{=}C(OEt)Ph - TiCl_4$ [31a], $WCl_6 - EtOH - Et_2AlCl$ [31b], $Re_2O_7$-$Al_2O_3$ [31c] these catalysts are also known to quickly undergo termination reactions. Secondly, the separation of cyclic oligomers has been done by precipitation in a non-solvent of the polymer. As shown below, this method gives unsatisfactorily results because of the similarity of solubility of a macrocyclic oligomer and a linear polymer chain.

a. Monomers and catalysts

We have chosen cyclooctene and COD as monomers, because of the experience we have acquired in handling them in our laboratory.[53-55] To date, no systematic data exist on the cyclics formation by so called well defined catalysts. We have used different well defined catalysts for carrying out this study (Figure 16). All these catalysts are active enough to allow polymerization of cyclooctene and COD, and react with acyclic double bonds. The use of more than a catalyst is necessary to check that equilibrium is reached: in this case the product distribution is independent on the catalyst choice. The three tungsten based catalysts and the molybdenum one will be described in details in the next chapters. The ruthenium catalyst has been recently developed.[5] This catalyst is slightly less active than tungsten based ones, so polymerization times of three days have been used (instead of 16 hours for the other catalysts). Realistically, the polymerization is terminated after 30 minutes, but the rest of the time is necessary for reaching equilibrium.

b.Separation of cyclic products from linear polymers

The usual method used to separate oligomers from high molecular weight polymers consists in adding a toluene solution of the macromolecules to methanol under high stirring. After filtration of the insoluble polymer, the solution, containing oligomers, monomer and organometallic fragment is analyzed. When the precipitated polymer is dissolved once again in toluene, and precipitated in methanol, a large

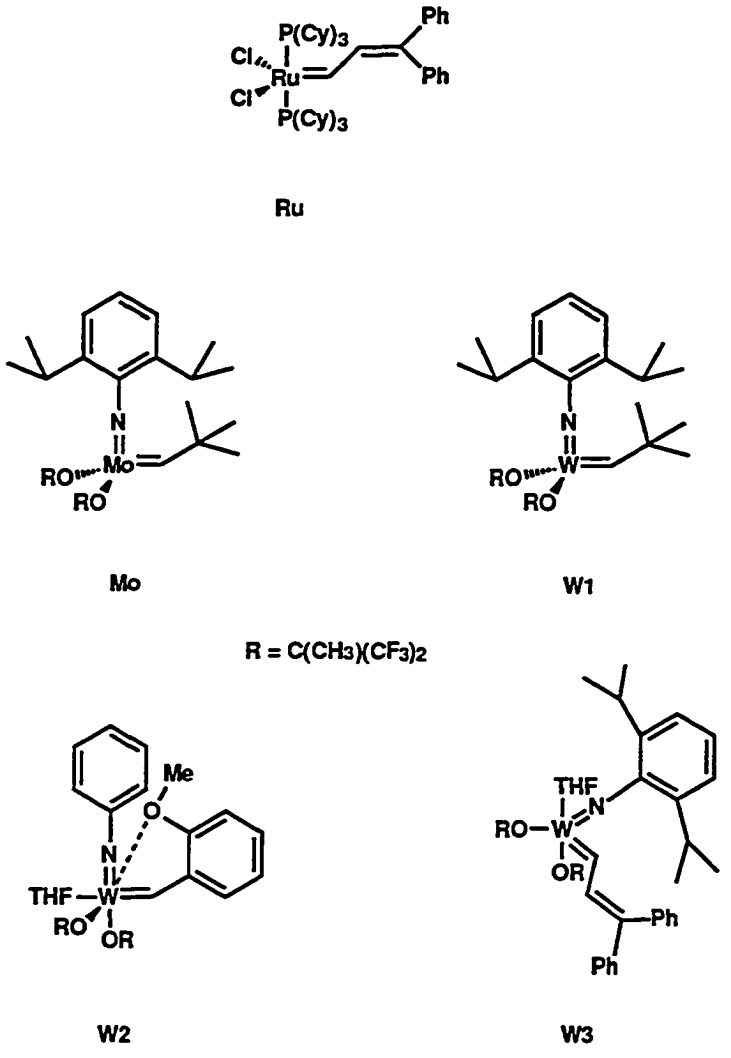


**Figure 16.** Catalysts used in our study

amount of cyclic oligomers is again found in the mother liquor. In fact, when compared to a method where the totality of the cyclic product is extracted, only 28% of the oligomers of COD are extracted by a single methanol extraction. The use of a Soxlet apparatus allows the extraction of 80% of the cyclic oligomers of COD, after a large number of rotations. Nevertheless, the Soxlet extraction is quantitative for the monomer and small size cyclics, but far from being efficient for larger size rings. In order to improve the

extraction process, a precipitating solvent in which hydrocarbons are more soluble was sought. After dissolution of the polymer in a minimum amount of hexane, isopropanol was added until induction of precipitation. The onset of precipitation occurs for a mixture which contains 50% isopropanol in volume. The analysis of cyclic products show that the extraction is nearly quantitative, yet some low molecular weight linear polymers are also extracted. To remedy this problem, this method is used when only very high molecular weight polymers are made, or when working with the ruthenium catalyst. It is also possible to separate the cyclic products from very high molecular weight linear products by simple flash chromatography on silica-gel (hexane - 10% $CH_2Cl_2$).

Since the separation of cyclic product appeared to be so difficult by the precipitation method, another route has been devised. This route does not apply for ruthenium catalyst, but for all other catalysts. For these catalysts, the typical way of quenching the reaction consists in adding an aldehyde (usually benzaldehyde) in order to promote a Wittig type reaction with the metallic carbene (Figure 17). When the aldehyde is supported on a crosslinked resin, then all the carbene-bound chains become grafted on the resin, making the separation of cyclic products trivial.[5] A few linear chains which do not contain a metal end could originate from cross metathesis of two living chains, giving a non substituted chain and a chain containing two metal ends. Experiments have been carried out at high dilution to minimize the probability of such a reaction to occur.

---

[5] The experiments described below have been done in the absence of chain transfer agents, therefore all linear chains are carbene bound. Adding or not a chain transfer agent is not changing the generality of our results (see this chapter, III.2.a).

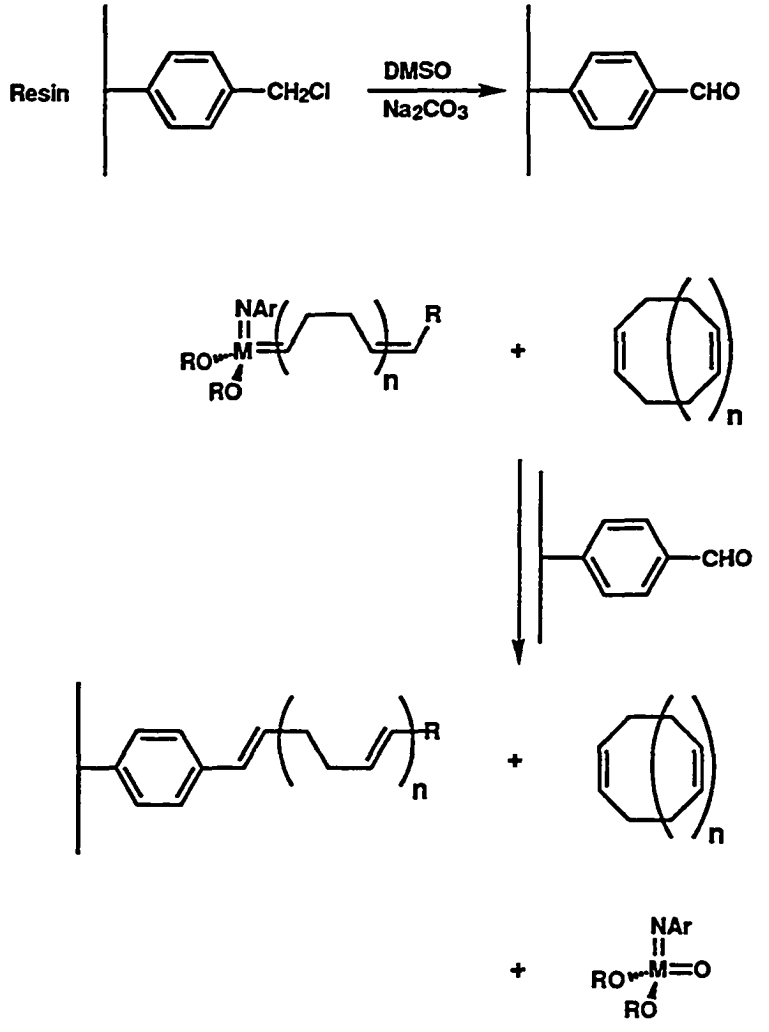


**Figure 17.** Separation of cyclic and linear products with a crosslinked resin. The resin has been synthesized from a commercial Merrifield resin (2% DVB), via a modified Swern oxidation.[56] The resulting oxo-imido metal complex is insoluble in the reaction medium.

c. Detection and identification of cyclic products

Cyclic oligomers have been analyzed by gas phase chromatography (GC) or gas-phase chromatography coupled with mass-spectrometer (GC-MS). Because high molecular weight cyclics contain many different cis/trans isomers, the samples have been hydrogenated on Pd/C (Figure 18). After

having analyzed each product, it has been possible to determine their amount by calibrating the response of the flame ionization detector of the GC (Figure 19). The calibration curve can be extrapolated to high molecular weight cycloalkanes, affording the quantitative analysis of hydrogenated products.

Injections in the GC have been made on a split type-injector, or a splitless injector, when precise quantitative measurements are needed. In these two injectors, the cyclic products containing more than 32 carbons are not vaporized efficiently. On-column injections, where the injector is short-circuited, have been made in a few occasions, and have allowed the detection of cyclic products up to 60 carbon atoms (Figure 20). Yet, this method cannot be used regularly, in reason of its detrimental effect on the column.

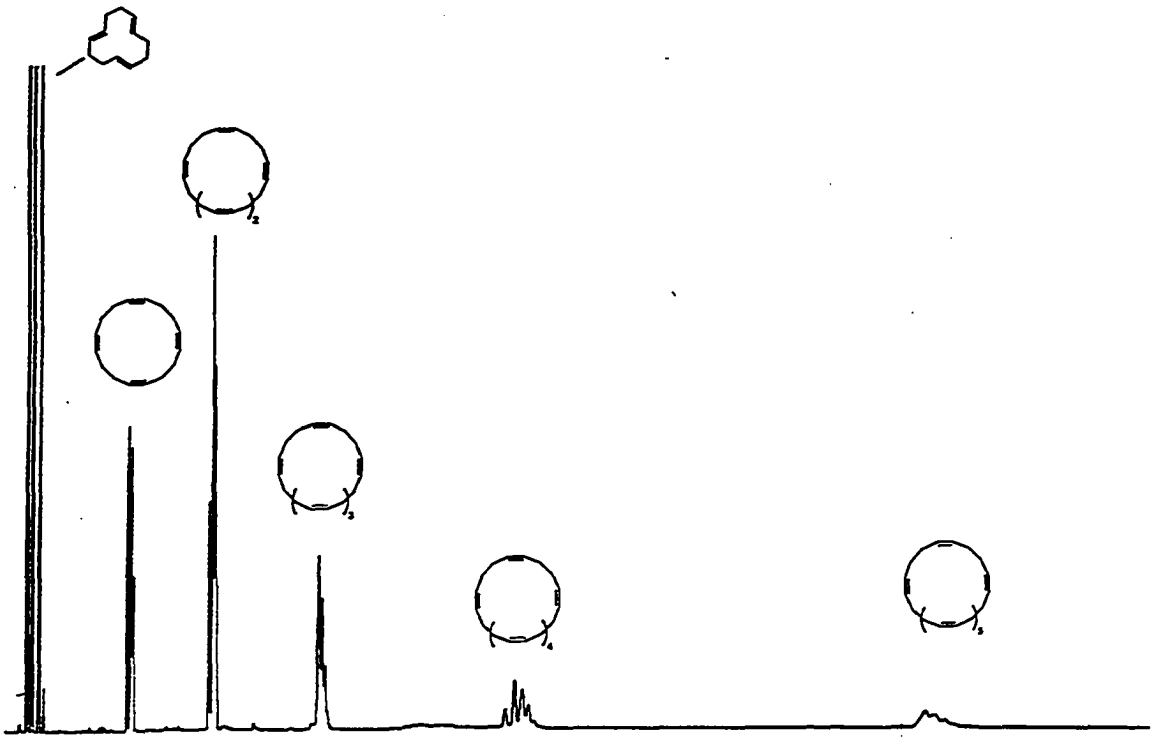

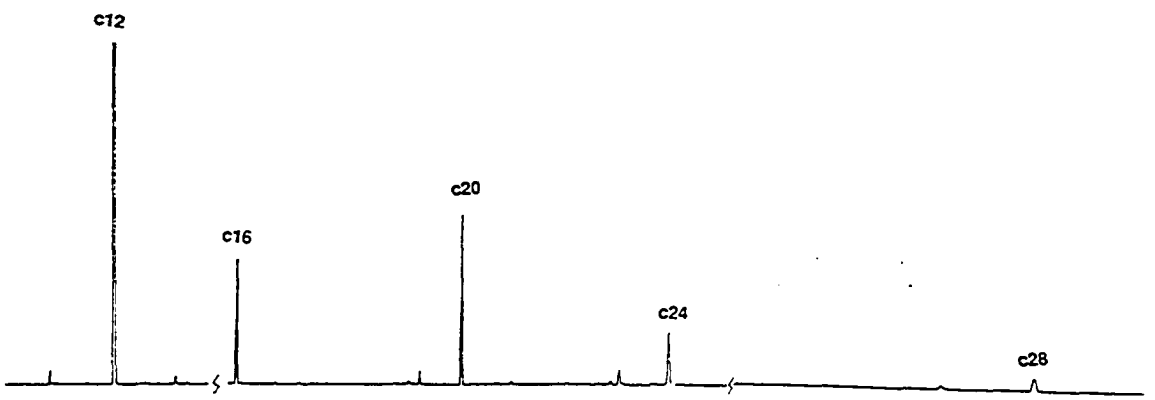


**Figure 18.** Chromatogram of a mixture of cyclic oligomers before hydrogenation (top) and after hydrogenation (bottom). This mixture is obtained by polymerization of COD at room temperature with W2 catalyst, for 150 minutes. [COD] = 0.072 mol/l, [COD] / [W2] = 1. 5 . The first five minutes of the chromatograms are not shown. The three first peaks correspond to respectively *cis,cis,trans, cis,trans,trans* and *trans,trans,trans*-cyclododecatriene.

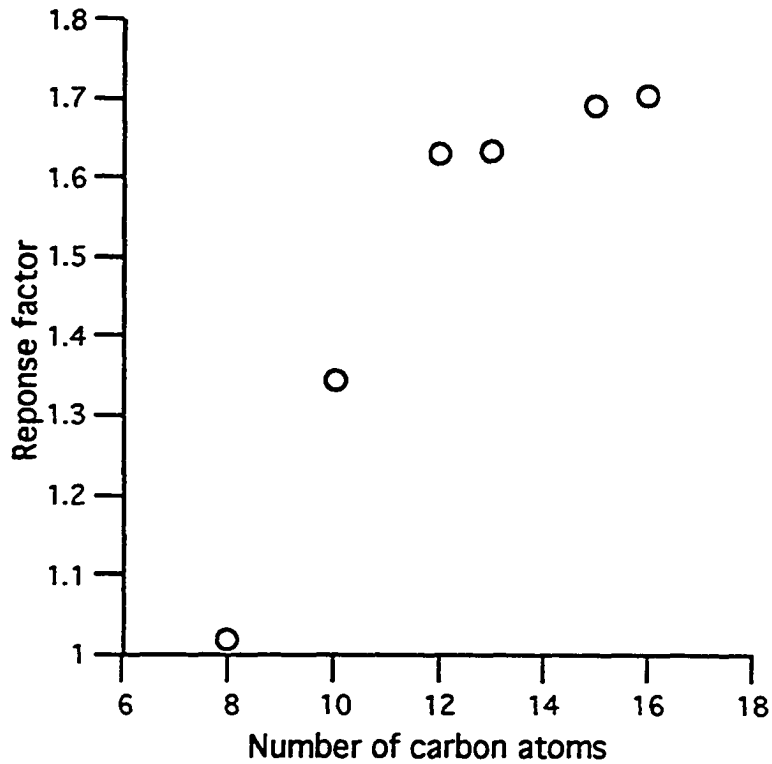


**Figure 19.** Calibration of the GC by cycloalkanes. The response factor is given relatively to the response of *p*-xylene.

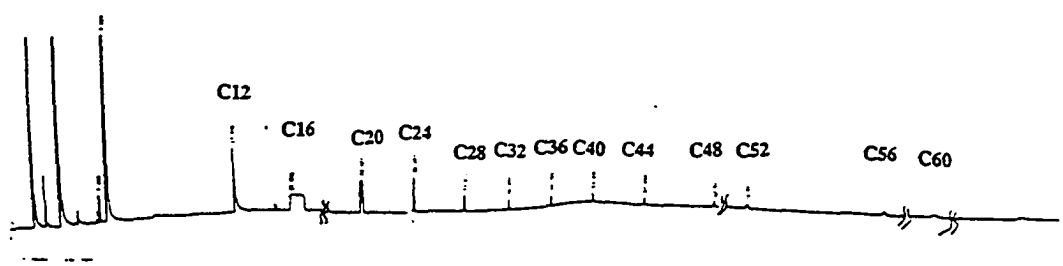


**Figure 20.** Chromatogram of hydrogenated cyclic oligomer mixture. This mixture is obtained by polymerization of COD at room temperature with W2 catalyst, for 150 minutes. [COD] = 0.072 mol/l, [COD] / [W2] = 23.5 . The first three minutes of the chromatograms are not shown. The C16 peak is contaminated by a printer mistake.

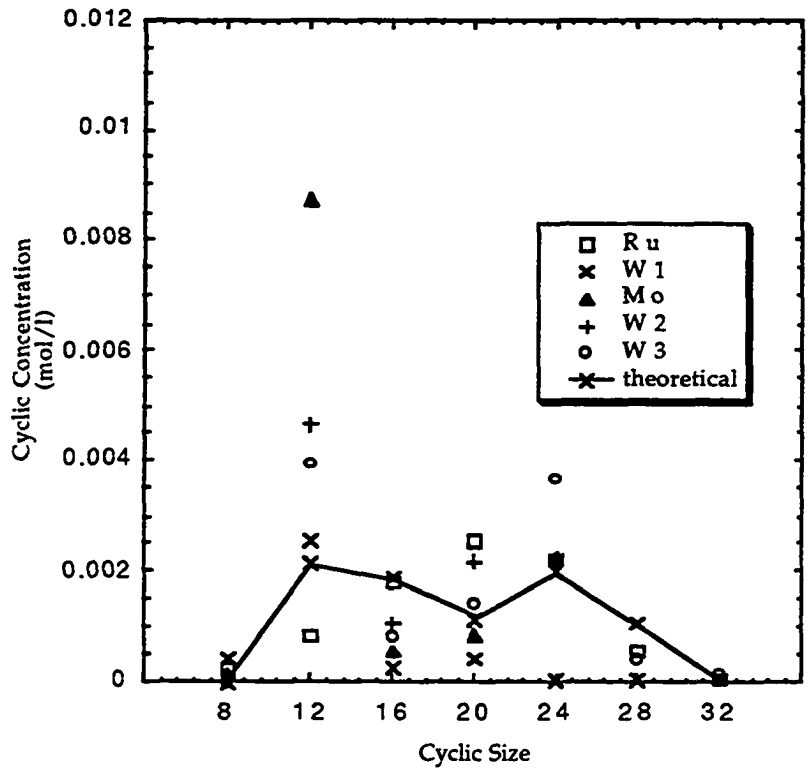


**Figure 21.** Cyclic products distribution in 1,5-cyclooctadiene (COD) polymerization. Ru : [COD] = 0.0702 mol/l , [COD] / [Ru] = 13.5; W1 : [COD] = 0.0702 mol/l , [COD] / [W1] = 1.5; W2 : [COD] = 0.0702 mol/l , [COD] / [W1] = 6.4; W3 : [COD] = 0.0702 mol/l , [COD] / [W1] = 13.5; Mo : [COD] = 0.0702 mol/l , [COD] / [Mo] = 5.29.

## 4. Experimental results and comparison with theory

### a. Cyclic distribution in the absence of chain transfer agent

The use of the resin described above allows the separation of cyclic from linear products. For the smallest cyclooligomers of COD, the results are presented in Figure 21. The detail calculations of the theoretical distribution are described in Appendix 2 of this chapter. For the experimental data, a significant amount of scattering is observed. However, for most catalysts, the dominant trend is closely related to the theoretical distribution. The

experimental data show large discrepancies for the concentration of the C12 cyclic (cyclododecatriene). At the exception of Ru catalyst, too large a value for the *trans,trans,trans*-cyclododecatriene is found. Intrigued by this phenomenon, we have carried out the polymerization of *trans,trans,trans*-cyclododecatriene in concentrated phase by catalysts W1 and W2, and found this polymerization to be very slow : after 3 days, under typical conditions, the polymerization is not complete. Therefore, it can be inferred that in the polymerization of COD, *trans,trans,trans*-cyclododecatriene acts as a kinetic trap. The ruthenium catalyst, which is not related to the family of molybdenum and tungsten catalysts, does not show the phenomenon of kinetic inhibition by cyclododecatriene.

The detection of high molecular weight cyclic oligomers has been done using on-column injection technique (Figure 22). Our theory predicts that, for large rings, the concentration $C_x$ of a cyclic of size x is proportional to $x^{-3\alpha-1}$ , where $\alpha$ is a factor which takes the quality of the solvent into account. If the solvent is theta, $\alpha$ is 0.5, whereas for a good solvent, $\alpha \geq 0.5$. In our case, we have found that, in toluene, $C_x$ varies like $x^{-2.1}$. The critical exponent (2.1) is slightly different from what is expected (2.5 to 2.8), but still in close agreement with the theory.

For cyclooctene polymerization, we have found a good agreement between theoretical and experimental results (Figure 23), at the exception of C16 (we suspect that for this particular cyclic product, the calculated strain energy (2.64 kJ/mol) is slightly too small). However, less results can be harvested because the higher molecular weight of the monomer unit.

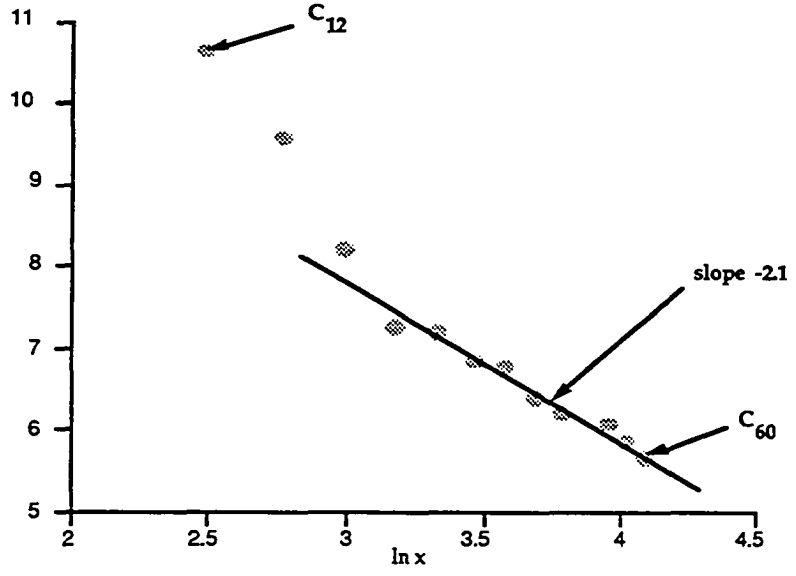


**Figure 22.** Distribution of COD cyclics of high molecular weight, versus carbon number, in logarithmic scale.

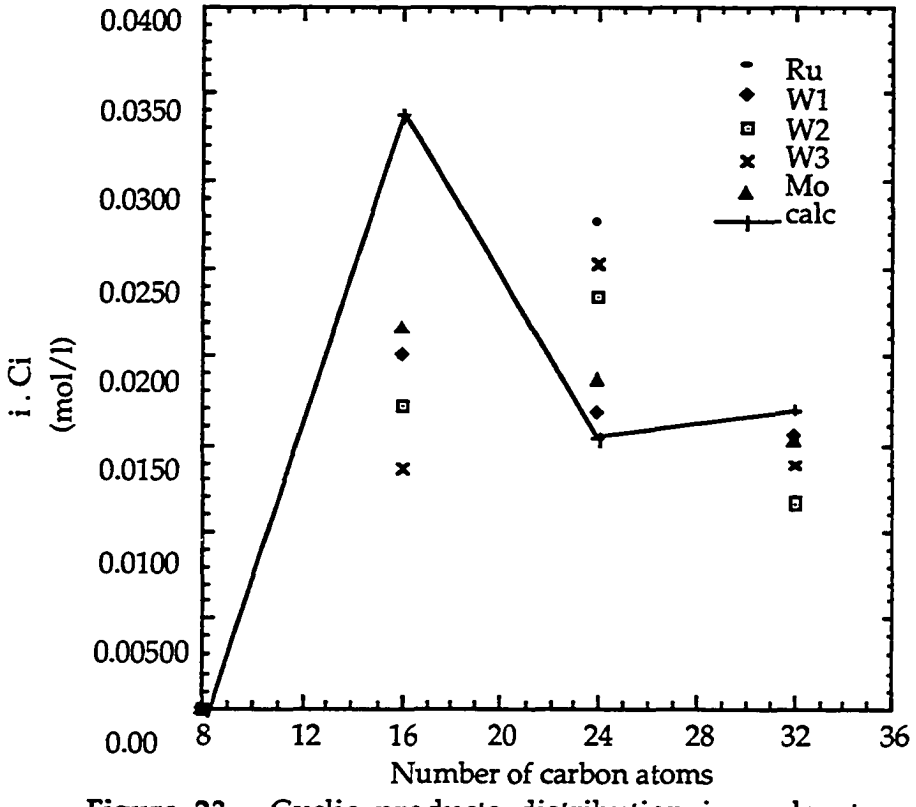


**Figure 23.** Cyclic products distribution in cyclooctene (COE) polymerization. Ru : [COE] = 0.1411 mol/l, [COE] / [Ru] = 37.5; W1 : [COE] = 0.1411 mol/l, [COE] / [W1] = 29.6; W2 : [COE] = 0.1411 mol/l, [COE] / [W2] = 63,5; W3 : [COE] = 0.1411 mol/l, [COE] / [W3] = 16.9; Mo : [COE] = 0.1411 mol/l, [COE] / [Mo] = 26.4.

b. Applications to ring closing metathesis

The experimental and theoretical distribution of COD indicates the presence of a concentration maximum for the cycles containing 24 carbon atoms as well as a maximum for cycles containing 12 carbon atoms (Figure 21). Interestingly, the relative predominance of the 2 maxima will be dependent on the degree of polymerization of the linear chains. This phenomenon prompts us to analyze the factor determining the selectivity of ring closing metathesis.

For example, a 0.1 mol/l solution of 1,5-hexadiene will give under dilute conditions a mixture of cyclic and linear products which are identical to those obtained by ring-opening of COD. Increasing the monomer concentration will obviously increase the fraction of linear polymers, compared to cyclic products (see Figure 15). In addition, the cyclic product distribution will be modified: at low monomer concentration, short cyclics will be made (cyclooctadiene, cyclododecatriene, eg), whereas at higher concentration, larger cyclics will be formed.

Less intuitive is the fact that, at fixed monomer concentration (0.1 mol/l), the catalyst concentration influences on the regioselectivity of the ring closing reaction. Figure 24 shows the variation of the concentration of cyclics having 12, 16, 20 and 24 carbon atoms when the catalyst concentration varies. When [cat] = $10^{-4}$ mol/l, the concentration of the C24 ring is larger than the one of C12 ring, whereas the situation is clearly inverted at higher catalyst concentrations.

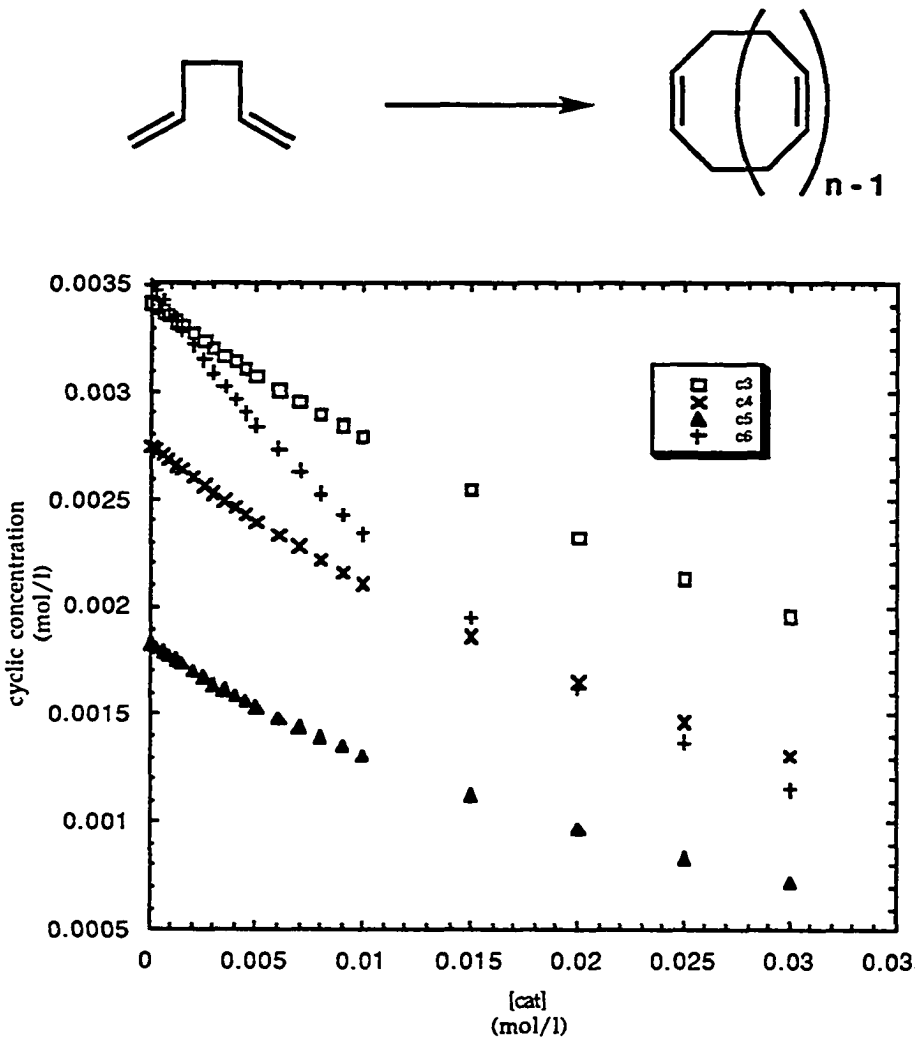


Figure 24. Calculated variation of the concentration of cyclic products with the concentration of catalyst, for a ring closing experiment. c3 : concentration of cyclododecatriene (C12), c4 : concentration of cyclohexadecatetraene (C16), c5 etc... The monomer concentration is kept constant at 0.1 mol/l, at 298 K.

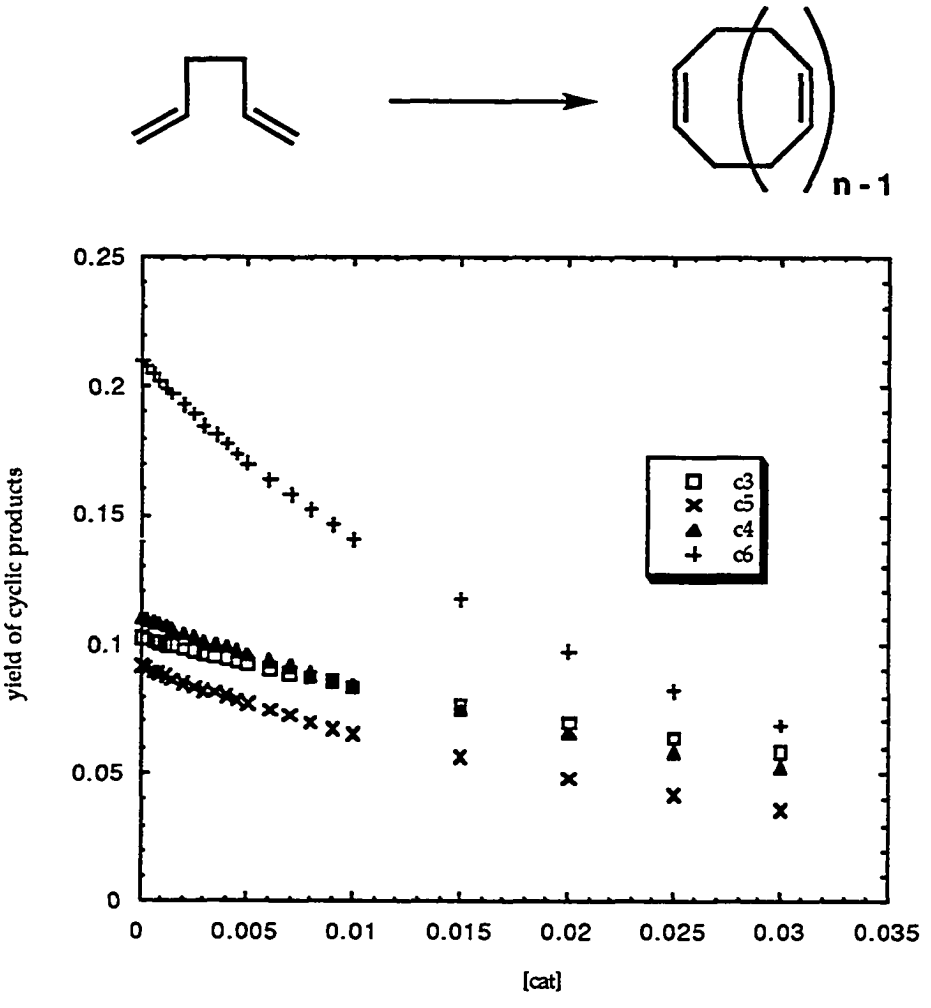


Figure 25. Calculated variation of the yield of cyclic products with the concentration of catalyst, for a ring closing experiment. c3 : yield of cyclododecatriene (C12), c4 : yield of cyclododecahexatetraene (C16), c5 etc... The monomer concentration is kept constant at 0.1 mol/l, at 298 K.

For a synthetic chemist, it is customary to describe the outcome of a reaction by giving the yield of the different products (instead of their concentration), relative to the starting material (Figure 25). Because larger rings consume larger amounts of monomer, the yield of C24 cyclic is twice larger (20%) than the yield of C12 cyclic (10%). Therefore, the ring-closing reaction shows a moderate selectivity toward C24 at low catalyst concentration. However, increasing the catalyst concentration to speed up the reaction leads to a dramatic loss of selectivity.

This result should be contrasted with the intuitive belief that the product selectivity at thermodynamic equilibrium is given by the difference of free energy between the products.[57] For example, for the reaction shown above, the free energy of cyclization for C12 and C24 are respectively 12.8 kJ/mol and 11.4 kJ/mol (Appendix 2). It could be concluded hastily that

$$\frac{\text{yield C24}}{\text{yield C12}} = \frac{24\ e^{-\frac{11.4}{RT}}}{12\ e^{-\frac{12.8}{RT}}} = 3.5 \qquad (29)$$

Nevertheless, as shown in Figure 25, the ratio of the yields never reach this value, and are additionally catalyst concentration dependent.

The origin of this catalyst concentration dependency comes once again between the distinction between catalyst and reaction promoter. In a ROMP polymerization, the metallic complex is effectively a catalyst if chain transfer agents have been intentionally added. In the case of Figures 22 and 23, one can argue that the metallic carbene which promotes the ring closing reaction is a catalyst, because it is not involved stoichiometrically in the reaction. However, the possibility of forming living linear polymers exists in a RCM experiment, thereby transforming the role of the carbene in a *reaction promoter*. Because there now exists a stoichiometric relation between the

"catalyst" and other components in the reaction, *the distribution of products at equilibrium in ring-closing metathesis depends on the amount of metallic carbene.*

There are some positive and negative aspects about this phenomenon:

1. In certain cases, the product distribution is strongly biased toward one product (such as a 6-membered ring). The influence of the "catalyst" concentration is then likely to be small.

2. When effective, the "catalyst" concentration dependence on the selectivity of the cyclization gives a remarkable handle to the synthetic chemist for selecting a product of given size.

3. Except when there is a very strong bias toward one cyclic product (like C6 and C5 rings), the general prediction of the cyclic products distribution is a difficult and lengthy task, which needs to be repeated in a case by case method. Appendix 2 gives an detailed example of such calculation.

c. Polymerizations in the presence of chain-transfer agents

In order to study the role of the monomer and chain transfer agent concentrations in a thermodynamically driven polymerization, a set of experiments has been conducted, where the ratios MON/CTA and CTA/CAT are held constant, but where the intrinsic concentrations of these reagents are varied from very concentrated to very dilute solution. We have chosen W1 for catalyst, *cis* β-methylstyrene for chain transfer agent and COD for monomer. The ratios MON/CTA and CTA/CAT are respectively 44.6 and 13.0. For these reactions, we have found that the yield of the polymerization (more precisely the yield in linear polymers) increases steeply until the concentration reaches a ceiling value (Figure 26).

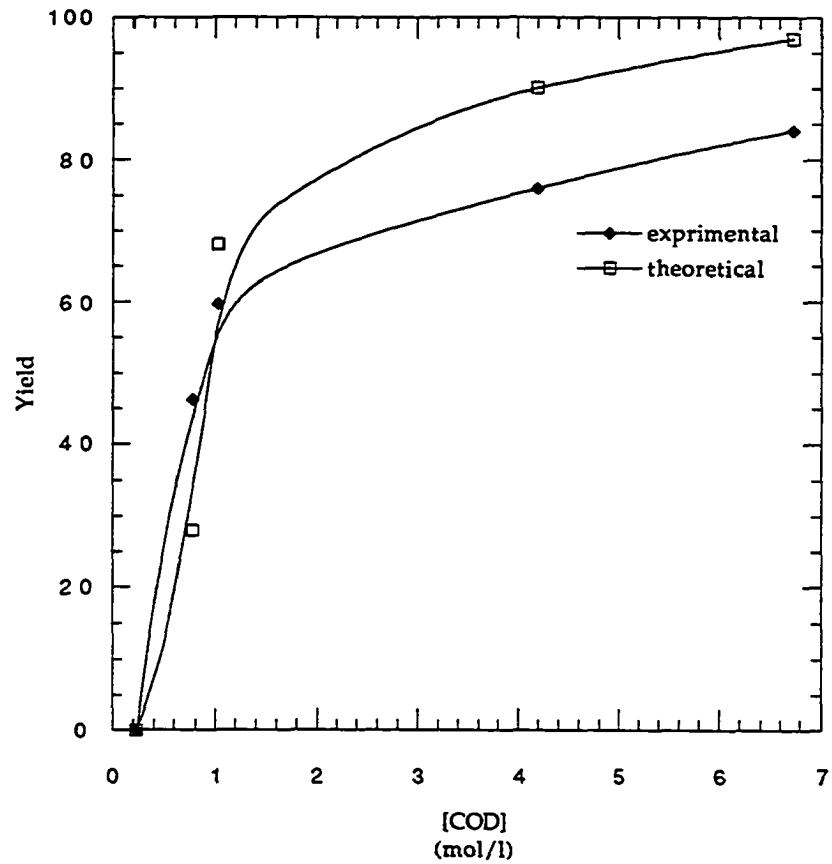


**Figure 26.** Variation of the yield of COD polymerization with the initial monomer concentration. The yield corresponds to the amount of isolated dried polymer.

The onset at which the ceiling value is reached corresponds to a monomer concentration of 1.5 mol/l. These results agree with Figure 15, which indicates that above a certain monomer concentration, the critical concentration reaches the value of 0.45 mol/l, and the rest of the monomer is incorporated in linear products. For high monomer concentrations, the theoretical yield is larger than the experimental one. This is likely to be due to the unavoidable losses during the isolation of the linear polymer.

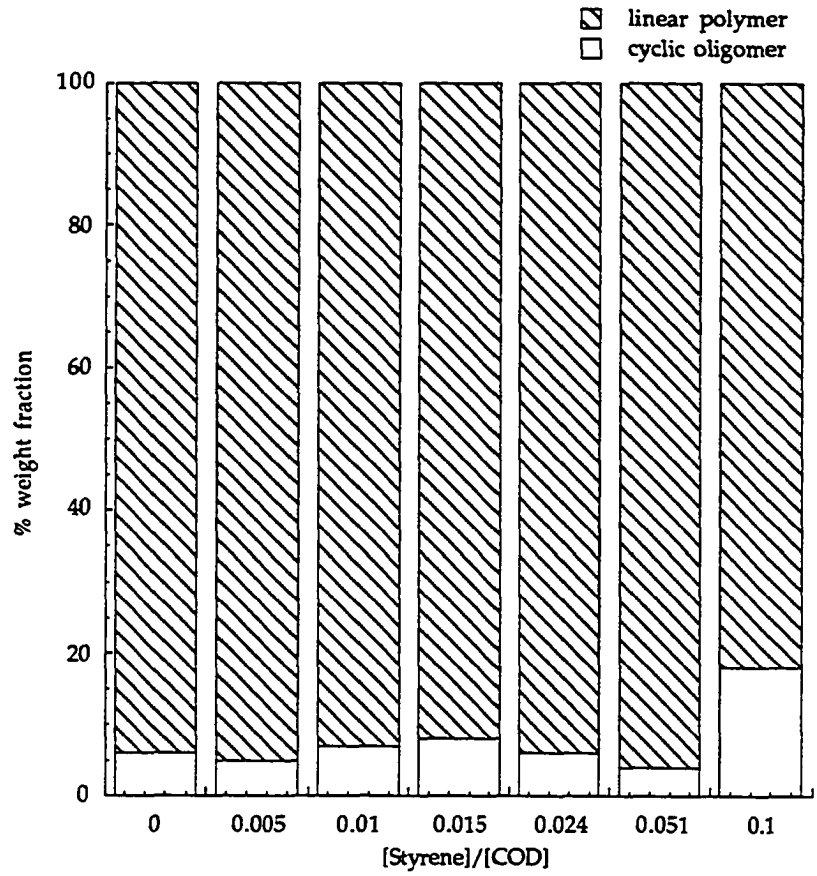


**Figure 27.** Weight fraction of linear polymer and cyclic oligomer with the ratio CTA / MON when the concentration of the chain transfer agent is varied. All the polymerizations have been done in neat monomer. The ratio MON/CAT is of 450.

Changing the ratio of the concentrations of monomer to chain transfer agent has little impact on the partition between cyclic and linear products, provided the monomer concentration is high enough (Figure 27). However, as stated above, changing this ratio affects directly the distribution of cyclic and linear products.

When very short chains are targeted, there seems to be an increase in the amount of cyclic products generated. This seemingly comes from the

competition between cyclization and monomer insertion in a linear chain: when little monomer is present, there is a strong trend to form cyclic products.

## 5. Regulation of the molecular weights: application to the synthesis of oligomers, and introduction to chapter 2.

### a. COD polymerization

The distribution of cyclic and linear products has now been established theoretically and experimentally. It has especially been found that, when the initial monomer concentration is large enough, the total amount of cyclic product does not vary. Under these conditions, the critical concentration $M_c$ is kept unchanged, and, according to equation 17, the molecular weight of the polymer varies linearly with the ratio MON/CTA. In addition, the totality of the monomer and chain transfer agents are consumed. Finally, in the case of COD, the yield of the polymerization is close to 90%. This set of conditions allow for optimal control on the molecular weight of the polymer by varying the ratio MON / CTA. For example, a Mayo plot for COD can be built, using styrene as a chain transfer agent (Figure 28). As expected, the molecular weight of the polymer is varying linearly with the ratio CAT/MON, and the slope of the graph is close to 1. A slope of 1 is to be expected for a *thermodynamically* driven polymerization in the absence of cyclic products. This value should be contrasted with the slope of the Mayo plot of a kinetically driven polymerization. In a kinetic regime, the slope is always less than 1, unless in the case of very fast transfer ($k_{tr} >> k_p$), for which a bimodal distribution is observed. Evidently, this polymerization has been made in very concentrated phase (using catalyst W1) to minimize the effects of cyclic

oligomers. We have also found that the PDI of the resulting polymers are close to 2 (typically 1.8), in agreement with a Flory type distribution.

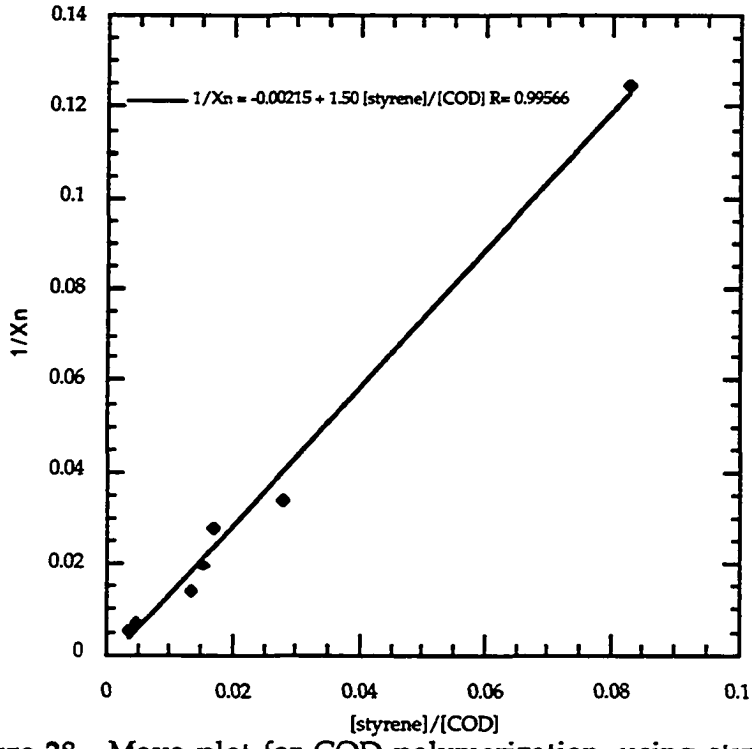


**Figure 28.** Mayo plot for COD polymerization, using styrene as a chain transfer agent. All polymerizations have been done neat, using catalyst W2. The ratio of CTA/ CAT is kept constant, equal to 41.

b. Polymerization of *sec*-butylcyclooctatetraene (sBCOT)

The polymerization of this monomer will be described in the next chapter. We have been interested in synthesizing short oligomers of polyacetylene, using the results established in this chapter. Polyacetylene oligomers effectively permit access to materials having non-linear optics properties. A simple calculation shows that if one desires to synthesize 10 g of polyacetylene oligomers in the absence of chain transfer agents (Figure 29), 60 g of catalyst W1 are necessary. Therefore, the chain transfer technique should be used.

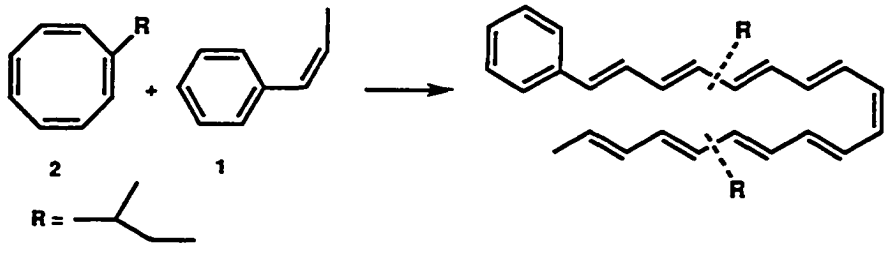


**Figure 29.** Synthesis of soluble polyacetylene oligomers

Very short sBCOT oligomers have been synthesized, using styrene and *cis*-β-methylstyrene as chain transfer agents (Figure 29). These oligomers have been analyzed by NMR and HPLC (Figure 30). There are a large number of difficulties associated with this polymerization. First, when only a small amount of catalyst is used (≈ 1%), the total conversion does not reach 15%. Arguably, catalysts W2 and W3 are poor polymerization catalysts of sBCOT, because of their mediocre initiation properties. Using larger catalyst amounts allows us to obtain these oligomers in higher yield (around 85%). Secondly, for unclear reasons, the yield in oligomers is depending on the ratio CTA / MON. When [s-BCOT]/[β-methylstyrene] = 1.1, the yield is only 11%, but this yield reaches 87% when the ratio of the concentrations is 2.5 . Finally, the oligomers are contaminated by the presence of *trans*-stilbene and *sec*-butylbenzene. *Trans*-stilbene is a product of the cross-metathesis of the chain transfer agent with itself, whereas *sec*-butylbenzene comes from the backbiting reaction of the propagating polyacetylene chain.

Despite these drawbacks, polyacetylene oligomers have been synthesized in good yield. Because of the large number of possibilities for the placement of the *sec*-butyl substituent, as well as the various cis/trans

addition, backbiting scrambles the end groups, making the micture even more complex. However, this experiment shows that the synthesis of polyacetylene oligomers is feasible. The amelioration of this process would imply finding a catalyst which is more adapted to the polymerization of sBCOT. In the next chapter, such catalysts will be studied.

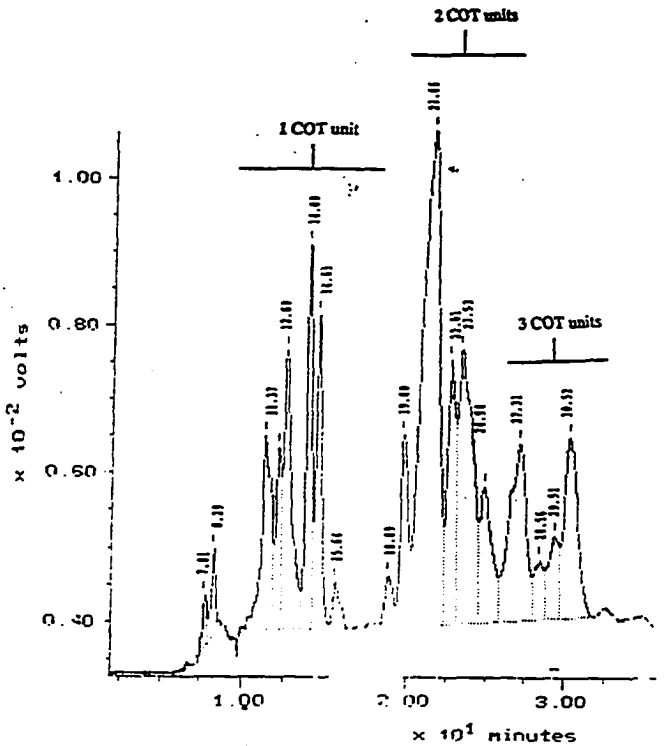


Figure 30. HPLC chromatogram of sBCOT oligomers, using styrene as chain transfer agent. [sBCOT] =5.4 mol/l, [sBCOT]/[styrene] = 1.9, [BCOT] / [W1] = 11.2. GPC analysis indicates a Mn of 190 (PDI of 1.9), relative to polystyrene standards.

## IV. Experimental Part

General methods are outlined in Chapter 2 of this thesis.

### Determination of kp/ki for catalyst 1

15.0 mg ($4.44\ 10^{-5}$ mol) of catalyst **1** are dissolved in 554.2 mg of benzene $d^6$. Norbornene (62.9 mg, 0.669 mmol) are dissolved in 584 mg of benzene $d^6$, giving a stock solution of 1.088 mol/l concentration. 100 ul of the stock solution are added to the catalyst solution, immediately stirred and rapidly monitored by NMR. 51% of the carbene **1** has been consumed. From these values, Gold equation gives a $k_p/k_i$ of 16.3.

### Determination of $k_{tr}$

11.4 mg of catalyst **2** ($2.34\ 10^{-5}$ mol, 1 eq) is added to 229 mg of benzene $d^6$ in a NMR tube. A stock solution of norbornene in benzene $d^6$ is prepared by adding 62.9 mg of norbornene in 584 mg of benzene $d^6$ (c = 1.088 mol/l). 295 mg of this solution are introduced in the NMR tube : $^1H$ NMR indicates that 85% of the carbene has been transformed in propagating carbene. Freshly distilled and dried styrene is introduced in a screw-cap vial, equipped with a Teflon liner cap. By the spectrometer, 2 ul of styrene are transferred to the NMR tube using a 1 ul syringe. The kinetics is monitored immediately after injection. The second order kinetics rate constant is extracted from plotting $( 1/ ( [sty]_o - [Mo]_o ) ) . \ln [ [Mo]_o / [sty]_o . ( [sty]_o - [Mo]_t) / ( [Mo]_o - [Mo]_t ) ]$ as a function of t.

### Determination of $k_p/k_i$ for catalyst 3

Catalyst 3 is prepared *in situ* by adding to a solution of 10.5 mg of **1** ($1.68\ 10^{-5}$ mol) in 255 mg of benzene $d^6$ and 200 ul of a 1.83 mol/l norbornene

solution in benzene $d^6$. To this solution 2.2 ul of styrene are added, and left for 6 hours at room temperature. $^1H$ NMR indicates that 78% of the molybdenum is under the form of **3**, 13 % under the form of **4** and 8% under **1**. Addition of norbornene (20 ul of the stock solution) shows that 81.2 % of **3** has initiated the polymerization. Using Gold equation, one finds $k_p/k_i$ = 1.5 .

**Polymerization with styrene as a chain transfer agent**

365 mg of norbornene are dissolved in 13.94g of toluene to form a stock solution of norbornene (0.241 mol/l)and 24.7 mg of catalyst **1** are dissolved in 466 mg of toluene to form a catalytic solution. 2 ml of monomer stock solution are added to 5 vials, labeled 1 to 5. 0 mg, 16.2 mg, 72.4 mg, 136.8 mg, and 10.8 mg of styrene are respectively added to vials 1 to 5. Under stirring, 50 ul of the catalytic solution are added, and the polymerization is left during 2 hours. Except for the vial which does not contain any styrene, the reaction mixture turns red rapidly. The polymers are purified by addition of methanol, and precipitation, followed by drying under vacuum. After weighing (y = 99%), the dried polymers are analyzed by GPC.

**Synthesis of the resin containing pending aldehyde groups**[56]

5 g of a Merrifield resin (purchased from Aldrich, 200-400 mesh, crosslinked at 5%) is dried *in vacuo* overnight at 110 °C. Under argon, 100 ml of dried DMSO are introduced. 10 g of $NaHCO_3$ (dried *in vacuo*) are suspended in 35 ml of DMSO, and the suspension is cannulated on the resin via a wide bore cannula. The reaction is heated at 160 °C for 12 hours, under an argon guard. After cooling the off-white powder is washed with DMSO,

hot water, acetone, then methanol. It is then dried under vacuum for a day. IR indicates a strong absorption band at 1697 $cm^{-1}$.

**Calibration of the GC**

Calibration of the GC has been made for cyclic and linear n-alkanes up to 16 carbons for cyclic compounds and up to 20 carbon atoms for linear compounds. Cyclic olefins of less than 15 carbons are commercial. Cyclohexadecane was synthesized as following:[62] 25 g ( 0.106 mol) of 8-cyclohexadecen-1-one (mixture of cis and trans, Aldrich) and 21 g (0.112 mol) of p-toluenesulfonhydrazide were placed in a 500 ml round bottom flask containing 200 ml of methanol. The flask is equipped of a reflux condenser and a bubbler. After 12 hours of reflux, the solution is cooled to ambient temperature, and transferred in a 1l round bottom flask. After cooling the solution to 10 °C, 25 g. (0.75 mol) of sodium borohydride is added by small portions, over a total time of 2 hours. The solution is then refluxed for 8 hours, and the solvent removed under reduced pressure. The residue is dissolved in ether, transferred to a separatory funnel, and successively washed with water, dilute hydrochloric acid and water. After drying over magnesium sulfate, and solvent removal, 22.2 g of a clear oil which crystallizes rapidly is obtained (yield 98%). The oil is further dried over calcium hydride and distilled under reduced pressure (200 mTorrs, 62 °C) to afford a white tacky solid Purity > 99 % as by GC. $^1H$ NMR in $CDCl_3$ 5.20 (m, 2, cis and trans olefinic H), 2.1 (m, 4, allylic H), 1.2 (m, 24). Freshly distilled cyclohexadecene (1g, 4.67 mmol) is dissolved in 50 ml of hexanes and ca 50 mg of Pd over activated carbon (Daegussa type, 5% metal content) is added to the solution. The mixture is capped by a septum, and purged with hydrogen. Then, during 8 hours, the mixture is vigorously stirred

under an atmosphere of hydrogen. The solid is then filtered away, the solvent evaporated, to leave 1g of a crystalline white solid (yield: 99%). $^{1}H$ NMR in $CDCl_3$: 1.308; $^{13}C$ NMR in $CDCl_3$: 26.6 ppm.

The calibration of the GC is effected relatively to p-xylene. For each standard, 5 points are taken corresponding to the ratio cycloalkane : *p*-xylene of 16:1, 4:1, 1:1, 1:4 and 1:16. The proportionality factor between the ratio of the areas of the GC peaks and the ratio of the concentrations is the response factor relative to *p*-xylene. Calibration settings: $T_{injection}$ = 300°C, $T_{FID}$ = 300 °C, $T_{init}$ = 50 °C for 1 minute, ramp at 30 °C/minute until 300 °C, with a 50 m capillary column SE-30 (Econosil, Alltech).

**Synthesis of cyclic oligomers**

A stock solution of COD in toluene (c = 0.0702 mol/l) is prepared, containing one equivalent of *p*-xylene. To 200 ul of this solution, 20 ul of a stock solution of catalyst **W1** (c = 0.02 mol/l) are added. The solution is stirred for 10 hours. To it, the crosslinked resin with pendant aldehyde groups (ca 20 mgs) is added, and the slurry is stirred for another 12 hours. The resin is filtered off, washed with toluene. An aliquot from the collected toluene fractions is analyzed by GC and GC-MS. Both indicate that mostly cyclic products is present. A few linear products can be detected, which likely originates from the decomposition of the propagating carbene. These linear products have 13 (3 unsaturations), 17 (4 unsaturations) and 21 (5 unsaturations) carbon atoms, as shown from GC-MS. The hydrogenation of the rest of the toluene solution is done by adding 5 mg of Pd over activated carbon (Daegussa type, 5% metal content), and stirring it over an atmosphere of hydrogen for 12 hours. The Pd is then filtered off, and the cycloalkanes are then analyzed by GC.

**Synthesis of sBCOT oligomers**

In a drybox, sBCOT (139.4 mg, 9.9 eq) and styrene (10.6 mg, 1) are stirred in a vial. 10.9 mg of catalyst W(=CH-*t*-Bu)(=N-2,6-*i*-$PrC_6H_3$)($OC(CH_3)(CF_3)_2$)$_2$ are added. In minutes a thick brown slurry is obtained, which solidifies rapidly. The mixture is washed with pentane, and dried under vacuo for a day in the dark. The mixture is analyzed by NMR, according to the method described by C. Gorman,[58] and by HPLC (1090 M, HP) equipped with a reverse phase column of 25 cm (C18) and a UV detector. The solvent is a mixture 90 : 5 : 5 acetonitrile : water : methylene chloride. After 30 minutes, water is gradually replaced by acetonitrile. Flow rate: 0.5 ml/min.[59]

## V. Appendix 1. Calculation of the molecular weight and PDI

The polymerization scheme corresponding to the polymerization of norbornene with catalyst **1**, using styrene as a chain transfer agent is:

$$V_0 + M \xrightarrow{k_o} W_1 \quad (30)$$

$$W_0 + M \xrightarrow{k_i} W_1 \quad (31)$$

$$W_n + M \xrightarrow{k_p} W_{n+1}\ ,\ n \geq 1 \quad (32)$$

$$W_n + P_0 \xrightarrow{k_{tr}} W_0 + P_n\ ,\quad n \geq 1 \quad (33)$$

The mass conservation laws are

$$MON = M + \sum_{n=0}^{\infty}(nW_n) + \sum_{n=0}^{\infty}(nP_n) \quad (34)$$

$$CAT = V_0 + \sum_{n=0}^{\infty}W_n \quad (35)$$

$$CTA = \sum_{n=0}^{\infty}P_n \quad (36)$$

The kinetic equations are

$$dM/dt = (k_p - k_i)\,M\,W_0 - (k_p\,CAT)\,M + (k_p - k_o)\,M\,V_0 \quad (37)$$

$$dV_0/dt = -k_o\,V_0\,M \quad (38)$$

$$dW_0/dt = (k_{tr}\,CAT)\,P_0 - k_i\,M\,W_0 - k_{tr}\,P_0\,(W_0 + V_0) \quad (39)$$

$$dP_0/dt = k_{tr}\,(W_0 + V_0)\,P_0 - (k_{tr}\,CAT)\,P_0 \quad (40)$$

$$dA/dt = -k_{tr}\,P_0\,A + (k_p\,CAT)\,M + (k_i - k_p)\,M\,W_0 + (k_o - k_p)\,MV_0 \quad (41)$$

$$dD/dt = k_{tr} P_0 A \quad (42)$$

$$dB/dt = -k_{tr} P_0 B + k_p M (CAT + 2A - W_0 - V_0) + (k_i W_0 + k_o V_0) M \quad (43)$$

$$dF/dt = k_{tr} P_0 B \quad (44)$$

with the notations:

$$A = \sum_{n=1}^{\infty}(nW_n) ,$$

$$B = \sum_{n=1}^{\infty}(n^2W_n) ,$$

$$D = \sum_{n=1}^{\infty}(nP_n)$$

$$F = \sum_{n=1}^{\infty}(n^2P_n) \quad (45)$$

The average degree of polymerization for living and dead chains are given by

$$\bar{X}_{ndead} = D/(CTA - P_0) \qquad \bar{X}_{nliving} = A/(CAT - W_0 - V_0) \quad (46)$$

and the PDI by

$$PDI_{dead} = [F (CTA - P_0)]/D^2$$

$$PDI_{living} = [B (CAT - W_0 - V_0)]/A^2 \quad (47)$$

The computer solves numerically the 8 differential equations 37 to 44, for a given set of concentrations (MON, CAT. CTA) and for a given set of rate constants ($k_i$, $k_p$, $k_{tr}$, $k_o$). The result is 8 interpolating functions, which are used to calculate $X_n$, PDI and any other desired quantity at any desired time.

## VI. Appendix 2. Calculation of the cyclics distribution for COD polymerization

This appendix describes how to calculate the distribution of cyclic and linear products in a thermodynamically controlled polymerization.

The first step consists in calculating the entropy of cyclization, given in equation 26. The only unknown parameter is the end to end distance $\langle r_x^2 \rangle$, which is given by:

$$\langle r_x^2 \rangle = C_x l_o x \qquad (48)$$

x is the degree of polymerization of the chain under consideration, $l_o$ is the length of a chain of one unit long, and $C_x$ is the characteristic ratio, calculated by RIS. The calculations of $\langle r_x^2 \rangle$ by R.I.S. have been effected by Zhong-Ren Chen using the Polymer software developed by Biosyn Tech., run on a Silicon Graphics computer (IRIS-4D1-4.0.5).

For COD polymerization, the RIS parameters are described in the data bank of the Polymer software (Biosyn). In all the rest of this appendix, a COD polymer which has a degree of polymerization of 1, 2, 3, ... contains 4, 8, 12 carbon atoms. Table 7 lists the characteristic ratio of the all cis and all trans polymer, as obtained by RIS.

The length $l_o$ of one monomer unit for COD (equation 48) is 2.969 Å. This allows to calculate the term $l_x = \langle r_x^2 \rangle^{1/2}$ for every different degree of polymerization. $l_x$ is the average end to end distance of a polymer of x unit long (Table 9). This average distance can also be calculated by direct minimization of the x-mer in molecular mechanics. This average distance is given in the third column of Table 9. Using equation 26, it is possible to calculate the entropy of cyclization of the x-mer. The entropy given in

equation 26 is a physical entropy in S.I. units. Chemists relate their entropy to a standard state, which corresponds to 1 mol/l in solution. Therefore the entropy listed in Table 9 is

$$\Delta S_{chemical} = -R \ln 10^3 + \Delta S_{physical} \qquad (49)$$

**Table 8.** Characteristic ratios of COD polymer, in a theta solvent at 298 K.

| X | $C_n$ (cis) | $C_n$ (trans) |
|---|---|---|
| 1 | 1.8857 | |
| 2 | 2.3186 | 3.6817 |
| 3 | 2.7097 | 4.2402 |
| 4 | 3.0141 | 4.5860 |
| 5 | 3.2458 | 4.8142 |
| 6 | 3.4231 | 4.9736 |
| 7 | 3.5607 | 5.0903 |
| 8 | 3.6693 | 5.1791 |
| 9 | 3.7566 | 5.2488 |
| 10 | 3.8278 | 5.3050 |
| 11 | 3.8868 | 5.3513 |
| 12 | 3.9300 | 5.3900 |
| 13 | 3.9786 | 5.4228 |
| 14 | 4.0149 | 5.4511 |
| 15 | 4.0464 | 5.4756 |
| 16 | 4.0740 | 5.4972 |
| 17 | 4.0985 | 5.5162 |
| 18 | 4.1202 | 5.5332 |
| 19 | 4.1397 | 5.5484 |
| 20 | 4.1573 | 5.5621 |
| 21 | 4.1731 | 5.5745 |
| 22 | 4.1876 | 5.5858 |
| 23 | 4.2008 | 5.5961 |
| 24 | 4.2129 | 5.6055 |
| 25 | 4.2241 | 5.6143 |
| 26 | 4.2343 | 5.6223 |
| 27 | 4.2438 | 5.6298 |
| 28 | 4.2527 | 5.6367 |
| 29 | 4.2610 | 5.6432 |

**Table 9.** End-to-end length and cyclization entropy

| $X_n$ | $l_x^1$ (Å) | | $l_x^2$ (Å) | | $\Delta S_x^1$ (J / K /mol) | | $\Delta S_x^2$ (J/K/mol) | |
|---|---|---|---|---|---|---|---|---|
| | cis | trans | cis | trans | cis | trans | cis | trans |
| 1 | 4.0782 | | | | 11.682 | | | |
| 2 | 6.3953 | 8.0589 | 7.5750 | 7.4142 | -5.3154 | -11.086 | -8.0294 | -9.0045 |
| 3 | 8.4675 | 10.592 | 9.9050 | 10.105 | -15.694 | -21.282 | -18.097 | -20.106 |
| 4 | 10.312 | 12.720 | 11.861 | 12.330 | -23.006 | -28.244 | -24.988 | -27.467 |
| 5 | 11.964 | 14.571 | 13.561 | 14.244 | -28.572 | -33.492 | -30.188 | -32.926 |
| 6 | 13.459 | 16.224 | 15.078 | 15.941 | -33.028 | -37.691 | -34.352 | -37.252 |
| 7 | 14.827 | 17.728 | 16.458 | | -36.726 | -41.186 | -37.821 | |
| 8 | 16.091 | 19.116 | 17.732 | 18.888 | -39.878 | -44.180 | -40.794 | -43.879 |
| 9 | 17.268 | 20.412 | 18.921 | 20.202 | -42.622 | -46.796 | -43.392 | -46.538 |
| 10 | 18.374 | 21.631 | 20.039 | 21.436 | -45.048 | -49.121 | -45.702 | -48.895 |
| 11 | 19.419 | 22.786 | | | -47.221 | -51.212 | | |
| 12 | 20.395 | 23.885 | | | -49.169 | -53.112 | | |
| 13 | 21.359 | 24.935 | | | -50.987 | -54.852 | | |
| 14 | 22.266 | 25.944 | | | -52.642 | -56.459 | | |
| 15 | 23.137 | 26.915 | | | -54.175 | -57.950 | | |
| 16 | 23.978 | 27.853 | | | -55.602 | -59.341 | | |
| 17 | 24.790 | 28.759 | | | -56.938 | -60.645 | | |
| 18 | 25.576 | 29.639 | | | -58.193 | -61.873 | | |
| 19 | 26.339 | 30.493 | | | -59.376 | -63.032 | | |
| 20 | 27.080 | 31.323 | | | -60.496 | -64.129 | | |
| 21 | 27.802 | 32.133 | | | -61.558 | -65.172 | | |
| 22 | 28.505 | 32.922 | | | -62.569 | -66.165 | | |
| 23 | 29.192 | 33.693 | | | -63.533 | -67.112 | | |
| 24 | 29.863 | 34.447 | | | -64.454 | -68.018 | | |
| 25 | 30.519 | 35.185 | | | -65.336 | -68.887 | | |
| 26 | 31.161 | 35.907 | | | -66.182 | -69.720 | | |
| 27 | 31.790 | 36.615 | | | -66.995 | -70.522 | | |
| 28 | 32.408 | 37.310 | | | -67.777 | -71.294 | | |
| 29 | 33.0130 | 37.992 | | | -68.532 | -72.038 | | |

1. Calculated using the values of Table 8
2. Calculated using the values of the most stable conformation found in molecular mechanics

The enthalpy of cyclization (or strain energy) are obtained for cycles of less than 32 carbon atoms. Above this limit, the cycles are supposed to be strainless. The energy calculations have been effected by a dynamic Monte Carlo search, using MM3 molecular field. The results are listed in Table 10.

**Table 10.** Steric energy, enthalpy, free energy and cyclization constant at 300 K, for COD polymerization. Each entry corresponds to the most stable arrangement of cis and trans double bonds. For exemple, monomer, dimer and trimer are *cis*-cyclobutene, *cis,cis*-cyclooctadiene, and *trans,trans,trans*-cyclododecatriene.

| $X_n$ | $SE_n$ (kJ/mol) | $\Delta H$ (kJ/mol) | $\Delta G$ (kJ/mol) | $K_x$ (mol/l) |
|---|---|---|---|---|
| 1 | 130 | 100.28 | 96.798 | $1.1078\ 10^{-17}$ |
| 2 | 83 | 32.98 | 34.565 | $8.8215\ 10^{-07}$ |
| 3 | 76.76 | 6.44 | 12.784 | 0.0057634 |
| 4 | 95.08 | 4.46 | 12.880 | 0.0055459 |
| 5 | 114.4 | 3.48 | 13.464 | 0.0043813 |
| 6 | 131.4 | 0.18 | 11.416 | 0.010009 |
| 7 | 152.24 | 0 | 12.278 | 0.0070700 |
| 8 | 171.91 | 0 | 13.170 | 0.0049327 |
| 9 | 190.27 | 0 | 13.950 | 0.0036015 |
| 10 | 216.2 | 0 | 14.643 | 0.0027232 |
| 11 | | 0 | 15.266 | 0.0021178 |
| 12 | | 0 | 15.833 | 0.0016853 |
| 13 | | 0 | 16.351 | 0.0013672 |
| 14 | | 0 | 16.830 | 0.0011270 |
| 15 | | 0 | 17.275 | 0.00094202 |
| 16 | | 0 | 17.690 | 0.00079680 |
| 17 | | 0 | 18.078 | 0.00068130 |
| 18 | | 0 | 18.444 | 0.00058778 |
| 19 | | 0 | 18.790 | 0.00051133 |
| 20 | | 0 | 19.117 | 0.00044814 |
| 21 | | 0 | 19.428 | 0.00039533 |
| 22 | | 0 | 19.724 | 0.00035084 |
| 23 | | 0 | 20.006 | 0.00031308 |
| 24 | | 0 | 20.276 | 0.00028077 |
| 25 | | 0 | 20.535 | 0.00025291 |
| 26 | | 0 | 20.784 | 0.00022881 |
| 27 | | 0 | 21.023 | 0.00020778 |
| 28 | | 0 | 21.253 | 0.00018936 |
| 29 | | 0 | 21.475 | 0.00017316 |

The only missing parameter is now p, the degree of polymerization for linear chains. It can be noticed that equation 18 is an intrinsic equation in p, which can be solved numerically. For example, the experimental conditions of polymerization in Figure 21 are [CAT] = 0.0052 mol/l, and

[MON] / [CAT] = 13.5. Using these parameters, the Mathematica input for obtaining p is:

```
In[22] := FindRoot[ (13.5 - p) * 0.0052 * 1000 == 2 * 0.000882 * (p/(1+p))^2 + 3
* 5.7632 * (p/(1+p))^3  +4 * 5.5459 * (p/(1+p))^4+5 * 4.3813 * (p/(1+p))^5 + 6
* 10.009 * (p/(1+p))^6 + 7 * 7.0070 *(p/(1+p))^7 + 8 * 4.90003*(p/(1+p))^8 +9
* 3.6015 * (p/(1+p))^9  + 10 * 2.7232 *(p/(1+p))^10 + 11 * 2.1178*
(p/(1+p))^11 + 12 * 1.6853 *(p/(1+p))^12+ 13 * 1.3672 * (p/(1+p))^13 + 14 *
1.1270 *(p/(1+p))^14+ 15 * 0.94202 * (p/(1+p))^15 + 16 * 0.7968 *
(p/(1+p))^16 + 17 * 0.6813 * (p/(1+p))^17 + 18 * 0.5877* (p/(1+p))^18 + 19 *
0.51133 * (p/(1+p))^19 + 20 * 0.4481 * (p/(1+p))^20 + 21 * 0.3953 *
(p/(1+p))^21, {p,0.01}]
```

The answer is p = 3.24.

It is now possible to obtain the distribution of cyclic and linear products, using equation 23 and 24. The results for the conditions described in Figure 21 are given in Table 11.

**Table 11.** Cyclic and linear polymer distibution, when [COD] = 0.07 mol/l and [CAT] = 0.0052 mol/l at 298 K in toluene. The distribution has been calculated, using p = 3.34.

| x | $C_x$ | $P_x$ |
|---|---|---|
| 1.0000 | 8.0769e-18 | 0.00093721 |
| 2.0000 | 5.0652e-07 | 0.00071616 |
| 3.0000 | 0.0025556 | 0.00054724 |
| 4.0000 | 0.0018790 | 0.00041816 |
| 5.0000 | 0.0011340 | 0.00031953 |
| 6.0000 | 0.0019815 | 0.00024417 |
| 7.0000 | 0.0010691 | 0.00018658 |
| 8.0000 | 0.00056972 | 0.00014257 |
| 9.0000 | 0.00031774 | 0.00010894 |
| 10.000 | 0.00018352 | 8.3246e-05 |
| 11.000 | 0.00010903 | 6.3611e-05 |
| 12.000 | 6.6279e-05 | 4.8607e-05 |
| 13.000 | 4.1075e-05 | 3.7142e-05 |
| 14.000 | 2.5867e-05 | 2.8382e-05 |
| 15.000 | 1.6518e-05 | 2.1688e-05 |
| 16.000 | 1.0674e-05 | 1.6572e-05 |
| 17.000 | 6.9728e-06 | 1.2663e-05 |
| 18.000 | 4.5960e-06 | 9.6765e-06 |
| 19.000 | 3.0546e-06 | 7.3941e-06 |
| 20.000 | 2.0454e-06 | 5.6501e-06 |
| 21.000 | 1.3785e-06 | 4.3174e-06 |
| 22.000 | 9.3470e-07 | 3.2991e-06 |
| 23.000 | 6.3728e-07 | 2.5210e-06 |
| 24.000 | 4.3665e-07 | 1.9263e-06 |
| 25.000 | 3.0052e-07 | 1.4720e-06 |
| 26.000 | 2.0773e-07 | 1.1248e-06 |
| 27.000 | 1.4412e-07 | 8.5949e-07 |
| 28.000 | 1.0036e-07 | 6.5677e-07 |
| 29.000 | 7.0117e-08 | 5.0186e-07 |

## VII. References

(1) Ivin, K. J. *Olefin Metathesis*; Academic: London, **1983**.

(2) Gilliom, L. R., Ph. D. Thesis, California Institute of Technology, 1986.

(3) (a) Bazan, G.C.; Khosravi, E.; Schrock, R.R.; Feast, W.J.; Gibson, V.C.; Regan, M.B., Thomas, J.K.; Davis, W.M. *J. Am. Chem.Soc.* **1990**, *112*, 8378. (b) Bazan, G.C.; Oskam, J.H.; Cho, H.N.; Park, L.Y.; Schrock, R.R.; *J. Am. Chem. Soc.* **1991**, *113*, 6899. (c) Crowe, W.E.; Michell, J.P.; Gibson, V.C.; Schrock, R.R. *Macromolecules* **1990**, *23*, 3534. (d) Bazan, G.C.; Schrock, R.R.; Cho, H.N.; Gibson, V.C. *Macromolecules* **1991**, *24*, 4495. (e) Mitchell, J.P.; Gibson, V.C.; Schrock, R.R. *Macromolecules* **1991**, *24*, 1220. (f) Schrock, R.R. *Acc. Chem. Res.* **1990**, *23*, 158. (g) Schrock, R.R.; DePue, R.T.; Feldman, J.; Yap, K.B.; Yang, D.C.; Davis, W.M.; Park, L.Y.; DiMare, M.; Schofield, M.; Anhaus, J.; Walborsky, E.; Evitt, E.; Kruger, C.; Betz, P. *Organometallics* **1990**, *9*, 2262.

(4) Wu, Z.; Wheeler, D. R.; Grubbs, R. H. *J. Am. Chem. Soc.* **1992**, *114*, 146-151.

(5) Nguyen, S. T.; Johnson, L. K.; Grubbs, R. H.; Ziller, J. W. *J. Am. Chem. Soc.* **1992**, *114*, 3974.

(6) These polymerizations are the work of B. Maughon, S. Kanaoka and D. Lynn. See also, Wu, Z.; Grubbs, R. H. *Macromolecules* **1995**, 10, 3502.

(7) Wu, Z.; Benedicto, A. D.; Grubbs, R. H. *Macromolecules* **1993**, *26*, 4975.

(8) Odian, G. *Principles of Polymerization*; John Wiley and Sons: New York, 1981; p 20.

(9) Flory, P. J. *Principles of Polymer Chemistry*; Cornell University Press, Ithaca, **1953**.

(10) Gold, L. *J. Chem. Phys.* **1958**, *28*, 91.

(11) Benedicto, A., Thesis, California Institute of Technology, 1994.

(12) Inoue, S.; Saegusa, T. in *Recent Advances in Mechanistic and Synthetic Aspects of Polymerization;* Guyot, A.; Fontanille, M. Eds.; **1987;** NATO ASI.

(13) Benedicto, A. D.; Claverie, J. P.; Grubbs, R. H. *Macromolecules* **1995,** *28(2),* 500-511.

(14) Heroguez, V.; Fontanille, M. *J. P. Sci. Part A* **1994,** *32,* 1755-1760.

(15) Schrock, R. R.; Murdzek, J. S.; Bazan, G. C.; Robbins, J.; Di-Mare, M.; O'Regan, M. *J. Am. Chem. Soc.* **1990,** *112,* 3875.

(16) (a) A. Benedicto is gratefully ackowledged for providing this table. (b) GPC has been calibrated before each set of experiment, see for example Schrock, R. R.; Feldman, J.; Cannizzo, L. F.; Grubbs, R. H. *Macromolecules* **1987,** *20,* 1169-1172. Calibration is time dependent, therefore correction factor may vary with time.

(17) (a) Flory, P.J. *Principles of Polymer Chemistry* ; Cornell University Press: New York, **1953.** (b) Gregg, R.A.; Mayo, F.R. *J. Am. Chem. Soc.***1948,** *70,* 2373. (c) Mayo, F.R. *J. Am. Chem. Soc.* **1943,** *65,* 2324.

(18) McKenna, J. M.; Wu, T. K.; Pruckmayr, G. *Macromolecules* **1977,** *10,* 877.

(19) Geiser, D.; Hocker, H. *Polym. Bull.* **1980,** *2,* 591.

(20) Geiser, D.; Hocker, H. *Macromolecules* **1980,** *13,* 653.

(21) Andrews, J. M., Ph.D. Thesis, University of New York, 1972.

(22) Jacobson, H.; Beckmann, C. O.; Stockmayer, W. H. *J. Chem. Phys.* **1950,** *18(12),* 1607-1612.

(23) Jacobson, H.; Stockmayer, W. H. *J. Chem. Phys.* **1950,** *18(12),* 1600-1606.

(24) Flory, J. P.; Jernigan, R. L. *J. Chem. Phys* **1965,** *42,* 3509.

(25) Flory, P. J.; Williams, A. D. *J. Polym. Sci., A2* **1967,** *5,* 399.

(26) Flory, P. J. *Macromolecules* **1974,** *7(3),* 381.

(27) Semlyen, J. A. *Cyclic Polymers*; Elsevier Applied Science Publishers: London and New York, **1986**.

(28) Clark, T. A. *A Handbook of Computational Chemistry*; Wiley: New York, **1985**.

(29) Scott, K. W.; Calderon, N.; Offstead, E. A.; Judy, W. A.; Ward, J. P. *Rubber Chem. Technol.* **1971**, *44*, 1341.

(30) Scott, K. W.; Calderon, N.; Offstead, E. A.; Judy, W. A.; Ward, J. P. *Am. Chem. Soc., Adv. Chem. Ser.* **1969**, *91*, 399.

(31) Gennes, P. G. d. *Scaling Concepts in Polymer Physics*; Cornell University, **1979**..

(32) Gennes, P. G. d. *C.R. Acad. Sci. Paris* **1990**, *310, II*, 1327.

(33) Ofstead, E. A.; Calderon, N. *Makromol. Chem.* **1972**, *154*, 21.

(34) Thorn-Csanyi, E.; Hammer, J.; Pflug, K. P.; Zilles, J. U. *Abstracts, MakroAkron 94, 35th IUPAC International Symposium on Macromolecules* **1994**, , 241.

(35) Hummel, K. *J.Mol.Sci.-Pure Appl. Chem.* **1993**, *A30*, 621.

(36) Fu, G. C.; Grubbs, R. H. *J. Am. Chem. Soc.* **1992**, *114*, 7324.

(37) Fu, G. C.; Nguyen, S. T.; Grubbs, R. H. *J. Am. Chem. Soc.* **1993**, *115*, 756.

(38) Kim, S. H.; Bowden, N.; Grubbs, R. H. *J. Am. Chem. Soc.* **1995**, 117, 2355.

(39) Fujimura, O.; Fu, G. C.; Grubbs, R. H. *J. Am. Chem. Soc.* **1995**, 117, 2108.

(40) Borer, B. C.; Deereenberg, S.; Bieraugel, H.; Pandit, U. K. *Tet. Lett.* **1994**, *35(19)*, 3191-3194.

(41) (a) Heroguez, V.; Soum, A.; Fontanille, M. *Polymer* **1992**, 33, 3302. (b) Cramail, H.; Fontanille, M.; Soum, A. *J. Mol. Catal.* **1991**, 65, 193 (a) Hillmyer, M.A.; Grubbs, R.H. *Macromolecules* **1993**, 26,872. (c) Hillmyer, M. H. Philosphy Doctorate, California Institute of Technology, **1994**.

(42) Chen, Z. R.; Claverie, J. P.; Grubbs, R. H.; Kornfield, J. A. *Macromolecules* **1995**, *28*, 2147.

(43) McQuarrie, D. A. *Statistical Mechanics*; Harper & Row: New York, **1976**.

(44) Thanks to Zhong-Ren Chen for providing this Figure.

(45) Reif, L.; Hocker, H. *Macromolecules* **1984**, *17*, 952.

(46) Hocker, L. *J. Mol. Catal.* **1980**, *8*, 202.

(47) Chauvin, y.; Commereuc, D.; Zaborowski, G. *Makromol. Chem.* **1978**, *179*, 1285-1290.

(48) Sato, H.; Tanaka, Y.; Taketomi, T. *Makromol. Chem.* **1977**, *178*, 1993-1999.

(49) Cherednichenko, V. M. *Polym. Sci. USSR* **1979**, *20*, 1225-1233.

(50) Lebedev, B. V.; Limiagov, B. I. *Vic. Soedin.* **1977**, , 824.

(51) Witte, J.; Hoffmann, M. *Makromol. Chem.* **1977**, *179*, 641-659.

(52) Ivin, K. J. *Makromol. Chem., Macromol. Symp.* **1991**, ,

(53) Hillmyer, M. A.; Grubbs, R. H., *Abs. Pap. ACS* **1993**, 206, 51.

(54) Hillmyer, M. A.; Grubbs, R. H. *Macromolecules* **1993**, *26(4)*, 872-874.

(55) Hillmyer, M. H.; Laredo, W.; Grubbs, R. H. *Manuscript in preparation* **1994**.

(56) Frechet, J. M. *Macromolecules* **1975**, *8*, 130.

(57) Miller, S. J.; Kim, S. H.; Chen, Z. R.; Grubbs, R. H. *J. Am. Chem. Soc.* **1995**, *117(7)*, 2108.

(58) Gorman, C. B.; Ginsburg, E. J.; Grubbs, R. H. *J. Am. Chem. Soc.* **1993**, *115(4)*, 1397-1409.

(59) Knoll, K.; Schrock, R. R. *J. Am. Chem. Soc.* **1989**, 11, 7989.

# CHAPTER 2

# SYNTHESIS, CHARACTERIZATION AND CATALYTIC PROPERTIES OF TUNGSTEN VINYL ALKYLIDENES

## I. Introduction

The metathesis reaction is catalyzed by numerous homogeneous or heterogeneous complexes, which are often tungsten-, molybdenum-, rhenium- or ruthenium-based. Representative examples can be found in the class of binary and ternary systems such as $Mo(NO)_2L_2Cl_2/RAlCl_2$, $WCl_6/EtOH/EtAlCl_2$, $WOCl_4/EtAlCl_2$, and $Re_2O_7/Al_2O_3$.[1] The most active ROMP catalysts have a tungsten (or molybdenum) core, surrounded by various ligands. In counterpart to their high activity, W based catalysts feature little tolerance for highly functionalized molecules. ROMP by tungsten and related molybdenum catalysts has been instrumental in the development of interesting polymers such as polynorbornene,[2-7] polycyclooctenes,[8,9] and polyacetylenes[10-13]. Since it has been shown that nucleophilic carbenes play a central role in the metathesis reaction,[14] the synthesis of tungsten carbenes has been the object of a flurry of activity. In what follows, a short overview of well-defined tungsten carbenes is presented.

The first examples of well-defined tungsten catalysts having a metathesis activity belong to the class of Fisher carbenes. These catalysts are active for alkyne polymerization, as well as for the polymerization of very strained cyclic olefins such as norbornene, but they do not catalyze the metathesis of low-strain olefins. Typical examples of these catalysts are the carbenes:

$(CO)_5W=C(Ph)(OMe)$,[15]

$(CO)_4W=C(OMe)[(CH_2)_3CH=CH_2]$,[16]

$(CO)_4W=C(Ph)[NHCH_2C(Me)_2CH=CH_2]$,[17]

and the carbyne $Br(CO)_4WCPh$ [18,19]

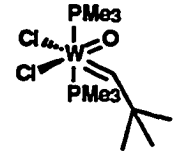

1

R. R. Schrock

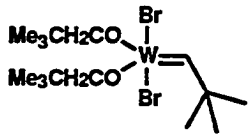

2

J. A. Osborn

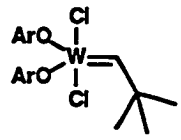

3

J. M. Basset

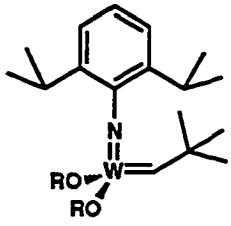

4

R. R. Schrock

M = W or Mo

R = $C(CH_3)_x(CF_3)_{3-x}$ x = 0, 1, 2

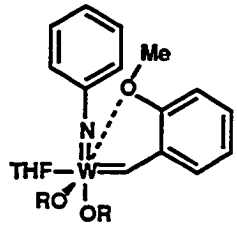

5

R. H. Grubbs

R = $C(CH_3)_x(CF_3)_{3-x}$ x = 0, 1, 2

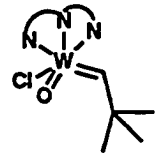

6

J. M. Boncella

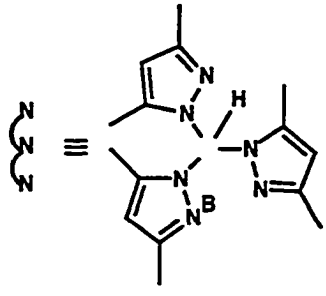

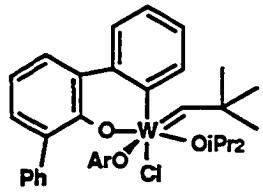

7

J. M. Basset

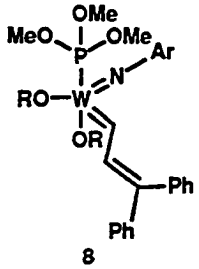

8

R. H. Grubbs

R = $C(CH_3)(CF_3)_2$

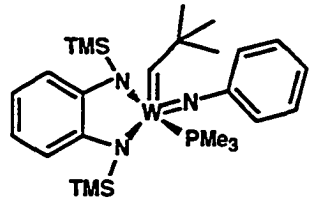

9

J. M. Boncella

Figure 1. Well-definednucleophilic tungsten carbenes

The first nucleophilic tungsten carbene (**1**) was reported by Schrock (Figure 1).[20] Successively, compounds **2** to **4** were described.[21-23] Catalyst **1** and **2** require the presence of a Lewis acid cocatalyst, whereas catalysts **3** and **4** are intrinsically active. It has been reported that the activity of **4** can be tuned by changing the basicity of the ancillary alkoxide ligand. This feature is advantageous because the alkoxide ligand is introduced at the last step of the synthesis (Figure 2). The key step for the synthesis of the carbenes **1** to **4** is a proton transfer reaction. This transfer can be effected by addition of an acidic proton to a carbyne,[24] or, more typically, by α-abstraction from a tungsten alkyl. α-Abstraction has also been used to synthesize catalysts **6** (which is air stable, and shows little activity),[25] **9** (little activity)[26] and **7**.[27-29] Catalyst **7** is obtained by intramolecular elimination, followed by orthometallation and has been reported to be the most active for the metathesis of 2-pentene.[30]

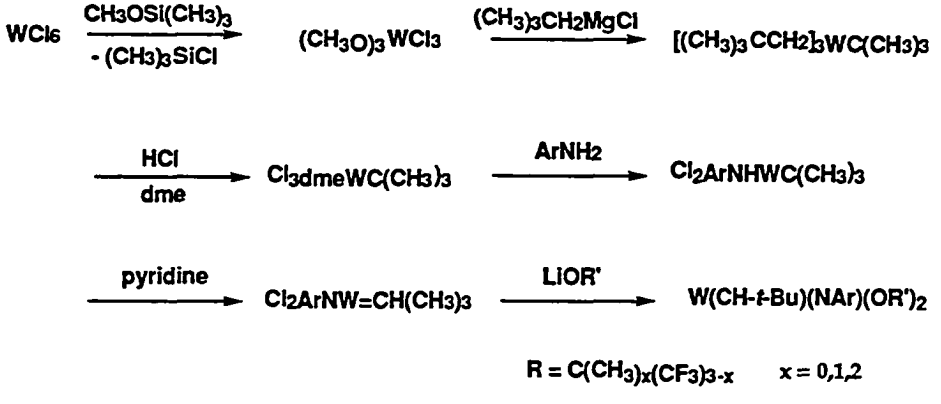


**Figure 2.** Synthesis of catalyst **4**

There are only two instances where reactions other than proton transfer have been used in the elaboration of tungsten carbenes. Catalyst **5** was synthesized via an ylide transfer by L. Johnson (see below).[31] Catalyst **8**

was also synthesized by L. Johnson,[32] using the ring-opening of diphenylcyclopropene, a method first established by Binger.[33] In this chapter, we will describe the catalytic properties of these two new classes of carbenes.

The impetus for this study finds its basis in the shortcomings characteristic of carbenes generated by proton transfer. Because an α-abstraction reaction is usually triggered by the bulkiness of the ligand environment, and by the absence of β protons, only very bulky alkylidenes (such as neopentylidenes) are obtained by this route. Consequently, althought these carbenes are usually very active catalysts, poor initiation of the polymerization by the bulky carbene is typical. Fast initiation relative to propagation has been achieved for the polymerization of strained olefins such as norbornene by slowing the propagation step.[2, 34, 35] This strategy has allowed the synthesis of *living* polymers with very low dispersities (PDI < 1.1) when using midly electrophilic catalysts such as $M(CH\text{-}t\text{-}Bu)(NAr)(OR)_2$ ( M = W or Mo, Ar = 2,6-$C_6H_3$-*i*-$Pr_2$, R = $C(CH_3)_3$ ). A similar result has also been obtained by adding a strong Lewis base, such as trimethyl phosphine, to the catalyst, and this method has been successful for the controlled polymerization of cyclobutenes.[36]

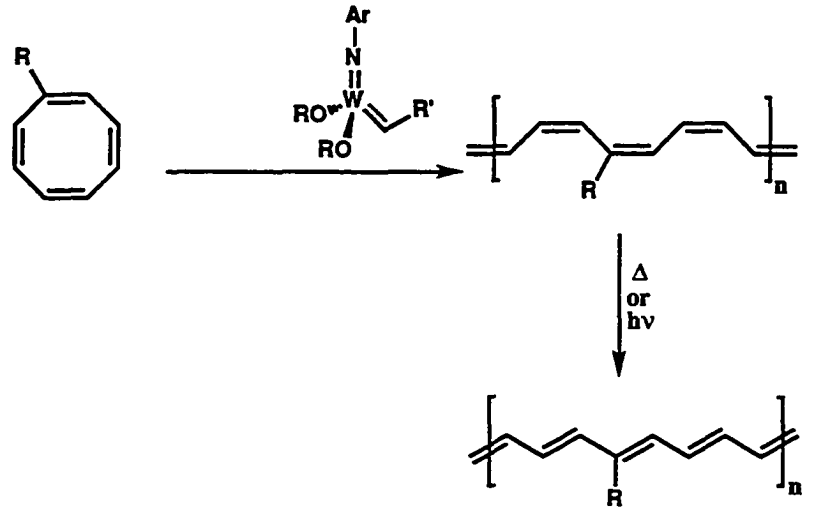


Figure 3. Synthesis of polyacetylene by ROMP. The polymer contains a high amount of cis double bonds which are isomerized under heat or light to trans double bonds. Catalyst **4** : Ar = 2,6-$C_6H_3$-*i*-$Pr_2$, R = $C(CF_3)_2(CH_3)$, R' = $C(CH_3)_3$. Catalyst **5** : Ar = 2,6-$C_6H_3$-*i*-$Pr_2$, R = $C(CF_3)_2(CH_3)$, R' = $C_6H_4$-*o*-OMe.

In contrast, living polymerization of low strain olefins presents a tougher challenge, because tuned down catalysts are not active enough to polymerize them. Finding a living catalyst for the ROMP of low strain olefins is of interest, in particular because the ROMP of cyclooctatetraene (COT) allows the synthesis of polyacetylene, an insoluble conducting polymer.[37-40] Several monosubstituted COTs have been polymerized by ROMP, using well-defined catalysts **4** and **5**, and this has permitted the synthesis of soluble polyacetylenes (Figure 3). It has been established[13] that those substituted COTs having secondary or tertiary alkyl substituents such as *sec*-butylCOT (sBCOT) give polymers which are soluble in the predominantly *cis* as well as the *trans* form, whereas less substituted COTs lead to polymers which are soluble in the predominantly *cis* form only. The soluble polyacetylenes obtained by this methodology demonstrate excellent

physical and chemical properties (high purity, high conductivity after doping) and show promising applications in the fabrication of microelectronic devices.[41] To this point, however, no control of the molecular weight distribution has been attained for this kind of polymerization. The molecular weight distribution in a typical polymerization of a highly conjugated substituted COTs is broad: the polydispersity index (PDI), as measured by size exclusion chromatography (SEC), has been reported to be typically of the order of 2 to 10. In addition, the ratio of monomer to catalyst has little or no influence on the molecular weight of the resulting polymer. As stated above, among the factors contributing to the lack of control in the polymerization are the poor initiation properties shown by **4** and **5**. For example, when the polymerization is monitored by NMR spectroscopy, no propagating carbene can be detected, indicating that the ratio of the rate of initiation to the rate of propagation is small (typically less than 0.1%). Additionally, the reaction is plagued by a backbiting reaction (Figure 4) which leads to the thermodynamically favorable production of an aromatic. To avoid this side reaction, the polymerization is usually run neat, so that secondary metathesis with the growing polymer chain becomes less favorable than monomer insertion. Running the polymerization neat is done at the expense of the control of the molecular weight distribution because of viscosity and diffusion problems.

To summarize, ROMP allows the synthesis of a variety of interesting polymers, such as polyacetylene, nevertheless, catalysts used to date are far from ideal. In this chapter new catalysts are described, and their properties in ROMP examined.

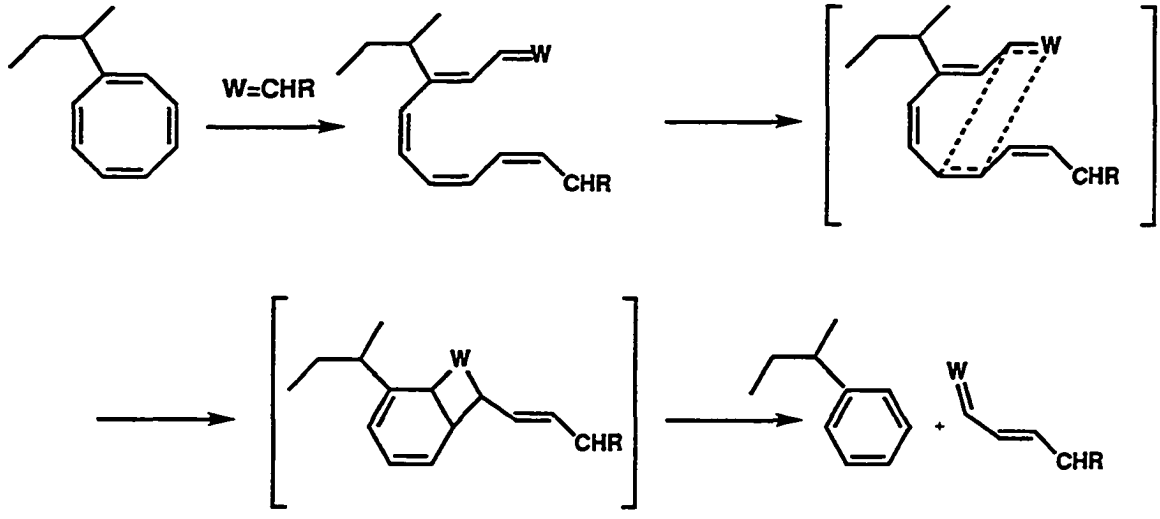


Figure 4. Mechanism of backbiting with catalysts 4 and 5. The *sec*-butyl substituent can be attached to other carbon atoms than the one drawn. It has been shown that no benzene forms during backbiting, which indicates that catalysts 4 and 5 do not attack trisubstituted double bonds.

## II. Synthesis of tungsten alkylidenes

### 1. Synthesis by ring-opening of diphenylcyclopropene

#### a. Synthesis of catalyst 8

Catalyst 8, obtained for the first time by L. Johnson,[32] has been syntheized via ring-opening of diphenylcyclopropene (Figure 5). The first step in the synthesis consists of exchange of the oxo ligand of tungsten oxytetrachloride for an imido ligand. We have found that despite its apparent simplicity, this step is tedious and complicated. The use of xylene as solvent, as recognized by L. Johnson, leads to good yields, but is of little practical use in large scale preparations because of the low volatility of the solvent. When octane is used instead, poorer yields are obtained (usually around 50%), but separation of the product is easier due to its insolubility at room temperature. In order to obtain acceptable materials at the end of the synthesis, purification of the imido complex is necessary. This purification is done by crystallization of the THF adduct of the imido complex in cold pentane. In the absence of recrystallization, the product is largely contaminated by the starting material, which is the same color. The starting material, if present, leads to the synthesis of the oxo analogue of the catalyst 8. This fact has been elegantly shown by J. De la Mata, who directly synthesized the oxo analogue of 8 (see below).

The use of a 1% sodium amalgam in the next step of the reaction makes this synthesis difficult to carry out on a large scale, and alternative reduction methods are actively researched (see below). Finally, it should be mentioned that the last synthesis step (the alkoxylation reaction) always occurs in yields less than 80%. One of the by-products found during the reaction is the alcohol derived from the alkoxide (see chapter 3). The origin

of the acidic protons as well as the nature of the remaining organometallic fragments are unknown.

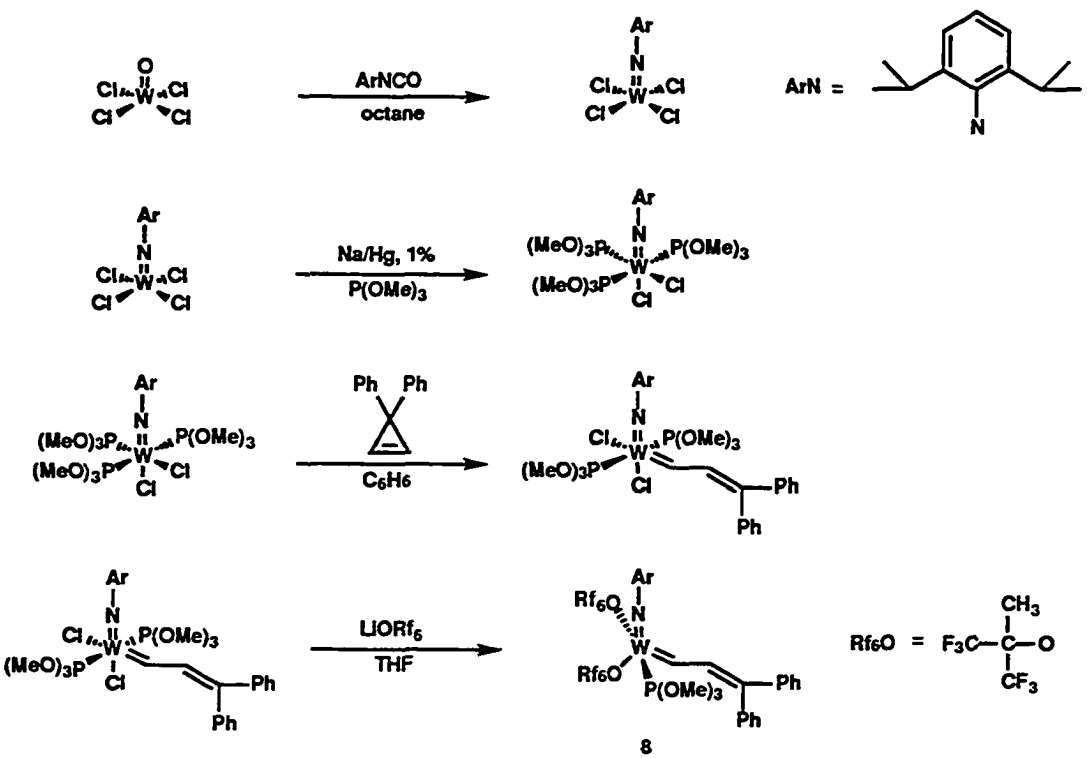


Figure 5. Synthesis of catalyst 8

b. Synthesis of oxo-carbenes

Tungsten oxo carbenes, first synthesized by J. De la Mata, are synthesized by a route which is identical to the synthesis of 8, except for the first step, which is skipped.[43] When using hexafluoro-*tert*-butoxide as ancillary alkoxide ligand, the resulting catalyst is stable in solution, but not in the solid state. This behavior has been attributed to the ease of the phosphite dissociation (see below). Yet, the use of the chiral ligand TBECLi$_2$,

developed by O. Fujimura, has allowed the isolation of oxo carbenes which are stable in the solid state (Figure 6). [42]

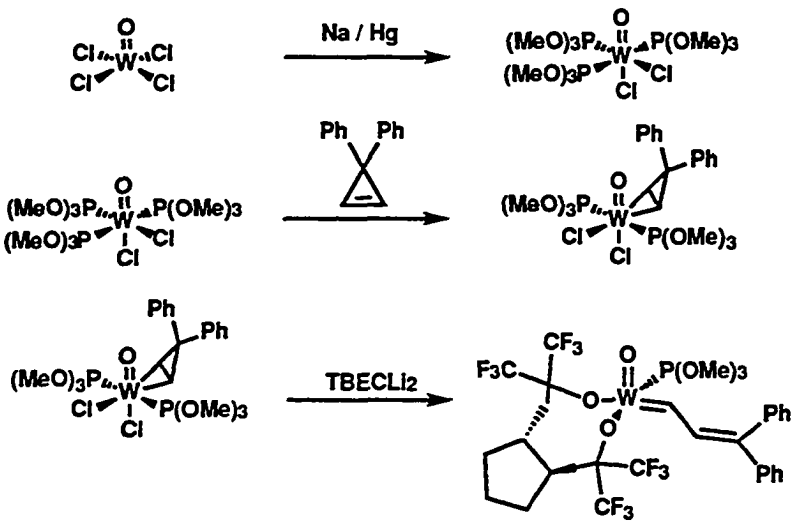


**Figure 6.** Synthesis of the oxo-tungsten carbene with the chiral $TBECLi_2$ ligand.

Although it has the merit of being the first synthesis of an oxo carbene catalyst, and providing a proof of principle, the route developed by J. de la Mata presents problems for large scale synthesis as well as for convenient use in polymerization : the use of sodium amalgam and the derivatization by a non-commercial chiral ligand. We therefore decided to develop a stable oxo-carbene which could be synthesized easily from commercial chemicals.[44]

The use of the amalgam has been circumvented by effecting the reduction from W(VI) to W(IV) with phosphines as the reducing agent. This route has been reported by Wilkinson[446] and by Carmona[46] separately, for trimethylphosphine, dimethylphenylphosphine and diphenylmethyl-phosphine. Triphenyl phosphine and trimethyl phosphite do not possess enough reducing character to allow direct transformation from W(VI) to W(IV). In the case of dimethylphenylphosphine and

diphenylmethylphosphine, the resulting paramagnetic, very slightly air sensitive, orange powders $WCl_4(PR_3)_2$ can be hydrolyzed in hot THF and excess phosphine to yield an oxotrisphosphine complex (Figure 7). The oxotrisphosphine complexes are air-stable 18-electron purple solids.

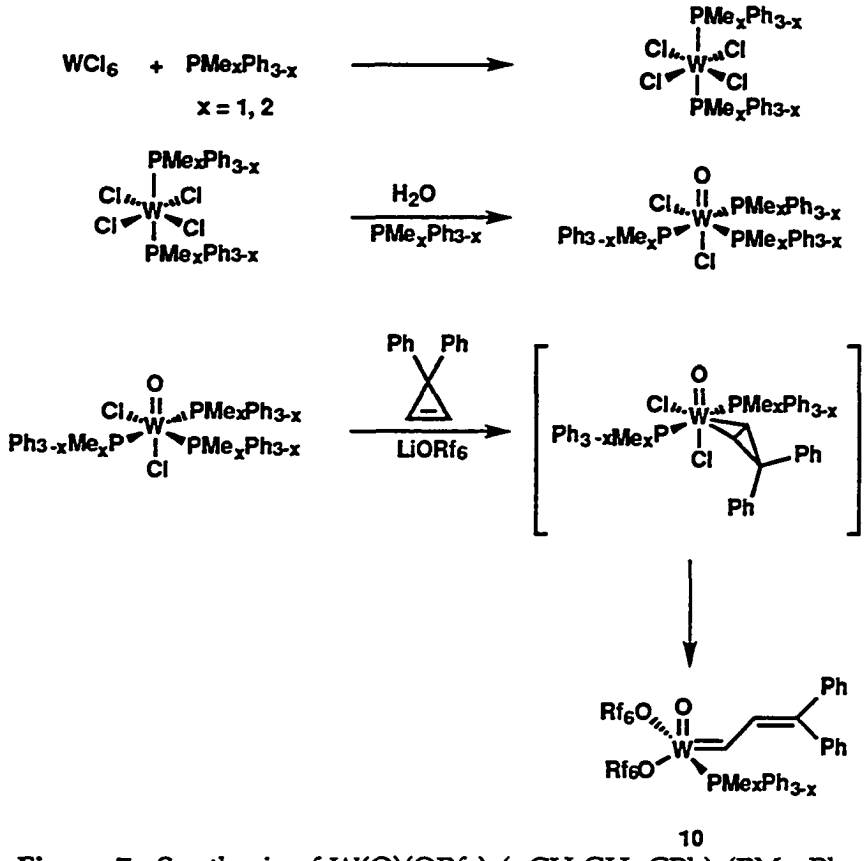


**Figure 7.** Synthesis of $W(O)(ORf_6)_2(=CH\text{-}CH=CPh)_2(PMe_xPh_{3-x})$ (**10**, when x = 1). $ORf_6 = OC(CF_3)_2(CH_3)$.

Reaction of diphenylcyclopropene with the oxotrisphosphine complex at room temperaure gives an olefin complex, which can then be ring-opened in the presence of the alkoxide to afford the carbene **10**. The ring-opening reaction occurs under the influence of heat, even in the absence of alkoxides, but, the resulting dichloro carbene is unstable, and yields dimeric products (Equation 1), unless substituted by alkoxides. Attempts to substitute the

chlorides of the oxo dichlorotrisphosphine complex prior to the formation of the olefin complex failed. Similarly, attempts to reduce oxo dichlorodialkoxytungsten (VI) to dialkoxytrisphosphine tungsten (IV) with two equivalents of sodium amalgam have also failed.

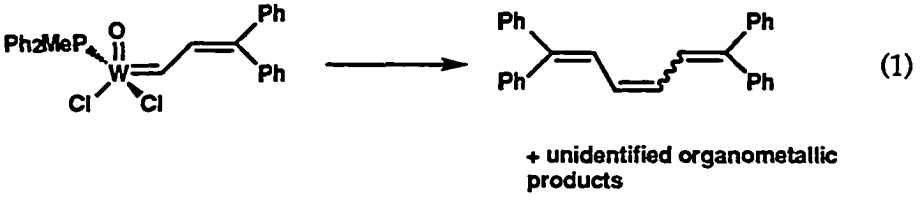


(1)

2. Synthesis by phosphorous ylide transfer

A large number of transition metal complexes having an ylide donor ligand are known,[47,48] nevertheless, elimination of a phosphonium moiety to yield an alkylidene is rarely observed.[49-51] L. Johnson has shown that this methodology can be used, however, to synthesize catalyst 5 from suitable W (IV) precursors (Figure 8). In terms of initiation properties, catalyst 5 presents two antagonistic features: the carbene is anti to the imido substituent, a feature reported by Schrock to be very favorable for rapid initiation,[52,53] and the carbene is chelating, which is obviously disfavorable. It will later be seen that catalyst 5 does not initiate well. Nevertheless, its poor initiation properties are compensated by the ease with which it is synthesized.

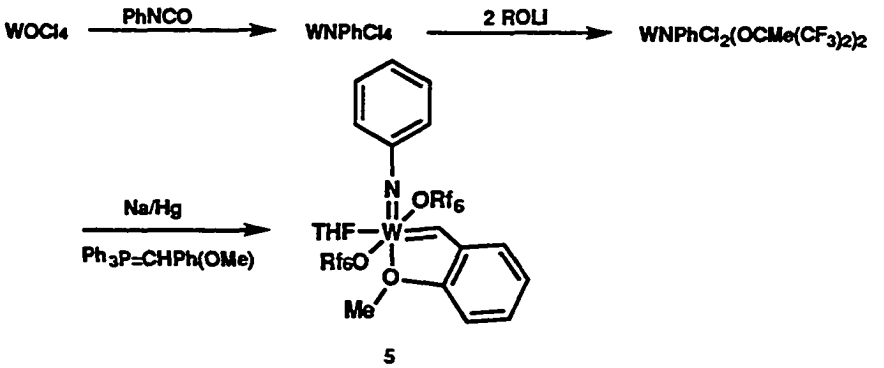


5

**Figure 8.** Synthesis of catalyst **5** by phosphorous ylide transfer

In order to combine the advantages of an easy synthesis, as well as of good initiation properties, a non-chelating carbene was targeted. Compound $WCl_2(=NPh)(=CH\text{-}CH=CMe_2)(PMePh_2)_2$, synthesized by L. Johnson, does not present any appreciable metathesis activity. We have effected in good yield the alkoxylation of this compound to yield the active catalyst **11**. In order to simplify the synthesis of **11**, the ylide transfer and the alkoxylation reactions have been carried out in one pot. The total yield for the three step synthesis is 55%.

The structure of catalyst **11** has been confirmed by X-ray analysis (Figure 10). The arrangement of the ligands is a distorted trigonal bipyramid, having one alkoxide and the phosphine in the axial position. Selected bonds and angles are listed in Table 1.

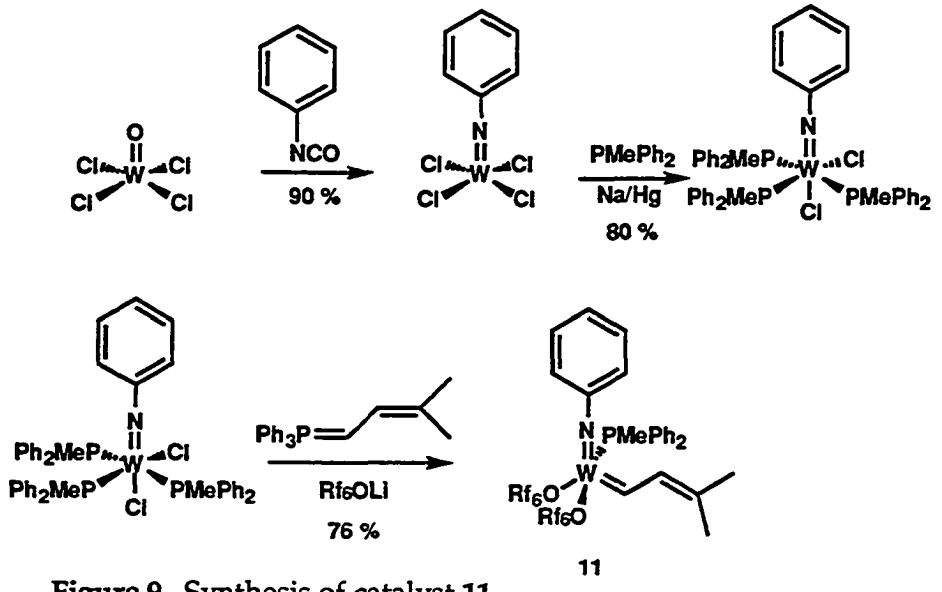


Figure 9. Synthesis of catalyst 11

Because ylide transfer is an easy procedure, the synthesis of tungsten oxo-carbenes by this route was attempted by this route. At 65 °C, in benzene-$d^6$, the ylide reacts in eight hours with dichlorotris(diphenylmethylphosphine)-oxotungsten (IV) in the presence of alkoxide, to yield a yellow adduct, which, by its spectroscopic characteristics, is likely to be the zwitterionic compound A (Figure 11). Similar zwitterionic intermediates have been postulated by L Johnson in the transfer mechanism of an ylide onto dichloro trisphosphine imido tungsten complexes. However, elimination of the phosphine to form the carbene does not occur at 65 °C.

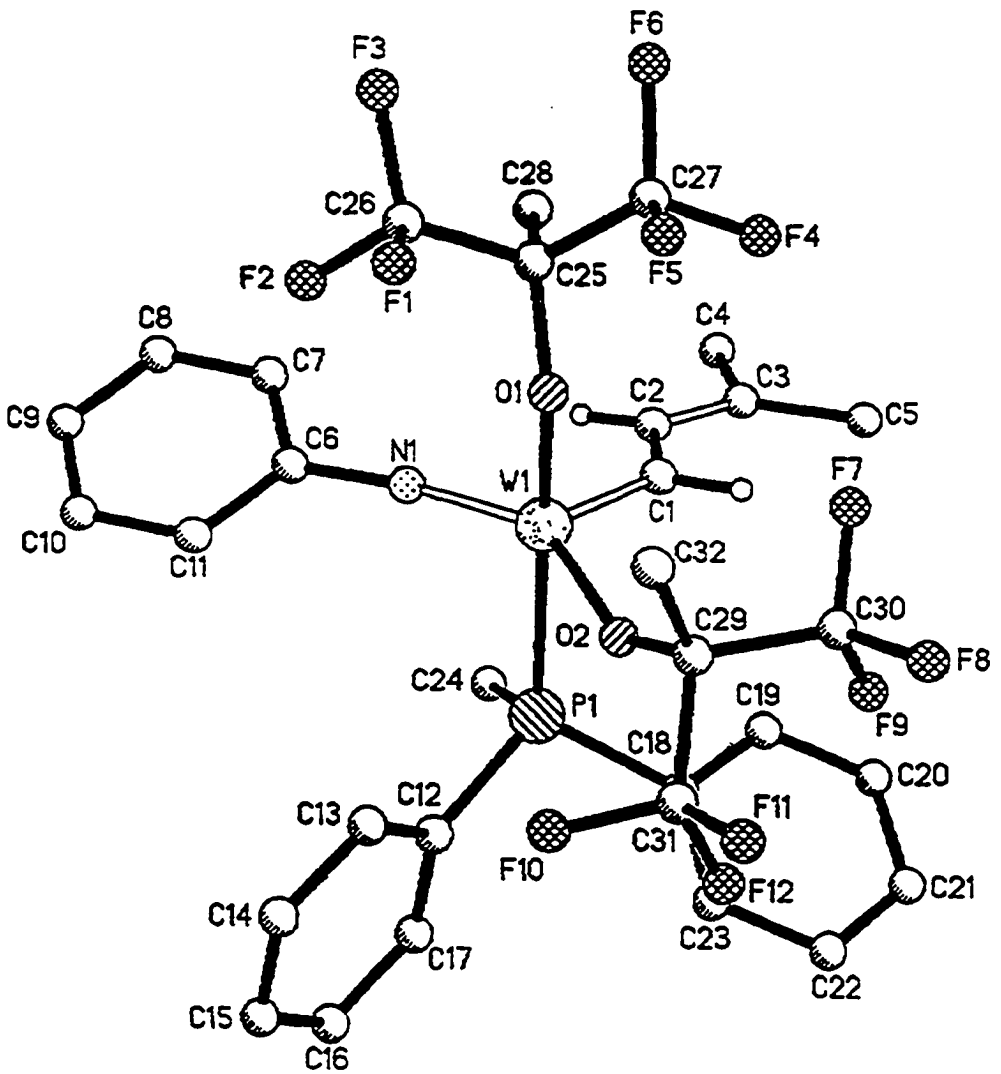


**Figure 10.** ORTEP plot of $W(ORf_6)_2(=NPh)(=CH-CH=CMe_2)(PMePh_2)$ (**11**). Thermal ellipsoids are drawn at the 50% probability level.

**Table 1** Selected bond lengths and angles for $W(ORf_6)_2(=NPh)(=CH-CH=CMe_2)(PMePh_2)$ **(11)**.

| Bond Lengths (Å) | | | |
|---|---|---|---|
| W1 P1 | 2.531(1) | W1 C1 | 1.911(3) |
| W1 O1 | 1.998(3) | C1 C2 | 1.446(5) |
| W1 O2 | 1.984(2) | C2 C3 | 1.341(5) |
| W1 N1 | 1.753(2) | C3 C4 | 1.503(6) |
| **Bond Angles (°)** | | | |
| O1 W1 P1 | 164.9(1) | C1 W1 O1 | 104.3(1) |
| O2 W1 P1 | 81.0(1) | C1 W1 O2 | 111.8(1) |
| O2 W1 O1 | 85.2(1) | C1 W1 N1 | 101.6(1) |
| N1 W1 P1 | 87.9(1) | C2 C1 W1 | 136.3(1) |
| N1 W1 O1 | 99.8(1) | W1 C1 H1A | 108(1) |
| N1 W1 O2 | 143.9(1) | C1 W1 P1 | 86.7(1) |

When the reaction is heated to 85 °C, small amounts of a carbene signal can be observed by $^1H$ NMR, accompanied by a large amount of decomposition. It has been established that phosphine elimination is very much accelerated by the steric bulk of the metal complex.[31] Due to the small steric bulk of the oxo complex, the elimination in **A** does not occur below temperatures at which the resulting carbene decomposes readily.

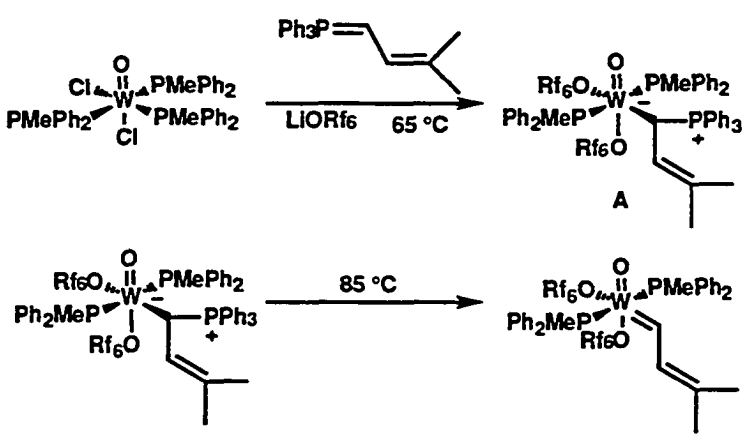


**Figure 11.** Synthesis of a vinyl alkylidene oxo tungsten complex by ylide transfer.

### 3. Carbene synthesis by phosphine and phosphite substitution

#### a. Phosphine and phosphite binding

The binding of phosphines and phosphites to tungsten alkylidenes is dependent on steric and electronic factors. The phosphine-bound and phosphine-free forms are in equilibrium in solution, with the equilibrium strongly favoring the bound form.[36] No phosphite- or phosphine-free carbenes can be observed by proton NMR in toluene, at temperatures ranging from 230 K to 330K. At room temperature in benzene, toluene, or THF, the dissociation reaction of the phosphite or phosphine is slow for catalysts **8**, **10** and **11**, as indicated by the presence in NMR of a distinct P-H coupling between the alkylidene proton and the phosphorous atom and distinct signals for the phosphine bound to W and free phosphine, even at temperatures as high as 80 °C.

For oxo carbenes, phosphine and phosphite are readily displaced by THF, whereas they are strongly bound in imido carbenes. For example, 30 equivalents of THF completely displace the $PMePh_2$ bound to **10** (at a concentration of $10^{-2}$ mol/l in benzene), to give a new oxo carbene **10'**.[1] By contrast, in pure THF, less than 5% of the phosphite in **8** is displaced. This behavior is clearly due to an electronic factor, which is still unclear at this time. It has been proposed[54] that, although imido ligands are usually more π-donating than oxo ligands, aryl-imido ligands could be less π-donating than oxo, which would explain the observed stronger phosphine binding for imido carbenes. Alternatively, it could be advanced that the hard oxo complex will bind preferentially to the hard THF, and the soft imido complex with the soft

---

[1] Primed compound numbers will be used in the following discussion to indicate THF adducts.

phosphine.[55] In the imido carbene series, the electron deficient character of the metal center strongly contributes to the stability of the W-P bond. For example, when *tert*-butoxides instead of hexafluoro-*tert*-butoxides are used as ancillary ligands (equation 2), the phosphite is completely displaced by small amounts of THF. Yet, bulky σ-donating phosphines (such as *tert*-butyl phosphine, or diphenylmethyl phosphine) are less strongly coordinated than the poor σ-donating phosphite, indicating that a steric component is also present in the thermodynamics of binding.

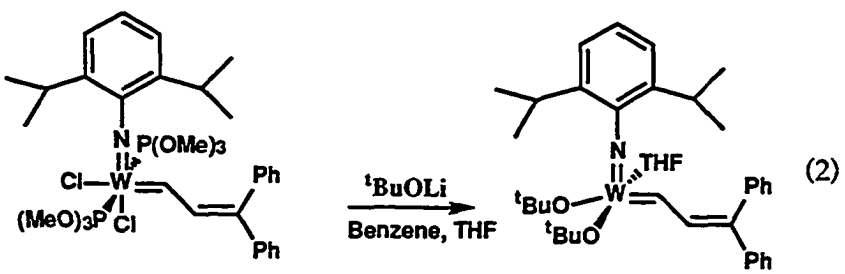


(2)

12

Since the trimethyl phosphite in 8 is not readily displaced, we have concentrated our efforts in finding a substitution pathway from 8 to the THF complex 8'. Quantitatively shifting the dissociation equilibrium toward the phosphite free form (8*tet*), or eventually the THF bound form (8') has been realized by using a phosphite sponge which binds the phosphite more strongly than the tungsten complex. The removal of the phosphite was performed in benzene, or in benzene/THF mixtures with 10 to 60 equivalents of THF relative to 8. Addition of THF enhances the removal of the phosphite and stabilizes the resulting compound. However, phosphite removal by this method leads to catalyst decomposition in pure THF. Both soluble and insolublephosphite sponges have been used.

**b. Homogeneous phosphite sponge**

The first route for phosphite abstraction involves the use of unsaturated soluble ruthenium complexes. In contrast to a heterogeneous process, which requires a reaction time of five to thirty minutes to be complete (see Experimental Section), a homogeneous reaction can potentially be instantaneous, giving an easy access to **8*tet*** and **8'**. Cp*RuCl [56] is a tetrameric, coordinately unsaturated complex that possesses a great affinity for phosphines. When two equivalents of Cp*RuCl are added to a brown solution of **8** in benzene, the solution immediately turns red, and no solid precipitates. Three sets of carbene complexes can be observed by $^1$H NMR. These complexes, which spectroscopically differ from the phosphite-free carbene **8*tet***, do not show activity in the polymerization of sBCOT or cyclooctene. It is likely that the chloride bridges between the Ru and W complexes, as observed in other ruthenium complexes.[57] $[Cp^*RuOMe]_2$ cannot provide a bridging halide, and, as expected, allows the generation of the phosphite-free catalyst **8*tet***.[56, 58, 59] When $[Cp^*RuOMe]_2$ is added to a solution of **8** in deuterated methylene chloride, two upfield doublets ($\delta$ = 10.37 and $\delta$ = 9.87) appear in the NMR, as well as a few other minor peaks. These two peaks are identical to those found by reaction of diphenyl-1,3-pentadiene with neopentylidene carbene **4** (Figure 12). As a result, we attribute these two peaks to the anti and syn rotamers of the phosphite-free complex, **8*tet***. Other smaller resonances have not been assigned.

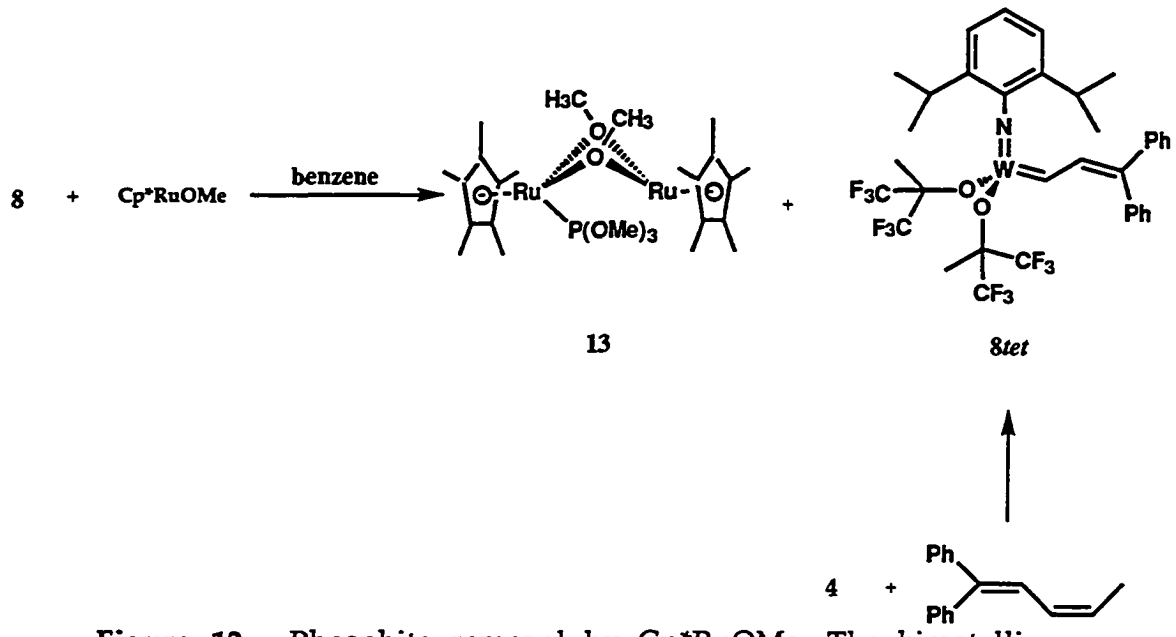


**Figure 12.** Phosphite removal by Cp*RuOMe. The bimetallic compound **13** has been identified from its literature spectroscopic characteristics.[58,59]

The equilibrium constant for the removal of phosphite by $[Cp^*RuOMe]_2$ is 0.12, indicating that only a small amount of phosphite-free catalyst is created for a 1 to 1 ratio Ru/W. In addition, *8tet* decomposes rapidly at room temperature (vide infra); at a concentration of $10^{-2}$ mol/l in dichloromethane at -40 °C, its half-life is about 4 hours. The fast decomposition as well as the poor yield for the generation of *8tet* prompted us to use THF as an ancillary ligand. A 1 : 2.8 : 21 mixture of W : Ru : THF gives at least 95% of 8', with virtually no decomposition. Minor resonances, observed from the reaction of 8 with $[Cp^*RuOMe]_2$ are also transformed into 8' ones upon addition of THF.

c. Use of a heterogeneous phosphite sponge

Although the use of $[Cp^*RuOMe]_2$ gives satisfactorily results, we have devised a simpler and more economical route to 8'. In benzene, copper(I) chloride (CuCl) is an insoluble solid, on which phosphites are readily adsorbed.[60] The reaction between CuCl and phosphite generates a CuCl phosphite polymer of undefined structure that is at least partially soluble in benzene in the case of trimethylphosphite. In benzene, methylene chloride, or toluene, a large excess of CuCl reacts with 8 to produce the species 8-*Cu* (Figure 13 and 14). We have determined that the species 8-*Cu* is a bimetallic compound containing the initial complex 8 and at least one molecule of CuCl.

The bimetallic structure of 8-*Cu* has been inferred from the following information. First, the $^1H$ carbene resonances of the bimetallic *8-Cu* do not match those of the phosphite free 8*tet*. Second, $^{31}P$ NMR (toluene, - 70 °C[2]) indicates that the phosphite of 8-*Cu* ($\delta$ =154 ppm, small peak) is not in the form of a phosphite-copper polymer ($\delta$ = 121 ppm, broad peak). In addition, $^{19}F$ NMR (in $CD_2Cl_2$ at - 50 °C) indicates that 4 different $CF_3$ groups ($\delta$ = -76.06, - 76.21, -76.51, -76.79) are present, which rules out the presence of a tetrahedral compound. Finally, $^1H$ NMR integration of the carbene signal of 8-*Cu* ($\delta$ = 10.7 ppm) compared to 8 shows that the equilibrium constant of this reaction is approximately 0.114 at 293 K ($\Delta H°$ = -3.2 kJ/mol, $\Delta S°$ = - 27 J/K·mol, Figure 14). Because of the negative enthalpy of reaction, the amount of 8 increases with decreasing temperature. If CuCl generated the phosphite-free isomer 8*tet* (instead of *8-Cu*), the amount of phosphite free

---

[2] The poor thermal stability of 8-*Cu* although higher than 8*tet*, forces one to use low temperatures for spectroscopic analyses.

isomer would likely increase with temperature. Even at low temperature (207 K) in toluene, *8-Cu* shows predominantly one rotamer (syn). The anti rotamer, present in very small quantities, is detectable by $^1$H NMR only after a large number of accumulations. Despite many attempts, we have not been able at this time to isolate a powder or a crystal of *8-Cu*, probably because of the equilibrium between *8-Cu* and **8**. Nevertheless, spectroscopic data allows us to guess a plausible structure for *8-Cu* (Figure 13).

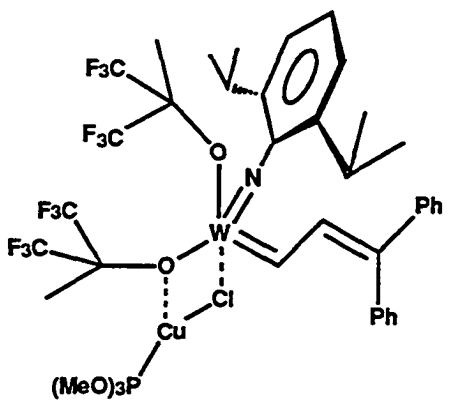


**Figure 13.** Possible structure for *8-Cu*. The carbene is represented in the syn position. Because the alkoxides are inequivalent, one of them is represented in axial position, and the other one in equatorial position.

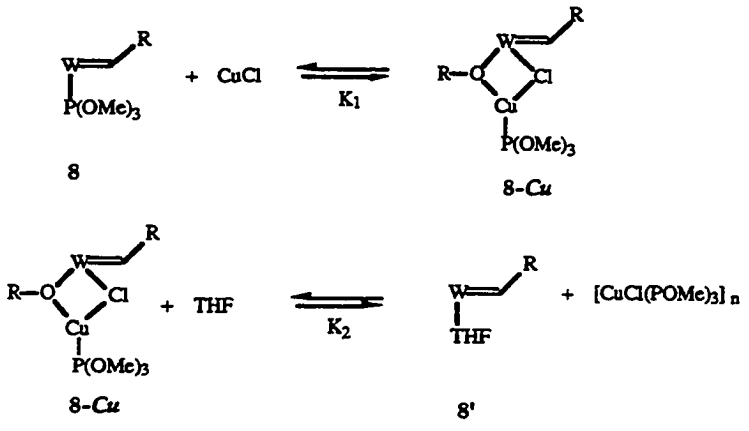


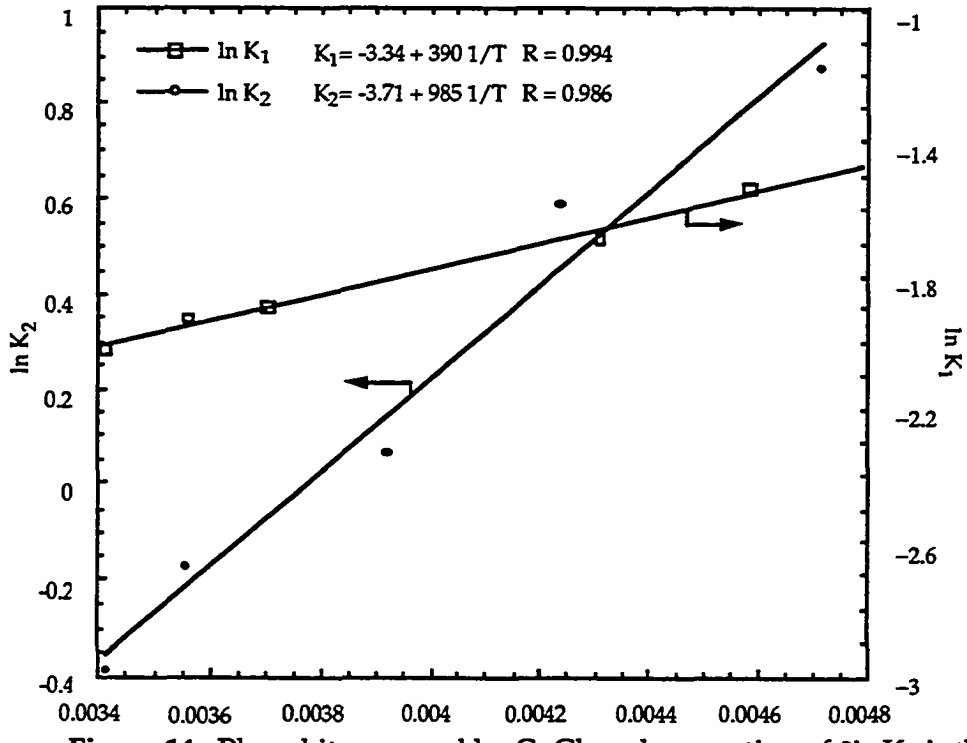


**Figure 14.** Phosphite removal by CuCl, and generation of 8'. $K_1$ is the equilibrium constant between 8 and *8-Cu* ( $\Delta H°$ = -3.2 kJ/mol, $\Delta S°$ = - 27 J/K/mol), and $K_2$ is the equilibrium constant between *8-Cu* and 8' ( $\Delta H°$ = -8.1 kJ/mol, $\Delta S°$ = - 31 J/K/mol ). The conditions of measurement are detailed in the experimental section.

Because CuCl does not quantitatively remove the phosphite in pure benzene, similar reactions were attempted with $PtCl_2$, AgCl, CuBr, CuI, and Pt black in place of CuCl. Pt black, CuBr, CuI and AgCl behave as very weak phosphite adsorbents. $PtCl_2$ partially removes the phosphite, giving ***8tet***, but reacts further, creating new ill-defined carbene complexes which do not exhibit any metathesis activity toward sBCOT. Longer reaction times of $PtCl_2$ with **8** (for a total duration of 2 hours) result in the decomposition of most of these new carbenes. Because the removal of the phosphite in the absence of another ligand seems to be thermodynamically uphill, THF has been added to the catalyst to drive the reaction to completion. When 30 equivalents of THF relative to **8** are added, the phosphite removal can be quantitative. After filtration of unreacted CuCl, NMR integration shows that less than 5% of **8** and trace amounts of ***8-Cu*** are present in solution, and that the generation of the new catalyst (**8'**) is nearly quantitative, with less than 5% decomposition.

The CuCl route can also be used for the generation of the THF adduct of catalyst **11, 11'**. Once again, a bimetallic adduct is formed, which, upon THF addition is cleaved to give the THF bound carbene **11'**.

d. Substitution of THF

The THF molecules in **8'** and **11'** are labile, and can be displaced by tri-*tert*-butylphosphine, acetonitrile, and triethylamine. Alternatively, tri-*tert*-butylphosphine, acetonitrile, and triethylamine adducts can be prepared through the CuCl route, in the absence of THF. The acetonitrile adduct decomposes rapidly, probably through nitrile metathesis. Ether, 2-methyl THF, and 2,5-dimethyl THF do not readily displace THF, so that very large amounts of Lewis base are necessary to prepare the corresponding adducts.

These adducts can be prepared directly from reaction of 8 with CuCl and the corresponding Lewis base. At the other end of the nucleophilicity scale, DBU, trimethylphosphine, pyridine and quinuclidine displace not only THF, but even trimethyl phosphite. Accordingly, the ligand strength scale for 8 is the following:

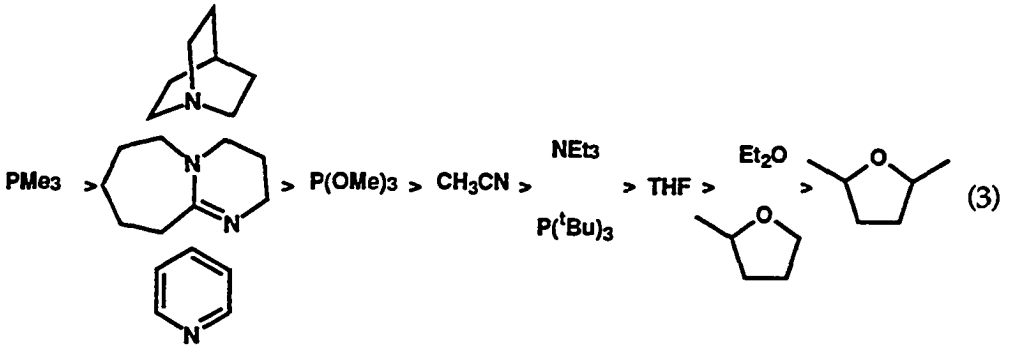


III. Characterization of tungsten carbenes

1. Stability of tungsten carbenes

As shown in Figure 15, the half-time of decomposition of 8*tet* in solution is greatly increased by the presence of THF. At room temperature, the THF-free catalyst 8*tet* has a half-life of 10.5 minutes, whereas this value is increased by up to 42 minutes when 10 equivalents of THF are present. When 73 equivalents of THF are used, no decomposition is observed over two hours. All attempts to prepare the phosphite-free catalyst in bulk have failed, suggesting that 8' is, if not totally unstable, very fragile in the solid state. This behavior is attributed to the high volatility of THF : when a sample of 8', concentrated *in vacuo*, is disolved rapidly in benzene-$d^6$, $^1H$ NMR indicates the presence of residual amounts of 8*tet*. This behavior is also observed for catalysts **10'**, **11'** and **12'**, which are all THF-bound. On the contrary, phosphine-bound catalysts, for which the phosphine is not volatile,

are stable in the solid state. Phosphite catalysts are stable if the phosphite is strongly bound (like 8 and the TBEC catalyst), but unstable if the phosphite is loosely bound (like $W(=O)(=CH\text{-}CH=CPh_2)(ORf_6)_2P(OMe)_3$).

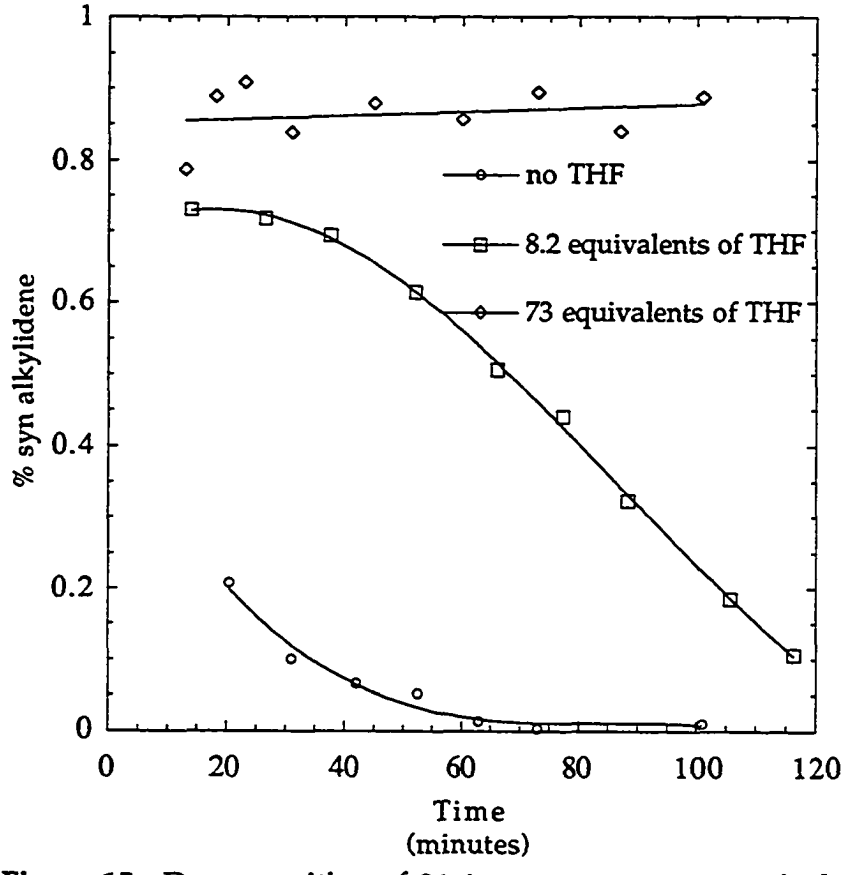


**Figure 15.** Decomposition of *8tet* at room temperature in benzene with different amounts of THF. For the 3 runs, the initial concentration of 8 is 0.012 mol/l and the concentration of $[Cp^*RuOMe]_2$ is 0.028 mol/l.

## 2. Spectroscopic characterization of W carbenes

### a. General features

Each carbene is a mixture of syn and anti rotamers. Syn carbenes have the carbene substituent pointing toward the imido or the oxo ligand (Figure 16). For vinyl alkylidenes, the coupling between the α proton and β proton is typically on the order of 12-15 Hz for anti rotamers and 9-12 Hz for syn rotamers.

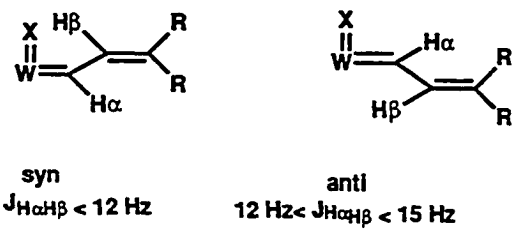


syn
$9\ Hz < J_{H\alpha H\beta} < 12\ Hz$

anti
$12\ Hz < J_{H\alpha H\beta} < 15\ Hz$

**Figure 16.** Syn and anti rotamers. X = imido or oxo, R = Ph, Me

In phosphine- and phosphite-bound catalysts, the ratio syn / anti is dependent on the batch of catalyst used. Usually, monocrystalline samples show exclusively one rotamer only. For THF adducts, the syn / anti ratio is independent of the batch of catalyst used and of the method used to generate it. It is believed that, for these complexes, the syn / anti ratio reflects the thermodynamic stability of the two rotamers. Table 2 and 3 list the principal spectroscopic characteristics of the vinyl-alkylidenes **8 - 14**.

Table 2. Selected $^1H$ NMR data for different adducts of catalyst 8

| ligand | carbene proton | | vinyl proton | | J syn (Hz) | J anti (Hz) | % syn |
|---|---|---|---|---|---|---|---|
| | δ syn | δ anti | δ syn | δ anti | | | |
| none | 10.1 | 11.5 | 7.9 | 9.1 | 9.9 | 15.2 | 78 |
| CuCl[a] | 10.7 | 11.55 | 8.75 | 9.1 | 13.3 | 13.9 | >99 |
| THF[a] | 10.2 | 11.3 | 9.0 | 9.2 | 11.2 | 15.0 | 87 |
| THF[b] | 10.2 | 11.4 | 9.1 | 9.3 | 11.1 | 14.6 | 88 |
| THF[c] | 9.9 | 11.2 | 8.8 | 8.9 | 11.1 | 14.6 | 88 |
| methyl-2-THF[b.d] | 10.2 | 11.6 | 9.1 | 9.15 | 10.9[e] | 14.7 | 87 |
| | 10.6 | 11.4 | 8.6 | 9.2 | 13.1 | 15.8 | |
| dimethyl-2.5- | 10.25 | 11.6 | -[f] | 9.15 | - | 14.1 | 97 |
| THF[b.d] | 10.55 | | 9.1 | | 10.9 | | |
| pyridine[b] | 11.5 | 11.8 | 9.3 | 9.45 | 12.2 | 14.6 | 25 |
| DBU[a.g] | 11.3 | 11.6 | 9.2 | 9.3 | 11.8 | 14.5 | 26 |
| quinuclidine[b] | 10.9 | 11.4 | 9.1 | 9.2 | 11.4 | 14.7 | 61 |
| acetonitrile[b] | 11.9 | 12.2 | 9.5 | 9.6 | 10.5 | 14.6 | 26 |
| triethylamine[b] | 10.15 | 10.2 | 9.1 | 8.6 | 11.5 | 13.5 | 33 |
| diethylether[b] | 10.1 | -[h] | 9.1 | - | - | - | > 95 |
| $^t$butylphosphine[b] | 12.4 | 11.9 | 8.9 | 9.1 | 10.8 | 14.2 | 55 |

a. in toluene-$d^8$.
b. in benzene-$d^6$.
c. in methylene chloride-d2.
d. at 259 K.
e. because of the fluxional behavior of this adduct, the coupling can only be observed at low temperature
f. resonance obscured by 8
g. an unidentified peak at 12.6 ppm is also present
h. signal not observed

Table 3. Selected $^1H$ NMR data for different catalysts in benzene $d^6$.

| catalyst | carbene proton | | vinyl proton | | J syn (Hz) | | J anti (Hz) | | %syn |
|---|---|---|---|---|---|---|---|---|---|
| | δ syn | δ anti | δ syn | δ anti | $J_{HH}$ | $J_{HP}$ | $J_{HH}$ | $J_{HP}$ | |
| **8** | 11.9 | 12.4 | 8.9 | 9.1 | 12.6 | 5.4 | 13.4 | 7.9 | 8[a] |
| **8'** | 10.2 | 11.4 | 9.1 | 9.3 | 11.2 | - | 15.0 | - | 87 |
| **10** | 11.5 | 12.1 | 8.5 | 8.9 | 11.4 | 1.8 | 14.7 | 2.1 | 63[a] |
| **10'** | 10.2 | 11.8 | 9.25 | 9.35 | 10.8 | - | 12.9 | - | 46 |
| **11** | 12.3 | 12.4 | 7.5 | 8.1 | 10.7 | 3.3 | 12.4 | 5.1 | 98[a] |
| **11'** | 10.0 | 10.5 | 7.6 | 8.3 | 10.4 | - | 11.3 | - | 40 |
| **12** | 9.7 | 10.0 | 9.0 | 9.35 | 11.8 | - | 15.3 | - | 54 |

a. % syn depends on the batch of catalyst considered

b. Characterization of 8'

Because 8' is not stable in the solid state, no X-ray structure could be obtained. Therefore, a detailed spectroscopic analysis was carried out. The $^1H$ NMR spectrum of 8' has been analyzed and all resonances assigned (Figure 17). When 8' is heated at 60 °C in toluene with 60 equivalents of THF, the two carbene peaks (syn and anti) coalesce in the $^1H$ NMR, giving one new average resonance. This phenomenon is reversible, but is accompanied each time by some decomposition, probably due to the high temperature. Thus the syn/anti interconversion is slow below 60 °C (compared to the NMR time scale). The equilibrium ratio of the *syn* and *anti* rotamers in 8' does not change from -30 °C to 46 °C. A similar observation in THF solvent has been made by Oskam and Schrock [53] for $Mo(NAr)(CHCMe_2Ph)(OR_{F6})_2$, the molybdenum analogue of 4. However, for the molybdenum catalyst, the anti isomer is only present in very small amounts.

For the sake of clarity, we will describe the NMR characteristics of the syn rotamer only: the anti rotamer behaves identically, and is in slow exchange with the syn rotamer, relative to NMR timescale, up to 60 °C.

At room temperature, $^1H$ NMR of 8' indicates one set of resonances for the methyl and methine protons of the isopropyl groups and for alkoxide methyl. This implies not only fast rotation of the N-C bond but also time-averaged mirror symmetry in the complex. The equivalence of these resonances is observed at temperatures as low as - 60 °C. The high fluxionality of 8' is unprecedented for pentacoordinated tungsten alkylidenes. The small size of the carbene ligand as well as the rapid dissociation of THF could provide a rationale for such a behavior.

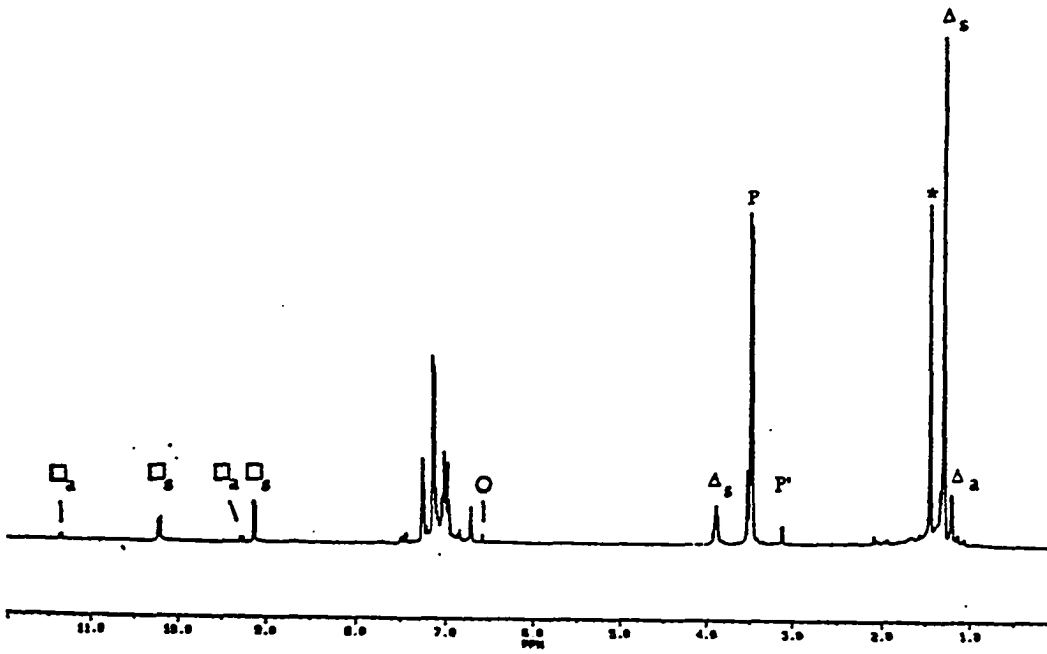


**Figure 17.** $^1$H NMR of 8' in deuterated benzene, with 60 equivalents of THF $d^8$. 8' was generated by the CuCl route. $\square_a$: anti carbene proton (downfield), and vinyl proton (upfield). $\square_s$: syn carbene proton (downfield), and vinyl proton (upfield). $\Delta_s$ syn methyne (downfield) and methyl (upfield) protons. $\Delta_a$ anti methyl protons (the methyne protons are obscured by the phosphite peak). P and P' : respectively copper bound and free phosphite. * : alkoxide methyl group. O: HFB, hydroxyl proton (see chapter 3). The methyl group of HFB is directly upfield of $\Delta_a$. The peaks on the shoulder of P and $\Delta_s$ correspond to THF.

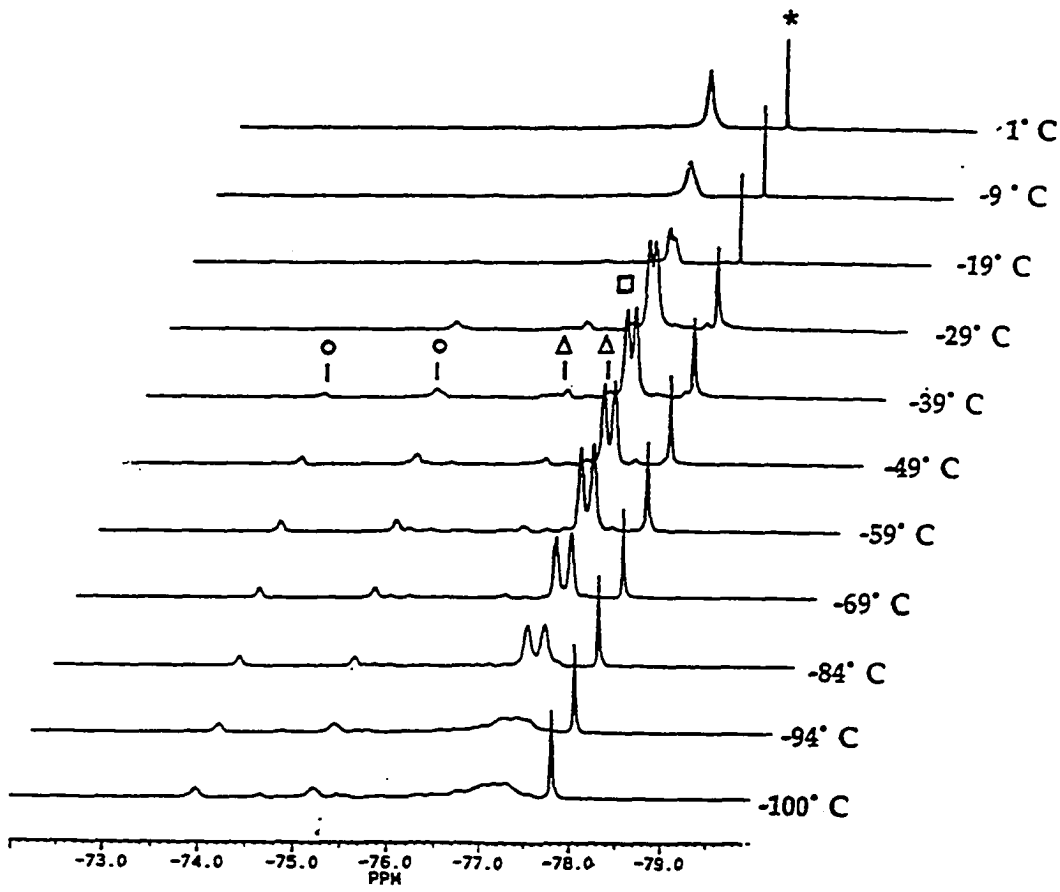


**Figure 18.** VT behavior of 8' ($^{19}F$ NMR in $CD_2Cl_2$). 8' was created by the CuCl route. □: syn alkoxide resonances, O: anti alkoxide resonances. Δ : two of the four resonances of 8-*Cu* . * : HFB (see chapter 3).

At room temperature, $^{19}F$ NMR shows only one resonance for the 4 $CF_3$ groups, which suggests an impossibly high (greater than $C_s$) symmetry for the complex. In order to shed some light on this phenomenon, VT $^{19}F$ NMR data were used (Figure 18). At high temperature one average peak is observed, which is split into two peaks at lower temperature. At very low temperature, a broad pattern (maybe four resonances) arises, likely from the absence of symmetry due to the freezing of molecular motions. At very low temperature, the complex behavior indicates that all four $CF_3$ groups are diasterotopic: therefore, there is no symmetry plane between the two alkoxides. This situation arises in a trigonal bipyramidal (tbp) or in a square pyramidal (sp) structure, when one alkoxide is axial and the other one is equatorial. It seems safe to rule out the presence of a sp structure, because of the extreme crowding created by the two alkoxides and imido ligands. This is also supported by the fact that, to date, square pyramidal carbenes of the type $W(=X)(=CHR)(OR)_2(L)$ have never been observed. The tbp arrangement which has one alkoxide equatorial and one alkoxide axial is a chiral structure.[61] This chiral structure is generated from THF coordinating to the CNO face of *8tet* (such as the phosphine in Figure 10). At intermediate temperatures, two resonances are only observed, because of the time averaging of the two enantiomeric structures. At these temperatures, a band shape analysis allows to find approximate activation parameters for the THF dissociation from 8': $\Delta H^{\ddagger}$ =24.2 kJ/mol and $\Delta S^{\ddagger}$ = - 55.2 J/K·mol.[3]

At higher temperature, the two peaks collapse to a single peak. One possible explanation for this phenomenon is alkoxide exchange. Alkoxide

---

[3] In the band shape analysis, the dissociation rate is supposed to be zero order in THF concetration, and first in 8'.

exchange has already been reported for $Mo(NAr)(CHCMe_2Ph)(OR)_2$.[62] We also observed that at - 70 °C, a mixture of lithium *tert*-butoxide and **8'** does not react over a duration of 15 minutes, but they do react in less than 30 seconds at -10 °C, to give a mixture of $Rf_6OLi$ and **12**. In chapter 3, it will be shown that exchange also occurs between free alcohol and bound alkoxide. However, under a variety of conditions, coalescence between bound alkoxide and free alkoxide or alcohol is *not* observed. Consequently, the observed coalescence (if coalescence there is) does not originate from an exchange process between tungsten alkoxide and free alkoxide or free alcohol. Additionally, when **8'** and **4** or **4** and $Mo(NAr)(CHCMe_2Ph)(OR)_2$ are mixed no coalescence is observed under a large temperature range, indicating that if bimolecular exchange occurs, it is slow on the NMR time scale. It therefore seems that, although alkoxide exchange occurs, this phenomenon is not responsible for the observed degeneracy of the $CF_3$ peak.

A more likely explanation for this degeneracy is accidental overlap of the signals of the two diastereotopic $CF_3$ groups, due to the temperature dependence of the chemical shift of each resonance. Such a degeneracy is also apparent in the VT $^{19}F$ NMR of $Mo(NAr)(CHCMe_2Ph)(OR)_2$.[63] At room temperature, the $^{19}F$ NMR shows one peak, whereas at higher temperature, two peaks are observed. Because this phenomenon appears by raising the temperature, an exchange process is clearly not occurring.

Because the THF dissociation is a rapid process for **8'**, the association constant for THF binding to the phosphite-free complex ***8tet*** could not be measured reliably. At room temperature, an estimate for the dissociation constant is about $2\ 10^{-4}$ mol/l, which can be compared with a dissociation constant of $6.5\ 10^{-2}$ mol/l for **4** .[64] The smaller value for ***8tet*** can be

explained by the relatively small steric hindrance compared to **4**, which favors the complexation of THF. This trend is even more drastic for **11'**, where THF dissociation is slow on the NMR scale, and for which the dissociation constant is 1.6 $10^{-5}$ mol/l. Binding decreases with the increasing bulk of the Lewis base: the dissociation constant for 2-methylTHF from **8'** is 3.4 $10^{-2}$ mol/l and for 2,5-dimethylTHF, 2.3 mol/l.

### 3. Evaluation of the initiation properties in polymerization

It will be shown in Chapter 3 that the rates of polymerization depend on the amount of alcohol (hexafluoro-*tert*-butanol, or HFB) present in the system. In the rest of this chapter, the amount of alcohol is between 0.8% and 1.5% for all catalysts except for **8'**, for which it is 9%. In order to assess accurately the efficiency of the initiation reaction, we have decided to use two different characteristic numbers (Table 4).

The first one is the ratio $k_p/k_i$, which enables to measure how much more reactive the propagating species is compared to the initiating one. For example, the use of a modified Gold's equation[65] (equation (7), appendix 1), leads to an apparent $k_p app/k_i app$, which, for **8'**, depends on the THF concentration. In the case where the THF binding characteristics to the propagating carbene are known, it is possible to obtain $k_p/k_i$ in the absence of THF, using the relationship $k_p/k_i = k_p app/k_i app \cdot K_{cat}/K_{prop}$ where $K_{prop}$ and $K_{cat}$ are the dissociation constants of THF for the propagating and initial carbenes respectively (see Appendix I). In most cases, it is difficult to obtain Kprop directly (only the value for sBCOT is presented here), because **8-*Cu*** or **8*tet*** cannot be generated quantitatively from **8**. Therefore, apparent ratios $k_p/k_i$ will be presented (typically using a ratio THF : catalyst of 65 : 1).

The other approach consists of comparing the $k_i$ of 8' to the $k_i$ of a different carbene. Since 4' and 8' have identical propagating carbenes, it is clear that, for the same concentration of THF, $k_i(8')/k_i(4') = k_iapp(8')/k_iapp(4') \cdot K_{cat}(4')/K_{cat}(8')$. Using the values found above, the ratio $K_{cat}(4')/K_{cat}(8')$ is $6.5\ 10^{-2}/\ 2.0\ 10^{-4} = 325$, so that $k_i(8')/k_i(4') = 325\ k_iapp(4')/k_iapp(8')$. The advantage of this last method is that it quantifies the initiation reaction independently of the characteristics of the propagating carbene and of the amount of THF used. When a phosphine-bound catalyst is used, the kinetic law is no longer first-order in catalyst, because of phosphine inhibition. Therefore, the Gold equation is not rigorously applicable (see first chapter). For sake of comparaison, Gold equation will be used, but resulting values shall not be used to calculate absolute kinetic rate constants.

On average, we observe that vinyl alkylidenes initiate much better than neopentylidenes (Tables 4 and 5). This is a consequence of the large steric difference between the two types of carbenes.[4] There does not seem to be a large difference between the initiating properties of oxo and imido complexes though the body of data on oxo catalysts is currently small.

---

[4] Electronic reasons could be invoked too.

**Table 4.** $k_p/k_i$ and initiation kinetic constant of 8' and 4' for different monomers

| monomer | $k_p app/k_i app$[a] | THF/CAT[a] | $k_i(8')/k_i(4')$ | Temperature[b] |
|---|---|---|---|---|
| norbornene | 9 | 59 | 8 | 293 K |
| COD | 82 | 65 | 370 | 293 K |
| COE[c] | 161 | 65 | 25 | 293 K |
| sBCOT | 1 | 52 | $> 10^5$ | 293 K |
| phenylCOT | 0.5 | 74 | - | 309 K |

a. for catalyst 8'.
b. in benzene
c, cyclooctene

**Table 5.** Apparent $k_p/k_i$ for different catalysts and monomers (at room tempertaure in benzene)

| catalyst | monomer | [MON] | MON/CAT | % initiated | $k_p/k_i$ |
|---|---|---|---|---|---|
| **4** | NBE | 0.13 | 14.2 | 31 | 227 |
| **8** | NBE | 0.14 | 13.6 | 86 | 11 |
| **8'** | NBE | 0.12 | 12.1 | 84 | 9 |
| **11** | NBE | 0.12 | 4 | 56 | 13 |
| **4** | COD | 0.13 | 14.2 | 7 | 5500 |
| **8'** | COD | 0.27 | 19.2 | 53 | 82 |
| **11** | COD | 0.12 | 7.8 | 33 | 9 |
| **8'** | sBCOT | 0.12 | 23 | 88 | 1 |
| **11** | sBCOT | 0.18 | 6 | 100 | < 1 |

## IV. Polymerizations with tungsten vinyl alkylidenes

### 1. General Features

Although they are slightly less active than **4**, because of Lewis base deactivation, tungsten vinylalkylidenes are usually quite active and the improvement in intiation properties makes them attractive ROMP catalysts. Only catalyst **8**, in which the phosphite is strongly bonded, and catalyst **12**, which is less electron-deficient, show inferior activity. In Table 6, an overview of the reactivity of the catalysts studied is presented.

**Table 6.** Polymerization of selected monomers by different catalysts, at room temperature (unless otherwise noted). x indicates no polymerization (under typical conditions), and y indicates polymerization occurred.

| catalyst | NBE | COD | COE | sBCOT |
|---|---|---|---|---|
| **4** | y | y | y | y |
| **8** | y | x | x | x |
| **8'** | y | y | y | y |
| **10** | y | y | y | y[a] |
| **10'** | y | y | y | y[a] |
| **11** | y | y | y | y[a] |
| **11'** | y | y | y | y |
| **12** | y | x | x | x |

a. Polymerization done at 35 °C. At room temperature, no polymerization occurs.

2. Polymerization of norbornene (NBE)

a. Polymerization by 8

Norbornene is rapidly polymerized by 8 in benzene and toluene, and at a slower rate in THF. The resulting polymer can be cleaved from the tungsten complex by reacting an aldehyde (typically benzaldehyde or pivaldehyde) with the growing chain in a Wittig-like reaction. The isolated polymer has a high molecular weight and relatively low polydispersity index (Table 7). All the samples prepared using 8 show a small additional high molecular weight peak, which has already been observed for the polymerization of norbornene by tungsten catalysts such as 4. This high molecular weight peak will be studied in more detail in the next chapter.

The polynorbornene obtained with 8 contains a high ratio of cis double bonds, which very slowly isomerizes to trans double bonds, by secondary metathesis with the internal double bonds of the polymer. For example, when a polymer is formed by addition of 93 equivalents of norbornene to 8, 92% of the double bonds are cis after 2 hours of reaction time and 86% after 2 weeks or 2 months. Therefore, very little chain transfer

to the polymer occurs in the time scale of the polymerization, but some does happen subsequently.

**Table 7.** ROMP of norbornene by **8**. All polymerizations were done for 5 hours at room temperature before quenching

| equivs norbonene | solvent | Mn (x $10^3$ g/mol) | Xn | PDI | % trans |
|---|---|---|---|---|---|
| 10.9 | toluene | 1.6 | 17 | 1.25 | 24 |
| 45.5 | toluene | 6.3 | 67 | 1.2 | 21 |
| 92.0 | toluene | 11.3 | 120.2 | 1.14 | 8 |
| 185.6 | toluene | 17.4 | 185.3 | 1.10 | 8 |
| 300.0 | toluene | 34.5 | 367.27 | 1.17 | 12 |
| 465.3 | toluene | 44.9 | 477.7 | 1.24 | 6 |
| 1747.0 | toluene | 205.1 | 2182.7 | 1.15 | 20 |
| 36 | benzene | 5.4 | 57 | 1.15 | 11 |
| 83 | benzene | 10.6 | 113 | 1.2 | 9 |

The living character of **8** has also been examined. A usual way to assess it is to plot the number-averaged molecular weight versus the ratio of monomer to catalyst. Over a broad range of molecular weights we have obtained a linear plot, as well as low PDIs (Figure 19). This result is to be contrasted with the polymerization of norbornene by **4**, where secondary metathesis is important, as proven by large polydispersity indices as well as a high ratio of trans double bonds. Because of the fast initiation of norbornene by **8**, a propagating carbene could be observed by proton NMR. When 53 equivalents of norbornene are added to **8**, only one broad peak for the propagating carbene is observed downfield, at 11.3 ppm in deuterated benzene. This peak is believed to correspond to the propagating carbene for the phosphite-bound complex (see Table 8). After 2 days, only 15% of this species has decomposed, whereas after 2 months, 70% has decomposed. **8** contains the mixture of syn and anti carbene rotamers. The syn / anti ratio

of 8 has been found to vary from batch to batch, with generally a high preference for the anti isomer (> 80%). It is unclear why only one rotamer is observed by NMR for the propagating carbene of 8 plus norbornene (contrasting with the observations for 8'). Schrock and coworkers[53] have shown that, for catalyst 4, the anti isomer initiates better than the syn one, but that syn propagating carbene predominates. This explanation could be applied to our observations. Nevertheless, for all other catalysts we have studied, both syn and anti propagating carbenes are usually observed (see Table 8).

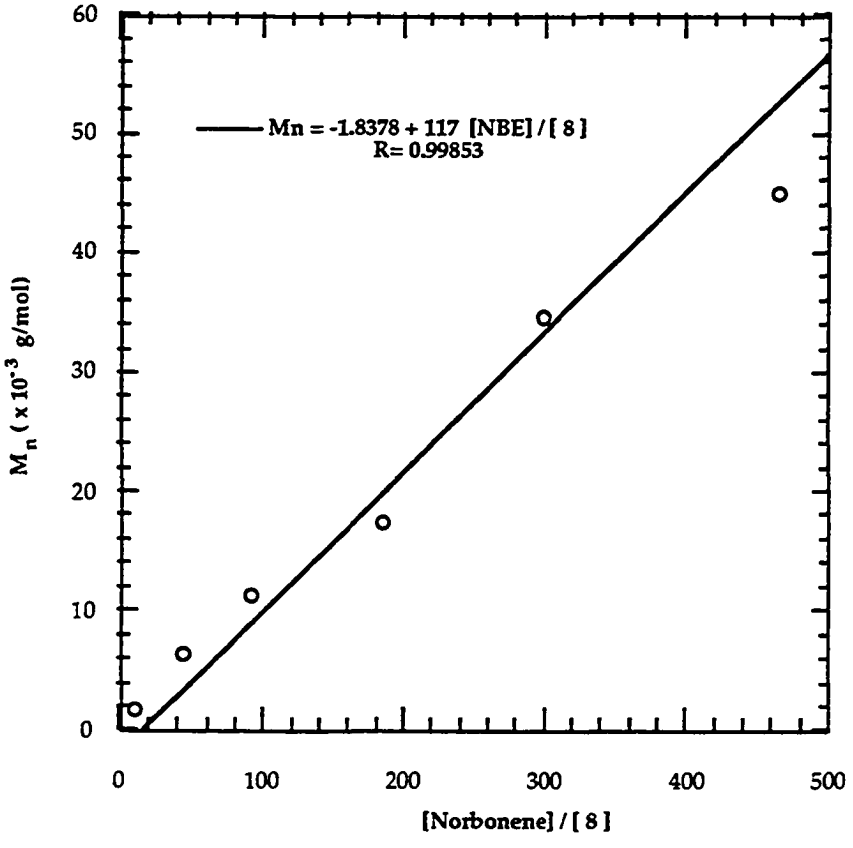


Figure 19. Polymerization of NBE by 8.

b. Polymerization by other catalysts

Norbornene is rapidly polymerized by 8' in benzene or toluene (with THF). The polymer initially contains a high ratio of *cis* olefin (93% cis by $^1H$ NMR, after a reaction time of 2 hours). Due to secondary metathesis with polymer double bonds, the *trans* amount increases with longer reaction times, even after completion of polymerization. After 2 days in benzene, the polymer is 20% *trans*, and after 2 months, 70% *trans*.

Proton NMR indicates the presence of two propagating carbenes (syn at 9.65 ppm, anti at 11.3 ppm, Table 8, Figure 20), which present an unresolved coupling pattern at room temperature. When a sample of polynorbornene[5] is prepared in toluene-$d^8$ at -65 °C, the polymer is observed to be highly cis (> 95 %). In this case, the syn propagating carbene is a doublet (J = 8.7 Hz) (Figure 20), whereas the anti propagating carbene is a broad signal which overlaps with the anti initiating carbene. When cis-trans isomerisation occurs, the syn propagating carbene shows a more complex pattern, which appears to be the resonance of the former carbene superimposed with a new doublet. This new doublet possibly corresponds to the propagating carbene having a *trans* double bond adjacent to the cyclopentyl ring.

---

[5] [8'] = 0.013 mol/l, [THF] = 0.21 mol/l, [norbornene] = 0.12 mol/l, in toluene d8.

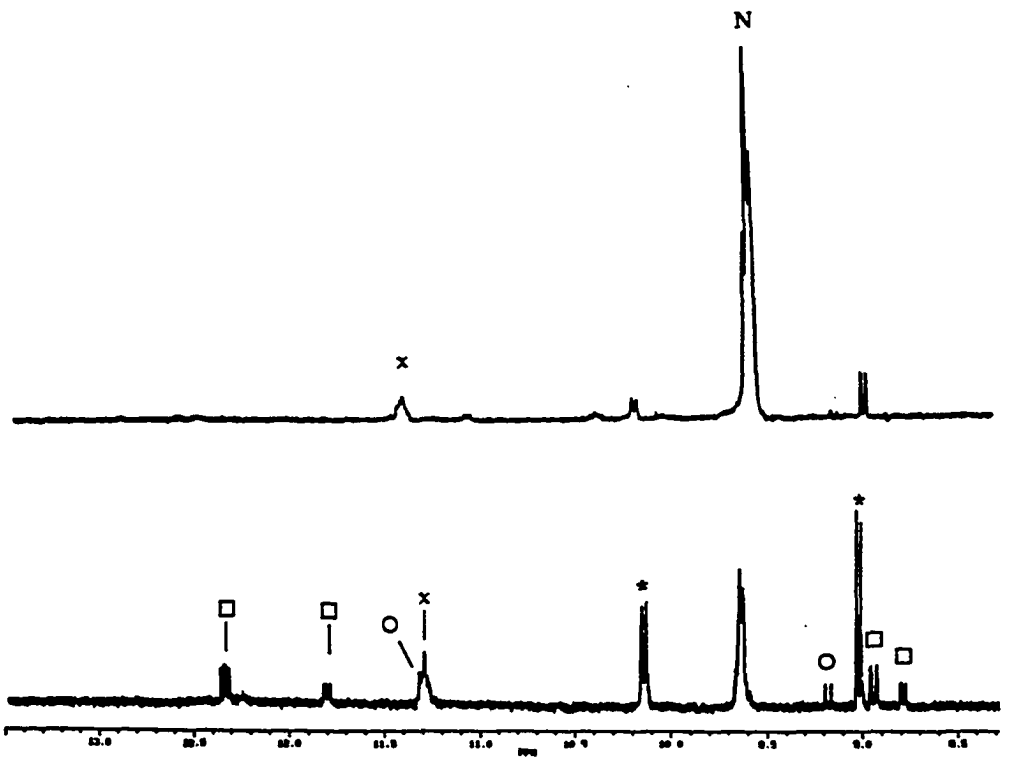


**Figure 20** $^{1}H$ NMR of the carbenic region of a polynorbornene sample with 8'. N: syn propagating carbene; x anti propagating carbenes, * syn 8' (carbene proton downfield, vinyl proton upfield); O anti 8' (carbene proton downfield, vinyl proton upfield); □ phosphite carbenes 8 (carbene proton downfield, vinyl proton upfield). Bottom spectrum: PNBE made at -65 °C; top spectrum, same sample after warming at room temperature.

Table 8. $^1H$ NMR data for the propagating carbenes of selected polymers. The data correspond to a benzene solution at room temperature.

| MON | catalyst | carbene | | J syn (Hz) | J anti (Hz) | % syn |
|---|---|---|---|---|---|---|
| | | δ syn | δ anti | | | |
| NBE | **8** | 11.3 | - | - | - | 100 |
| NBE | **8'** | 9.7 | 11.3 | 8.7 | - | 93 |
| COE | **8'** | 9.8 | 11.2 | 6.5 | - | > 95 |
| COD | **8'** | 9.8 | 11.2 | - | - | > 95 |
| PhCOT | **8'** | 10.0 | 11.0 | 11.45 | 12.97 | 80 |
| PhCOT | **8'** | 9.9 | - | 11.45 | - | |
| sBCOT | **8'** | 11 - 10 | 11.5 - 11.3 | - | - | 85 |
| NBE | **10** | 10.87 | - | | - | > 95 |
| COD | **10** | 11.1 | - | - | - | > 95 |
| NBE | **11** | 11.6 | 11.19 | 8.1 | - | 95 |
| COD | **11** | 11.75 | 11.65 | - | - | 85 |
| sBCOT | **11** | 12.3-12.8 | - | - | - | - |

The propagating carbene of norbornene with **8'** slowly decomposes: 30% of it is still present after 2 days. An identical propagating carbene could be observed (but in a smaller amount), with **4'** as a catalyst in benzene. Using Gold's equation, it was found that **8'** initiates the polymerization of norbornene nine times better than **4'** (Table 4). This result is easily understandable because of the steric hindrance of the neopentylidene carbene **4'**. The polymers obtained from **8'** show a relatively narrow molecular weight distribution (Table 9), however it is too broad to consider the polymerization as living (typically 1.3). Noticeably, because the polymerization is rapidly initiated, the molecular weight depends linearly with the ratio of monomer to catalyst (Figure 21), in contrast with norbornene polymerizations by **4**.[2] As is usually the case for norbornene polymerization with tungsten catalysts, the polymer exhibits a very high molecular weight shoulder.

Polymerization by **11** is similar to polymerization by **8'**. However, it seems that the high molecular weight shoulder can be quite important, even

predominant (entry 6 of Table 9). In addition, the PDIs seem larger than for **8'**.

**Table 9.** ROMP of norbornene using **8'** or **11.** All polymerizations were done for 30 minutes at room temperature in toluene before quenching with benzaldehyde. The ratio of THF to **8'** is 20 ± 5.

| catalyst | [MON] (mol/l) | equivs norbonene | Mn (x $10^3$ g/mol) | Xn | PDI |
|---|---|---|---|---|---|
| **8'** | 0.13 | 24 | 2.4 | 26 | 1.30 |
| **8'** | 0.13 | 46 | 5.2 | 55 | 1.45 |
| **8'** | 0.13 | 78 | 6.6 | 70 | 1.25 |
| **8'** | 0.13 | 150 | 13.8 | 147 | 1.30 |
| **8'** | 0.13 | 312 | 27.4 | 291 | 1.25 |
| **11** | 0.67 | 33 | 95.0 | 1010 | 2 |
| **11** | 0.67 | 71 | 3.6 | 38 | 1.4 |
| **11** | 0.67 | 118 | 11.7 | 124 | 1.9 |
| **11** | 0.67 | 260 | 29.0 | 276 | 1.4 |
| **11** | 0.67 | 451 | 42.4 | 451 | 2.1 |

### 3. Polymerization of cyclooctadiene (COD) and cyclooctene (COE)

**8'** and **11** polymerize COD and COE neat or in solution, giving high molecular weight polymers of low or medium PDIs. A typical polymerization by **8'** (typically 2 hours) is faster than for **11** (typically 2 days). Propagating carbenes can be detected readily by proton NMR for **8'** : COE gives rise to a poorly resolved triplet at 9.85 ppm (J = 6.5 Hz), whereas COD shows a broad resonance at 9.8 ppm. Anti rotamers can be detected, though in small amounts, at 11.2 ppm. Similar propagating carbenes can be detected in small amounts when **4'** is used under identical conditions.

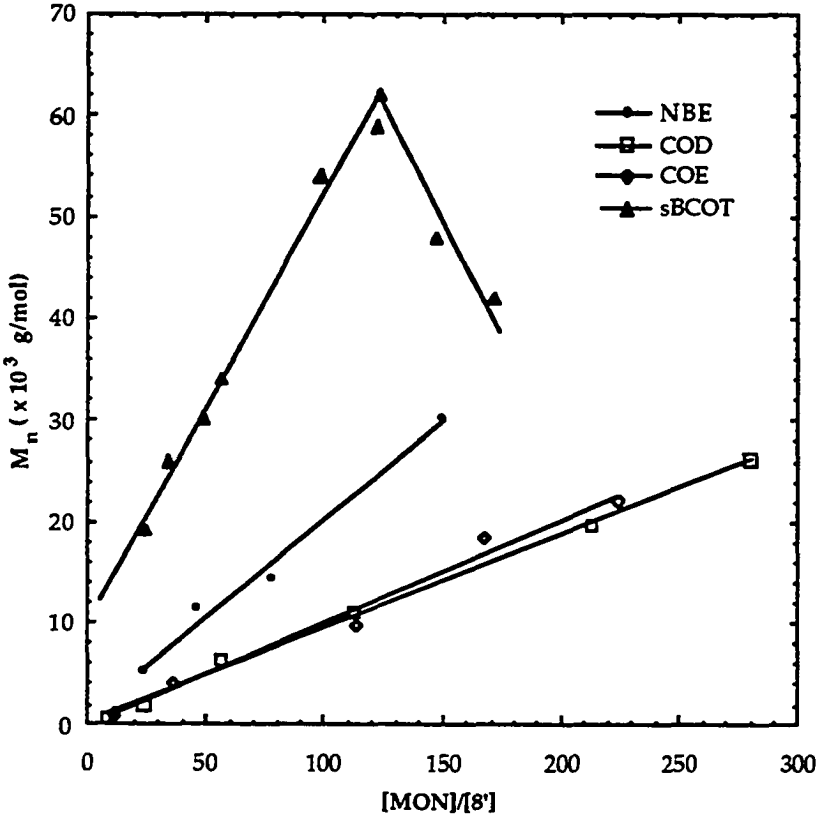


**Figure 21.** Molecular weight of the ROMP polymers of norbornene (NBE), cyclooctene (COE), cyclooctadiene (COD) and *sec*-butylcyclooctatetraene (sBCOT) by **8'**. The exact polymerization conditions are shown in the tables 9, 12 and 13. The aspect of the sBCOT curve is explained in the text.

These carbenes decompose slowly at room temperature over a period of 2 days. In contrast, the sluggish **11** is able to initiate the polymerization of COD (see Table 5), giving a propagating carbene which is stable for days in solution.

**8'** produces a significant amount of backbiting, and reaches thermodynamic equilibrium rapidly (see previous chapter). For example, when the polymerization of COD is done in benzene at 281K for 6 hours, the polymer is 75 % cis, and the PDI is 1.61. If the polymerization is done under the same conditions, and then left at room temperature for 48 hours, the polymer is 91% trans, with a PDI of 1.72. On the other hand, after one week, **11** produces a very small amount of cyclic oligomers, and does not reach thermodynamic equilibrium.

The microstructure of the polymer of COD (that is to say polybutadiene) is strongly dependent on the history of the polymerization (see Tables 10 and 11). Because backbiting scrambles cis and trans double bonds, statistical arguments have been used to calculate the amount of cis and trans double bonds prior to any backbiting (Appendix 2). For that purpose, we have used the fact that in COD polymerization, trans-trans sequences are only formed by backbiting. We found that the polymer contains 95% cis double bond before backbiting, independently of the polymerization temperature. Because 50% of the cis double bonds present in the monomer are not touched during the ring-opening, we can conclude that, during the ROMP reaction, in only 10% of the insertion steps is a trans double bond created. It is therefore possible to conclude that the addition of COD monomer to **8'** or **11** is very regioselective.

In contrast to **8'**, we found that the amount of trans-trans dyads, which is a fingerprint of the backbiting reaction, is zero (to the resolution of $^{13}C$

NMR) for the polymerization of COD by **11**. Nevertheless, the PDIs of the polymers are typically about 1.6 (Table 12), indicating that some backbiting has occurred. It should be noticed that only one backbiting reaction per chain is necessary to generate a polymer distribution with a PDI between 1.5 to 2.[66] However such a small amount of backbiting is not going to be detected by NMR. The relationship between COD/CAT and the molecular weight of the polymer is linear for both catalysts **8'** and **11** (See Table 12 and Figure 21). The linearity is greater for **11**, which merely produce cyclics, than for **8'**.

**Table 10.** Polymerization of COD by **8'** and **11** at different temperatures. These same entries are also used in Table 11.

| Temp. (°C) | Catalyst | [COD] / [CAT] | [THF] / [CAT] | [MON] (mol/l) | reaction time | Mn ($x10^3$ g/mol) | PDI |
|---|---|---|---|---|---|---|---|
| 16 | 8' | 153 | 73 | 0.93 | 3 hours | 33 | 1.65 |
| 4 | 8' | 142 | 73 | 0.86 | 3 hours | 30 | 1.6 |
| -6 | 8' | 126 | 73 | 0.77 | 5 hours | 41 | 1.55 |
| -16 | 8' | 250 | 117 | 1.3 | 2 days | 23 | 1.6 |
| -46 | 8' | 420 | 117 | 2.0 | 2 days | 39 | 1.8 |
| 16 | 11 | 164 | 0 | 0.6 | 1 day | 30 | 1.7 |

**Table 11.** Dyad analysis of polybutadiene, and calculation of cis/trans ratio in the absence of backbiting. Experimental conditions are detailed in Table 10.

| Temperature (°C) | catalyst | % t/t dyads | % c/c dyads | % cis without backbiting | % trans without backbiting |
|---|---|---|---|---|---|
| 16 | 8' | 13.7 | 49.2 | -a | -a |
| 4 | 8' | 10.8 | 40.3 | -a | -a |
| -6 | 8' | 1.7 | 75.3 | 94.5 | 5.5 |
| -16 | 8' | 5.1 | 57.9 | 92.2 | 7.8 |
| -46 | 8' | 2.15 | 72.65 | 94.1 | 5.9 |
| 16 | 11 | 0 | 92.23 | 92.2 | 7.8 |

a. cis:trans ratio cannot be calculated for polymers which are not highly cis (see Appendix 2).

**Table 12.** ROMP of COD and COE catalyzed by 8' and **11.** All polymerizations were done for 3 hours at room temperature in toluene. The ratio of THF to 8' is 20 ± 5.

| Monomer | Catalyst | [MON] / [CAT] | $M_n$ ($x10^3$ g/mol) | $X_n$ | PDI |
|---|---|---|---|---|---|
| COD | 8' | 9 | 0.6 | 5.6 | 1.6 |
| COD | 8' | 24 | 1.9 | 17.5 | 1.8 |
| COD | 8' | 56 | 6.3 | 58.3 | 2.1 |
| COD | 8' | 112 | 11.0 | 101.8 | 1.45 |
| COD | 8' | 213 | 19.7 | 182.4 | 2.5 |
| COD | 8' | 280 | 26.3 | 243.5 | 1.6 |
| COD | 8' | 505 | 61.2 | 566.7 | 1.6 |
| COE | 8' | 12 | 1.0 | 9.3 | 1.6 |
| COE | 8' | 36 | 4.1 | 37.5 | 1.9 |
| COE | 8' | 113 | 9.9 | 90.7 | 1.5 |
| COE | 8' | 167 | 18.4 | 167.2 | 2.0 |
| COE | 8' | 224 | 22.1 | 200.9 | 1.6 |
| COD | **11** | 49 | 7.5 | 69 | 2.1 |
| COD | **11** | 106 | 14 | 129 | 2.1 |
| COD | **11** | 177 | 19 | 175 | 2.1 |
| COD | **11** | 266 | 26 | 240 | 2.1 |
| COD | **11** | 355 | 36 | 333 | 2.1 |

4. Polymerization of *s*BCOT

8' and **11** are conjugated carbenes and therefore resemble the propagating carbene of *s*BCOT. As a consequence, the rates of propagation should not be extremely different from the rates of initiation. When 6.2 equivalents of *s*BCOT are added to a solution of 8', most of the initial carbenes disappear within 5 minutes. The starting carbenes resonances are replaced by a set of doublets between 10.9 ppm and 10.5 ppm (Figure 22). These resonances are tentatively attributed to propagating carbenes. When, instead of THF, 2-methylTHF is used for complexing 8', the resonances are slightly shifted, indicating that the detected species include THF. If the new resonances are attributed to propagating carbenes, it is then possible to

calculate the $k_i/k_p$ by the use of Gold's equation. In the presence of 42 equivalents of THF, the apparent $k_i/k_p$ is 1 for **8'**. In similar conditions, no propagating carbene can be detected by proton NMR when **4** is used as a catalyst. For **11**, as for **8'**, complete disappearance of the initiating carbene upon addition of sBCOT gives very broad resonances between 12.3 and 12.8, which are assigned to phosphine-bound propagating carbenes.

Because the NMR of sBCOT carbenes is very complicated, the case of benzoCOT has been studied (**14**). In this case, 3 propagating carbenes are possible (Figure 23). Because one of them would be a disubstituted carbene, only two of them can be observed by $^1H$ NMR. In Figure 23, 2 syn propagating carbenes are observed, and 2 smaller anti propagating carbenes (Table 8). The relative amounts of these carbenes yields information on the regioselectivity of the attack of the catalyst **8'** on phenylCOT. Interestingly, we found that the double bond in alpha position to the benzo group is preferred (Figure 24). The boat type geometry of the monomer may furnish a possible interpretation of this result: the phenyl group blocks the access to the lower face of the monomer, whereas the alpha double bonds are accessible.

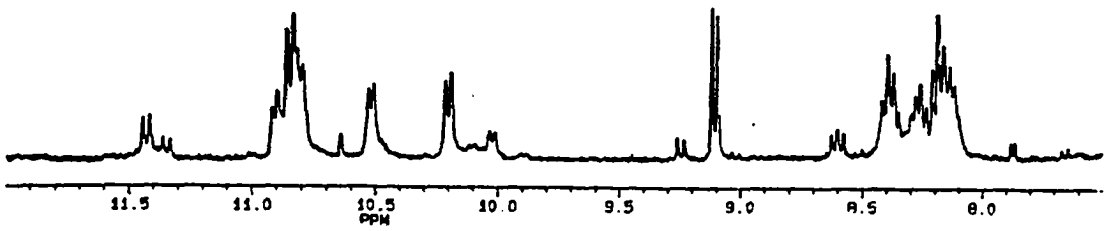


**Figure 22.** Carbene region of sBCOT, in the presence of 8' (toluene d8, - 55 °C)

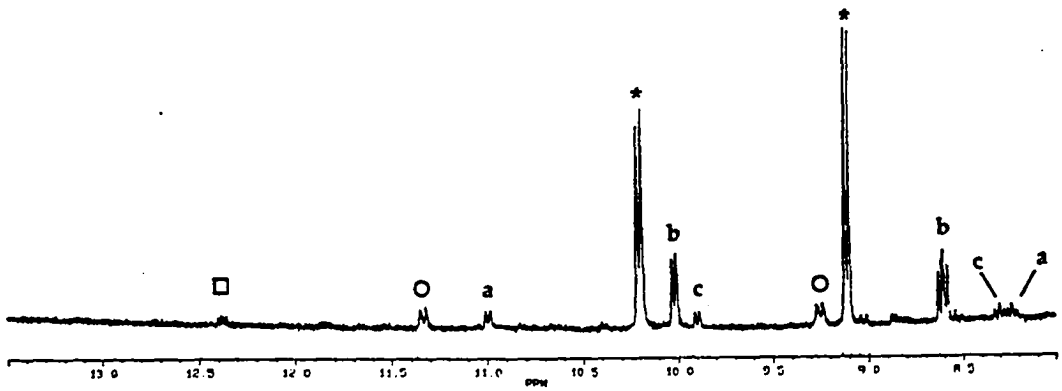


**Figure 23.** Carbene region of benzoCOT, in the presence of 8' (in benzene $d^6$ at 40 °C). Carbene peaks are downfield (> 9.5 ppm) and vinyl protons are upfield ( < 9.5 ppm).
□ : 8, anti carbene; O : 8', anti rotamer; a : poly(benzoCOT) carbene, anti rotamer; b and c : poly(benzoCOT) carbene, syn rotamer; another anti carbene of poly(benzoCOT) shows a resonance at 10.8 ppm.

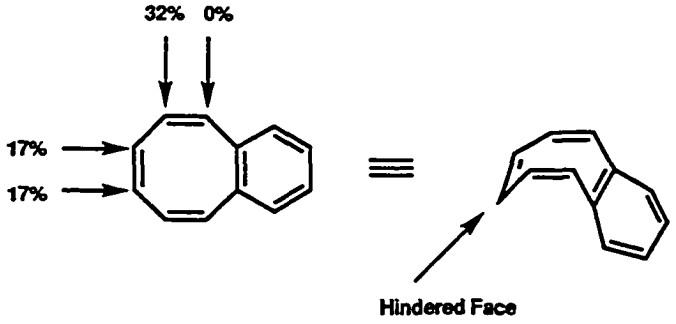


**Figure 24.** Regioselectivity of the attack of 8' on benzoCOT. The percentages of attack vary slightly during the reaction and the experimental conditions. Conditions used in this case: benzene-$d^6$ at 40 °C, [8'] = 0.0008 mol/l, [phenylCOT] = 0.014 mol/l.

Since good initiation is achieved, it is now possible to assess the reactivity of 8' or 11 toward sBCOT. This was not possible beforehand, because the amount of initiated species by 4 is unknown. Kinetics of polymerization were studied at different temperatures using NMR (see experimental section).

We found that in the presence of an excess of THF, the polymerization is first order in monomer, and first order in catalyst for catalyst 8' (Table 13). When very little THF is used, there seems to be slight deviations to the first order behavior in monomer, at least at the start of the polymerization. This behavior is expected because THF behaves as a competitive inhibitor of the polymerization, and at low THF concentrations, there is competition between monomer and THF coordination to the catalyst. The rate of polymerization in this case is :

$$\text{Rate} = k_p [\text{MON}] \frac{[\text{CAT}]}{\frac{[\text{THF}]}{K_d} + \frac{[\text{MON}]}{K'}} \qquad (4)$$

**Table 13.** Kinetics of polymerization of sBCOT by 8'. All the polymerizations have been carried out in toluene-d8.

| Temp (°C) | [sBCOT] (mol/l) | [THF] (mol/l) | [sBCOT] /[8'] | %bb[a] | $k_p$ ($l.mol^{-1}.min^{-1}$) | [HFB][b] /[8'] |
|---|---|---|---|---|---|---|
| 20 | 0.28 | 0.28 | 44 | 17 | 1.02 | 0.12 |
| 28 | 0.28 | 0.28 | 49 | 23 | 1.80 | 0.12 |
| 36 | 0.28 | 0.28 | 48 | 26 | 3.78 | 0.12 |
| 44 | 0.28 | 0.28 | 48 | 24 | 5.91 | 0.12 |
| 52 | 0.28 | 0.28 | 48 | 32 | 11.12 | 0.12 |
| 18 | 0.22 | 0.095 | 66 | 23 | 1.82 | 0.12 |
| 18 | 0.20 | 0.14 | 52 | 20 | 1.64 | 0.12 |
| 18 | 0.22 | 0.21 | 56 | 19 | 0.70 | 0.12 |
| 18 | 0.26 | 0.39 | 65 | 17 | 0.45 | 0.12 |
| 40 | 0.25 | 0.036 | 59 | 26 | 11.2 | 0.12 |
| 40 | 0.25 | 0.082 | 57 | 25 | 6.57 | 0.12 |
| 40 | 0.27 | 0.156 | 64 | 24 | 5.99 | 0.12 |
| 40 | 0.18 | 0.28 | 66 | 20 | 4.85 | 0.12 |
| 18 | 0.47 | 0.80 | 82 | 7 | 0.44 | 0.03 |
| 18 | 0.47 | 0.80 | 82 | 15[c] | 0.53 | 3.22 |
| 18 | 0.47 | 0.80 | 82 | 21[c] | 0.60 | 24 |

a. percentage of monomer converted in sec-butylbenzene.
b. amount of alcool, as measured by $^{19}F$ NMR (see chapter 3).
c. the amount of backbiting increases with time (see chapter 3).

where $k_p$ is the rate constant of propagation, $K_d$ is the dissociation constant of THF and K' is a constant that is unneeded for our purpose. The apparent rate of propagation $k_p$app can be equated to $k_p K_d$ [CAT] / [THF]. Plotting $1/k_p$app versus [THF] (Figure 25) allows one to find the rate of polymerization in the absence of THF (using the dissociation constant found for the initiating carbene). These rates are 33 l $mol^{-1}$ $s^{-1}$ at 18 °C, and of 500 l $mol^{-1}$ $s^{-1}$ at 40 °C. Finally, activation parameters can be calculated by an Eyring plot (Figure 26). The large negative entropy ( $\Delta\Delta S^{\ddagger}$ = -21 Cal/K) suggests that for the polymerization of sBCOT, olefin coordination is the

slow step. In many other ROMP polymerizations, the rate determining step is believed to be the cleavage of the metallacycle.[36, 64]

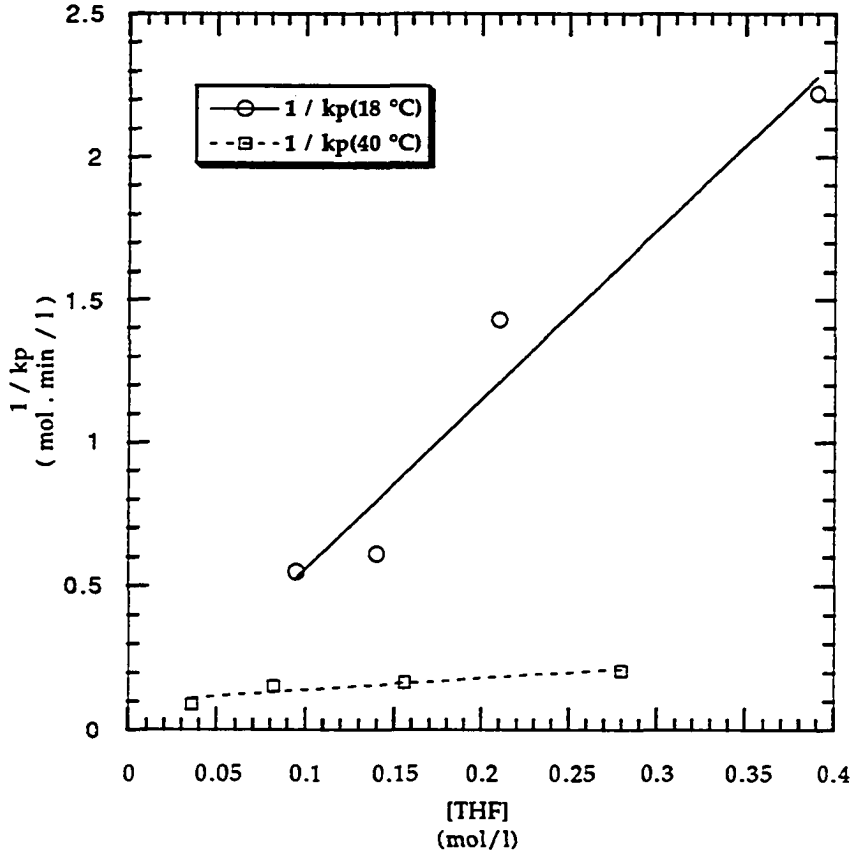


**Figure 25.** Inverse of the apparent rate of polymerization of sBCOT by 8' versus THF concentration. The polymerization conditions are listed in Table 13.

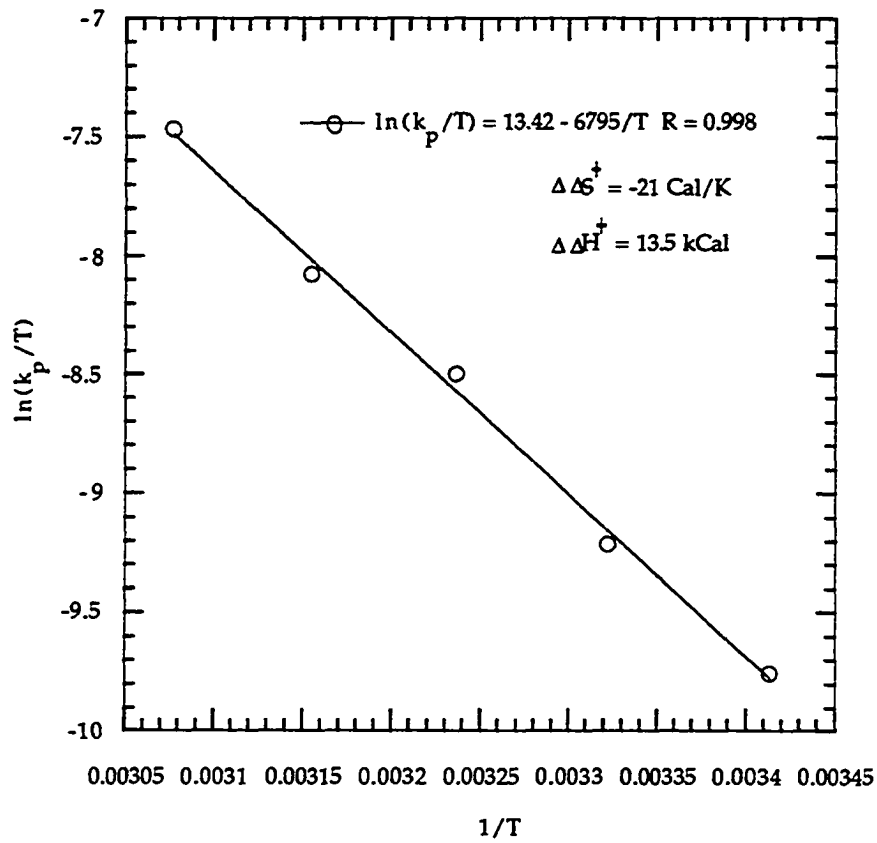


**Figure 26.** Eyring plot for the polymerization of sBCOT by **8'**. The polymerization conditions are listed in Table 13.

Kinetics of sBCOT polymerization by **11** is much slower than polymerization by **8'**. For example, it has been found that polymerization by **11** takes two days at room temperature under usual conditions. Nevertheless, slight warming greatly accelerates the polymerization: at 35 °C, the polymerization goes at a rate comparable to that of **8'** at room temperature (Figure 27). As observed in Figure 27, the reaction appears to show a mixture of zero-order kinetics at high monomer concentration and first-order kintics at low monomer concentration. This behavior is typical of phosphine inhibition. At high monomer concentration, all the active sites are saturated by the monomer, and the kinetics is controlled by the rate of

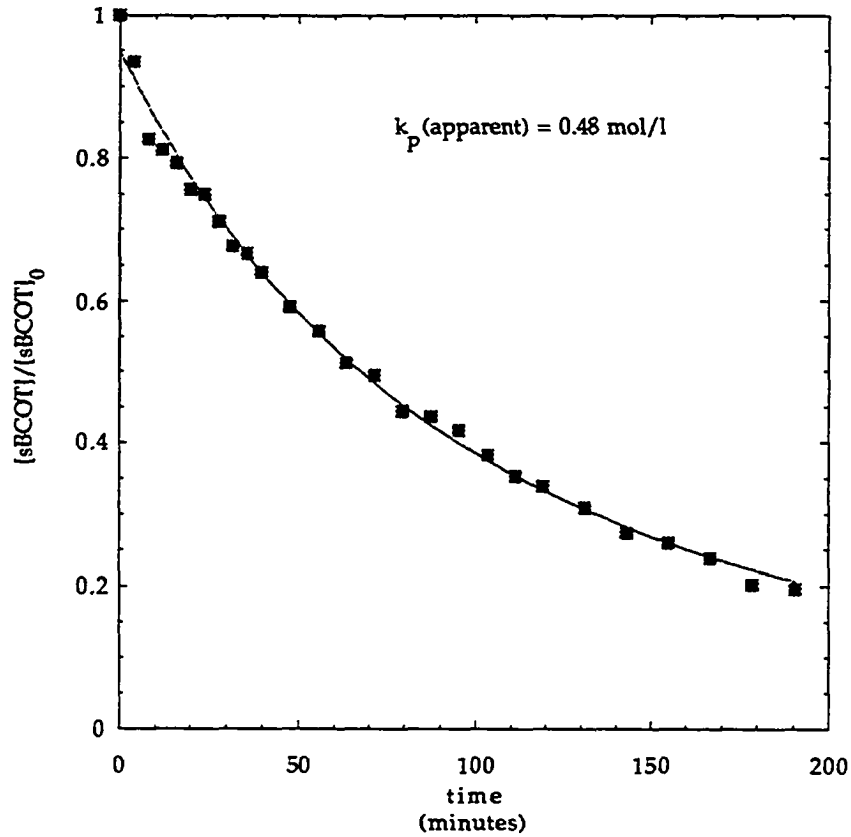


**Figure 27.** Kinetics of polymerization of sBCOT by **11** at 35 °C in toluene $d^8$. [sBCOT] = 0.27 mol/l, [sBCOT] / [**11**] = 12.

formation of the metallacycle, whereas at low concentration of monomer, a competition exists between the phosphine and monomer occupancy of the active site.

Finally, polymers of sBCOT have been synthesized in solution using **8'**. In contrast with process in neat monomer, solution polymerization reduces the viscosity build-up and permits the reaction to go to higher conversion. After 8 hours of polymerization, 99 % of the monomer is consumed and the reaction mixture is still a liquid (Table 14). Because it has

been possible to improve initiation drastically, as well as to inhibit the backbiting reaction, the PDIs of the resulting polyacetylenes samples are extremely low (< 1.2) . In addition, for low and medium molecular weight samples, there is a linear relationship between the molecular weight of the polymer and the ratio of monomer to catalyst (Figure 21). We are currently analyzing the reasons for the breakdown of this linear relationship for high molecular weight samples (Figure 21). It is possible that, because of their intrinsic chemical fragility, high molecular weight polyacetylenes are degraded during the GPC analysis. Since polymerizations by **11** are slower, monodisperse materials are not obtained. On the other hand, polymerizations with **11'** are rapid (typically done in less than 1 hour), and afford monodisperse polymers.

**Table 14.** ROMP of sBCOT using **8'** and **11'**. All polymerizations were done for 16 hours at room temperature in toluene, then quenched with benzaldehyde. The ratio [THF ]/[**8'**] is 48, the ratio [THF] /[**11'**] is 53.

| catalyst | [MON]/ [CAT] | [MON] (mol/l) | $M_n$ ($\times 10^3$ g/mol) | PDI | %bb[a] |
|---|---|---|---|---|---|
| **8'** | 24.5 | 0.51 | 19.2 | 1.4 | 13 |
| **8'** | 49 | 0.94 | 30.2 | 1.25 | 16 |
| **8'** | 98 | 1.6 | 54 | 1.1 | 14 |
| **8'** | 122 | 1.8 | 59 | 1.1 | 15 |
| **8'** | 123 | 1.1 | 62 | 1.1 | 13 |
| **8'** | 147 | 2.1 | 48 | 1.1 | 17 |
| **8'** | 171 | 2.3 | 42 | 1.3 | 14 |
| **8'** | 34 | 1.0 | 26 | 1.3 | 6[b] |
| **8'** | 56 | 1.0 | 34 | 1.2 | 5[b] |
| **11'** | 32 | 1.1 | 24.1 | 1.1 | 12 |
| **11'** | 46 | 1.1 | 32.3 | 1.1 | 12 |
| **11'** | 79 | 1.1 | 48 | 1.2 | 9 |

a. determined by $^1H$ NMR in $CDCl_3$ using the method described by C. Gorman.[13]

b. polymerizations done using a new batch of **8'**, which contains little HFB

## V. Experimental Section

**General Methods.** All manipulations of air- or moisture-sensitive compounds were carried out under a nitrogen atmosphere in a Vacuum Atmospheres dry box equipped with a MO-40-1 purification train, or under an argon atmosphere , using standard Schlenk techniques on a vacuum line. Solids were weighed in dry box. Toluene, ether, benzene and THF were distilled from sodium benzophenone ketyl, and stored under an argon atmosphere. THF was stored under argon over activated 4Å molecular sieves (activation during 12 hours at 200 °C *in vacuo*). Pentane was separated from olefinic residues by trituration on concetrated sulfuric acid before drying. Prior to use, solvents were passed through a small column of silica gel (activited *in vacuo* for 12h at 350 °C). Cyclooctene (COE) and cyclooctadiene (COD) were distilled from calcium hydride and freeze-pump-thaw three times before use. Norbornene (NBE) was stirred with sodium at 60 °C, distilled into a Schlenk flask and degassed. *Sec*-butylcyclooctatetraene (*s*BCOT) was prepared as described in the literature, and passed through a small column of silicagel before use. $W(CHR')(NAr)(OR)_2$ (Ar = 2,6-$C_6H_3$-*i*-$Pr_2$; OR = $OC(CF_3)_2(CH_3)$) (4 and 5), $W(CH{=}CH{=}C(C_6H_5)_2)(NAr)(OR)_2{\cdot}P(OMe)_3$ (8) (Ar = 2,6-$C_6H_3$-*i*-$Pr_2$; OR = $OC(CF_3)_2(CH_3)$) and $(Cp^*RuOMe)_2$ were prepared as described in the literature, except for $W(=NAr)Cl_4$ and $WCl_2$[N-2,6-$C_6H_3$-(*i*-Pr)$_2$][$P(OMe)_3$]$_3$. $WCl_2$[NPh][$PMe(Ph)_2$]$_3$ was graciously prepared by L. Johnson. All the glassware of NMR experiments, including storage vials and NMR tubes, was washed with concentrated ammonia, and then dried in an oven at 150 °C for 12 hours. CuCl (Aldrich) was dried under vacuum, and used without further purification. NMR experiments were effected on a Brucker 500 AM spectrometer (500.138 MHz $^1H$, 470.56 $^{19}F$, 202.69 $^{31}P$). Kinetics

measurement for sBCOT polymerization were effectued on a QE Plus-300 MHz spectrometer. Polymer molecular weights were analyzed on Waters 150-C ALC/GPC (gel permeation chromatography in toluene equipped with columns Waters Ultrastyragel 105, 104, 103, 500A and a refractometer). The GPC analyses were done at 65 °C, and the molecular weight distribution were calibrated with polystyrene standards for polynorbonene and poly(sBCOT) and with polybutadiene standards for poly(COD) and poly(COE). In the case of polysBCOT, degased, oxygen free toluene was used in the GPC and the temperature was lowered to 55 °C.

**- Preparation of $WCl_4$(=N-Ar), Ar = 2,6-$C_6H_3$-*i*-$Pr_2$**

In a 1l-three-neck round-bottom flask, $WCl_4(O)$ (15.96 g, 46.7 mmol), purchased from Aldrich, is added to 250 ml of octane (distilled from $CaH_2$ and FPT 3 times). Freshly distilled 2,6-diisopropylphenylisocyanate (9.5 g, 46.7 mmol) is added dropwise to the slurry. The slurry rapidly turns darker, and is heated to reflux. Large amounts of $CO_2$ are evolved during the first hour of reflux. After 16 hours of reflux, the homogeneous dark brown solution is cooled to room temperature, and is settled for one hour. A dark powder precipitates out and is filtered through a fritted funnel, and washed with octane then pentane, to afford 13.4 g of a red-brick powder. This powder is a mixture of starting material and product. The powder is dissolved in ca 25 ml of THF, giving a very dark green solution. If the solution is not completely homogeneous, a filtration through a bed of celite is done, to separate insoluble impurities. The celite is washed with additional THF. To the THF solution, pentane (ca 300 ml) is added until the solution become slightly cloudy. The mixture is then cooled to -50 °C for 48 hours,

inducing the crystallization of feathery green needles, which are collected, and washed with pentane (11.4 g, 41%).

$^1H$ ($C_6D_6$) δ 7.20 (d, 2, J = 7.78, H*m*), 6.23 (t, 1, J = 7.78, H*p*), 4.95 (septet, 2, J = 6.68, C*H*Me$_2$), 4.44 (m, 4, $CH_2O$), 1.35 (d, 12, J = 6.68, CH*Me*$_2$), 1.25 (m, 4, $CH_2$).

$^{13}C$ (C6D6) δ 155.98 (Cipso), 146 (Co), 134.26, (Cp), 122.06 (Cm), 73.6 (THF), 27.73 (C*H*(CH$_3$)$_2$), 26.25 (CH(C*H*$_3$)$_2$), 25.36 (THF).

Data for $WCl_4$[N-2,6-$C_6H_3$-(*i*-Pr)$_2$]: $^1H$ ($C_6D_6$) δ 7.05 (d, 2, J = 7.83, H*m*), 6.19 (t, 1, J = 7.80, H*p*), 4.63 (septet, 2, J = 6.68, C*H*Me$_2$), 1.2 (d, 12, J = 6.81, CH*Me*$_2$).

**- Preparation of $WCl_2$[N-2,6-$C_6H_3$-(*i*-Pr)$_2$][P(OMe)$_3$]$_3$**

In a 500 ml Schlenk, a 1% sodium amalgam ( 0.8 g Na, 34.5 mmol, 2.1 eq) is prepared under Ar flow. $WCl_4$[N-2,6-$C_6H_3$-(*i*-Pr)$_2$](THF) (9.4 g, 16.4 mmol) is dissolved in 100 ml of benzene (requiring vigorous stirring). P(OMe)$_3$ (7.73 ml, 65.2 mmol, 4 eq) is added, and the benzene solution is cannula filtered to the sodium amalgam, which is kept at room temperature (the reaction is slightly exothermic). The reaction is vigorously stirred for at least 90 minutes, until the solution is grayish (with a small green tinge). In case $WCl_4$(O) is a contaminant of the starting material, the solution turns gray purple. The slurry is settled overnight and the maximum amount of solution is cannula filtered. It is essential that the minimum amount of spent amalgam gets transferred with the solution, since it seems to interfere with the next step. The spent amalgam may be washed with aliquots of benzene. The collected fractions are then evaporated under reduced pressure and subsequently dried for 12 hours. The solid (or oily) complex is then dissolved in THF and recrystallized from pentane at -50 °C. The first crop affords 6.4 g of a gray powder (49%), and the second 4.2 g (32%).

$^1H$ ($C_6D_6$) δ 7.23 (t, 1, J = 8.5, H*p*), 7.14 (d, 2, J = 8.5, H*m*), 4.6 (septet, 2, J = 6.65, C*H*$Me_2$), 3.76 (t, 18, J = 5.2, *trans*-$P(OMe)_3$), 3.67 (d, 9, J = 10.4, *cis*-$P(OMe)_3$), 1.42 (d, 12, J = 6.65, CH*Me*$_2$).

$^{13}C$ ($C_6D_6$) δ 126.7, 123.8, 52.87, 53.04, 53.14, 27.72, 27.55.

data for $WCl_2O[P(OMe)_3]_3$ (purple impurity)

$^1H$ ($C_6D_6$) δ 3.65 (t, J = 5.4, *trans*-$P(OMe)_3$), 3.62 (d, J = 10.8, *cis*-$P(OMe)_3$).

**- Preparation of $W(=CH-CH=CMe_2)(NPh)(ORf_6)_2.PMePh_2$ (11)**

1.5 g of $W(CH=CH=C(C_6H_5)_2)(NPh)Cl_2.(PMePh_2)_2$ (1.84 mmol, 1 eq.) are dissolved in 20 ml of THF. The solution is cooled at -78 °C. 1g (5.31 mmol, 2.9 eq) of $LiOC(CF_3)_2(CH_3)$ (freshly sublimed) are dissolved in THF, and this solution is added dropwise to the cold solution of the carbene, over 35 minutes. Then the solution is slowly warmed over a period of 12 hours to room temperature. The THF is then evaporated, and the catalyst dissolved in 50 ml of ether. The insoluble LiCl is filtered, and washed again with 50 ml of ether, and the combined ether solutions are concentrated, until 1 ml of ether is left. The thick brown liquid is placed in a small Schlenk tube, which is capped by a septum, and left in the dry box. After two days, crystals have precipitated, and the residual liquid is filtered for a second crop. First crop : 650 mg ( y = 40.6 %), second crop : 312 mg ( y = 19.5 %). The monocrystalline sample is constituted of only the syn rotamer. Less crystalline samples contain both rotamers.

$^1H$ NMR ($C_6D_6$) δ 12.27 (dd, $J_{HH}$ = 10.63 Hz, $J_{PH}$ = 3.27 Hz, 1, W=CHR), 7.49 (dd, $J_{HH}$ = 10.63 Hz, $J_{PH}$ = 1.02 Hz, W=CH-CHR), 7.54 -6.6 (complex m, $H_{aryl}$), 2.09 (s, 3, $O(CF_3)_2(CH_3)$), 2.04 (s, 3, $O(CF_3)_2(CH'_3)$), 1.88 (d, $J_{PH}$ = 3.4 Hz, 3, $PPh_2Me$), 1.85 (s, 3, CMeMe' ), 1.57 (s, 3, CMeMe' ).

$^{13}C$ NMR ($C_6D_6$) syn δ : 259.5, $J_{CP}$ = 12.72 Hz ($C_\alpha$), 154.9 (Cipso, NAr), 137.25, $J_{CP}$ = 3.08 Hz ($C_\beta$), 133.54 (C*o*, NAr), 132.83 (C*p*, NAr), 131.0 ($C_\gamma$), 130.27 (Cδ) 27.45 (Me), 23.87 (Me), 18.4 (C($O^tBuF_6$)).

$^{19}F$ NMR ($C_6D_6$, ref $CFCl_3$): δ : - 76.5, -75.53, 77.94, 78.06

$^{31}P$ NMR ($C_6D_6$): δ : 30.6 ($J_{PW}$ = 154.1 Hz).

**-Observation of W(CH=CH=C($C_6H_5$)$_2$)(NAr)(OR)$_2$ (8*tet*)**

10.4 mg of **5** are dissolved in 712 mg of $CD_2Cl_2$. 4 mg of *cis*-diphenyl-1,3-pentadiene (1.4 eq, prepared by action of ethyledene phopshorous ylide on diphenyl acroleine) are added, and the evolution of the cross metathesis reaction is observed by NMR. After 1 hour at 18 °C, some decomposition has occurred (white precipitate), the cis diene is mainly isomerized to the trans diene, and ca 25 % of **8*tet*** has appeared.

$^1H$ NMR ($CD_2Cl_2$) syn: δ 9.9 (d, J = 9.3 Hz, 1, W=CHR), 8.6 (d, J = 9.3 Hz, W=CH-CHR), 7.5 -6.7 (complex m, $H_{aryl}$), 3.6 (septet, J = 6.9 Hz, 2, $CHMe_2$), 1.40 (s, 6, O($CF_3$)$_2$($CH_3$)), 1.27 (d, J = 6.9 Hz, 12, $CHMe_2$). anti[6]: 10.37 (d, J = 11.4 Hz, 1, W=CHR), 8.3 (d, J = 14.6 Hz, W=CH-CHR)

**-Observation of W(CH=CH=C($C_6H_5$)$_2$)(NAr)(OR)$_2$.CuCl.P(OMe)$_3$ (8-*Cu*)**

3.4 mg of **8** are added to 429 mg of toluene-d8 in a NMR tube. 55 mg of CuCl are added to this tube, the mixture is shaken for 5 minutes at room temperature and then is introduced in the NMR probe at low temperature.

---

[6] The methine protons of this isomer are obscured by the protons of the copper phosphite polymer at 3.45 (d, J = 12.6 Hz).

$^1H$ NMR ($C_8D_8$) syn: δ 10.7 (d, J = 13.3 Hz, 1, W=CHR), 8.75 (d, J = 13.3 Hz, W=CH-CHR), 7.5 -6.7 (complex m, $H_{aryl}$), 3.6 (septet, J = 6.9 Hz, 2, $CHMe_2$), 1.40 (s, 6, $O(CF_3)_2(CH_3)$), 1.27 (d, J = 6.9 Hz, 12, $CHMe_2$), 4.4 (m, $CHMe_2$), 3.6 (m, $CH'Me_2$), 2.05 (s, $O(CF_3)_2(CH_3)$), 1.55 (s, $O(CF_3)_2(CH'_3)$), 1.4 (d, J = 6.2 Hz, $CHMe_2$ ), 1.05 (d, J = 6.2 Hz, $CHMe'_2$). anti: 11.55 (d, J = 13.9 Hz, 1, W=CHR), 9.1 (d, J = 13.9 Hz, W=CH-CHR),

$^{19}F$ NMR (ref $CFCl_3$, in $CD_2Cl_2$): syn δ: - 76.05, -76.21, -76.56, -76.81

$^{31}P$ NMR (ref $P(OMe)_3$[7], in $C_8D_8$): 154 ppm, broad

**-Observation of $W(CH=CH=C(C_6H_5)_2)(NAr)(OR)_2$·THF (12) (Ar = 2,6-$C_6H_3$-*i* $Pr_2$; OR = $OC(CH_3)_3$.**

In a NMR tube, 20.8 mg of $W(CH=CH=C(C_6H_5)_2)(NAr)Cl_2(P(OMe)_3)_2$ and 4.0 mg of lithium *tert*-butoxides are dissolved in benzene d6 (500 ul) and THF d8 (20 ul). The color turns slowly red. After 3 hours at room temperature, NMR indicates that the reaction is complete. **12** is stable in solution, but when the solvent is pumped off, **12** decomposes, making its isolation difficult.

$^1H$ NMR ($C_8D_8$) syn: δ 9.67 (d, J = 11.8 Hz, 1, W=CHR), 9.0 (d, J = 11.8 Hz, W=CH-CHR), 7.5 -6.7 (complex m, $H_{aryl}$), 3.6-3.4 (septet, J = 6.9 Hz, 2, $CHMe_2$), 1.40-1.0 (m) anti: 10.03 (d, J = 15.3 Hz, 1, W=CHR), 9.35 (d, J = 15.3 Hz, W=CH-CHR). syn/anti = 54/46

**-Preparation of $W(CH=CH=C(C_6H_5)_2)(NAr)(OR)_2$·THF (8') (Ar = 2,6-$C_6H_3$-*i* $Pr_2$; OR = $OC(CF_3)_2(CH_3)$).**

---

[7] The phosphorous NMR were assigned using for reference $\delta(P(OMe)_3)$ = 140 ppm.

Preparation with $(Cp^*RuOMe)_2$ In a typical experiment, 6.9 mg of 8 ($7.55\ 10^{-3}$ mmol) and 5.6 mg of Cp*RuOMe (Ru:W = 2.76:1) are disolved in 456.8 mg of benzene. Immediately, to the dark red solution, 11.7 mg of THF are added at once (THF: W = 21.5:1).

Preparation with CuCl In a typical experiment, 4.4 mg of 8 ($4.24\ 10^{-3}$ mmol) and 99 mgs of CuCl ( Cu:W = 84:1) are stirred for half an hour in 437 mg of benzene, containing deuterated THF at a concentration of 0.33 Mol/l (THF:W = 38:1). The excess CuCl is then removed by filtration through a 0.5um micropore filter. The solution still contains a copper chloride phosphite polymer.

$^1H$ NMR ($C_6D_6$) syn: δ 10.2 (d, J = 11.1 Hz, 1, W=CHR), 9.1 (d, J = 11.1 Hz, W=CH-CHR), 7.5 -6.7 (complex m, $H_{aryl}$), 3.9 (septet, J = 6.9 Hz, 2, $CHMe_2$), 1.45 (s, 6, $O(CF_3)_2(CH_3)$), 1.3 (d, J = 6.9 Hz, 12, $CHMe_2$). anti[8]: 11.4 (d, J = 14.6 Hz, 1, W=CHR), 9.3 (d, J = 14.6 Hz, W=CH-CHR), 7.5 -6.7 (complex m, $H_{aryl}$), 1.34 (s, 6, $O(CF_3)_2(CH_3)$), 1.21 (d, J = 6.45 Hz, 12, $CHMe_2$ ).

$^{13}C$ NMR[9] ($C_6D_6$) syn δ : 251.92 ($C_\alpha$), 151.07 (Cipso, NAr), 146.91 ($C_o$, NAr), 138.27 (Cipso, -Ph), 137.98 (Cipso, -Ph), 133.70 ($C_\gamma$), 131.7 ($C_p$, NAr), 123.09 ($C_\beta$), 28.31 (methine), 23.87 (methyl), 18.4 ($C(O^tBuF_6)$).

anti δ : 254.99 ($C_\alpha$), 151.17 (Cipso, NAr), 145.2 ($C_o$, NAr), 139.07 (Cipso, -Ph), 138.59 (Cipso, -Ph), 132.21 ($C_\gamma$), 131.7 ($C_p$, NAr), 29.0 (methine), 23.64 (methyl), 19.24 ($C(O^tBuF_6)$).

$^{19}F$ NMR ($C_6D_6$, ref $CFCl_3$): δ : - 78.35

---

[8] The methine protons of this isomer are obscured by the protons of the copper phosphite polymer at 3.45 (d, J = 12.6 Hz).

[9] Because the NMR is done in benzene, some resonances are overlapped by the solvent, leading to an incomplete assignment.

**-Measurement of $K_1$ and $K_2$.**

In a NMR tube, 11.0 mg of 8 are dissolved in 462 mg of toluene d8. 89 mg of CuCl are added at once, and a $^1H$ NMR spectrum is registered as soon as possible at 281 K. Then, aliquots of THF d8 are added with a gas-tight syringe. Spectra are recorded until 26 ul of THF are added. At this concentration of THF, the CuCl concentration in solution begins to be important, because of the formation of a CuCl.THF complex. $K_1$ and $K_2$ are extracted by linearization at low THF concentrations (until 6 ul).

**-Typical measurement of $k_p/k_i$.**

In a vial, 6.0 mg of catalyst and 17.5 mg of CuCl are stirred in 1ml of deuterated benzene and 30 ul of deuterated THF for half an hour. After filtration through a 0.5 um Millipore filter, 20 ul of a 0.0182 molar solution of ferrocene in deuterated benzene are added (as reference for integration). Precisely 20ul of COD are added at once in the NMR tube through a septum, and the NMR tube is stirred immediatly. The NMR analysis is performed as soon as possible in order to minimize the decomposition. The measurement is repeated three times.

**-Typical sBCOT polymerization.**

In a small round bottom flask, 3.0 mg of 8, 11.7 mg of CuCl and 10 ul of THF are added to 200 ul of toluene. The mixture is stirred for half an hour, and 77 ul of sBCOT is then added at once. The polymerization takes between 8 to 16 hours. A small aliquot of the polymer is withdrawn for NMR analysis and 10 ul of benzaldehyde are then added to the rest of the dark violet solution. The solution is stirred for 1 hour, and the polymer

solution is then passed through a plug of silicagel, and filtered for GPC analysis. The small aliquot is dried under high vacuum, to leave a dark residue which is then analyzed by $^1H$ NMR, according to the litterature.[13]

**- Typical polymerization of COD**

In the dry-box, 307 mg of a toluene $d^8$ solution of 8' ($1.0\ 10^{-5}$ mol complexed by 1.17 mmol of THF) are added to a NMR tube. The tube is capped by a septum wrapped in parafilm. The tube is cooled at - 46 °C for 20 minutes, and 75 ul of COD are added at once from a cold gas-tight syringe. After the 2 reactants have been cooled, the tube is shaken, and left at this temperature for 2 days. Then 100 ul of acetone is added to the viscous solution at that temperature, the tube warmed to room temperature, the solvents are evaporated and the polymer is disolved in $CDCl_3$ for NMR analysis. The deutero solvent is then evaporated, the polymer is disolved in toluene, and is filtered through 0.5 um filter for GPC analysis.

**- Typical kinetic measurement**

A stock solution containing 24.7 mg of 8 ($2.38\ 10^{-5}$ mol), 96 ul of THF d8, 3.815 g of toluene d8, 16 mg of ferrocene (internal standard), and 93 mg of CuCl is prepared. 550 mg of this solution is added to a NMR tube, as well as 25 ul of sBCOT. After 2 minutes the first NMR spectrum is recorded (8 scans, recycling delay of 3 seconds), and subsequently every 6 minutes for 8 hours. All spectra are Fourier transformed, phased and integrated with identical adjustable parameters. The amount of polymer formed and %bb are calculated according to the procedure established by Grubbs and Gorman.[13] The propagation rate is extracted after exponential fit of the monomer decay. Because of the imprecision of the method, the values of $k_p$ in table 10 are

given with 10% error. The amount of HFB was measured by $^{19}F$ NMR (non proton decoupled).

## VI. Appendix 1 : Gold equation when excess THF is present.

The polymerization scheme for the polymerization in presence of THF is:

$$I + L \rightleftharpoons IL$$

$$N_x + L \rightleftharpoons N_xL$$

$$M + I \xrightarrow{k_i} N_1$$

$$N_x + M \xrightarrow{k_p} N_{x+1} \qquad (1)$$

where

L is the amount of THF at time t,

M is the amount of monomer,

I is the amount of THF free initiator,

IL is the amount of THF bound initiator,

$N_x$ is the amount of THF free catalyst with x units of monomer attached,

$N_xL$ is the amount of THF bound catalyst with x units of monomer attached.

If the polymerization is fast, or the polymerization is run in excess of THF, then the conservation law for the catalyst is (no free carbenes are observed):

$$(IL)_0 = (IL) + \sum_{x=1}^{\infty} (N_xL) \qquad (2)$$

The following equations describe the temporal evolution of the catalyst and the monomer:

$$-\frac{d(I)}{dt} = k_i (I)(M) \qquad (3)$$

$$-\frac{d(M)}{dt} = k_p \sum_{x=1}^{\infty} (N_x)(M) + k_i (I)(M) \quad (4)$$

with the outcome:

$$\frac{d(M)}{d(L)} = \frac{K_{cat}}{(L)} \left[ (1 - R) + R \frac{(IL)_0}{(IL)} \right] \quad (5)$$

$$\text{where } R = \frac{k_p \, K_{prop}}{k_i \, K_{cat}} \quad (6)$$

The integration of the above equation yields:

$$R = \frac{\frac{(L)}{K_{cat}}[(M) - (M)_0] + (IL)_0 - (IL)}{\ln((IL)/(IL)_0) + (IL)_0 - (IL)} \quad (7)$$

If there is no THF present, Gold's equation gives:

$$r = \frac{(M) - (M)_0 + (I)_0 - (I)}{\ln((I)/(I)_0) + (I)_0 - (I)} \quad (8)$$

where r is $k_p/k_i$ .

## VII. Appendix 2 : Calculation of the ratio cis/trans due to ring-opening for a highly cis polymer.

Because the ring-opening of COD produces a polymer where every other double bond is cis, the t/t dyads are only due to secondary metathesis (backbiting) of the growing polymer chain. Prior to backbiting, the dyad analysis should be

| | |
|---|---|
| c/t | $\frac{1-a}{2}$ |
| t/t | 0 |
| c/c | a |
| t/c | $\frac{1-a}{2}$ |

giving a ratio cis:trans equal to $\frac{1+a}{2} : \frac{1-a}{2}$ .

When backbiting occurs, x t/t dyads are created. Under the hypothesis that backbiting is not predominant in the reaction (that is to say that the resulting polymer is still high cis), the t/t dyads will occur from t/c and c/t dyads, which are in the total number of 1-a. Therefore, the probability of getting a trans double bond due to secondary metathesis is x / (1 - a). Secondary metathesis does not only convert cis double bonds to trans, but also trans to cis, in a proportion $\alpha$ which can be determined by the anlysis of the isomerisation of *cis*-3-hexene to *trans*-3-hexene (*vide infra*). Accordingly, the probability of getting a cis double bond due backbiting is $\alpha$ x / (1 - a). c/c dyads in the final polymer come from the original c/c dyads ( total a) and the c/t and t/c dyads which have been isomerized to c/c (total $2 \cdot \frac{1-a}{2} \cdot \frac{\alpha x}{1-a}$ ). However, some of the original c/c dyads have been transformed to t/c

and c/t, for a total number of a $\cdot\frac{x}{1-a}$ . After backbiting, the dyad analysis is:

c/t $\quad \frac{1-a}{2} + \frac{1}{2}\cdot\frac{a\,x}{1-a} - \frac{1+\alpha}{2}\cdot x$

t/t $\quad x$

c/c $\quad a - \frac{a\,x}{1-a} + \alpha\,x$

t/c $\quad \frac{1-a}{2} + \frac{1}{2}\cdot\frac{a\,x}{1-a} - \frac{1+\alpha}{2}\cdot x$

The $^{13}C$ NMR analysis provides the values of the amount of each of these dyads. Knowing x (t/t dyad), and u (c/c dyad), a can be calculated by:

$$\frac{1+u-x-\alpha x+\sqrt{1-2u+u^2-2x+2\alpha x-2ux-2\alpha ux+x^2+2\alpha x^2+\alpha^2 x^2}}{2}$$

It is important to notice that this expression has been obtained by statistical argument, and therefore is only approximate. Nevertheless, for chains long enough, this expression should be correct, as long as the ratio of cis double bonds is high. Anyway, in most cases, this approximate value is likely to be offset from the real value by a margin which is below the experimental error.

## VIII. References

(1) Ivin, K. J. *Olefin Metathesis*; Academic: London, **1983**.

(2) Schrock, R. R.; Feldman, J.; Cannizzo, L. F.; Grubbs, R. H. *Macromolecules* **1987**, *20*, 1169-1172.

(3) Schrock, R. R.; Mcconville, D.; Oskam, J.; Odell, R.; Hofmeister, G. *Abstracts Of Papers Of The American Chemical Society* **1994**, *207*, 342-POLY.

(4) Chan, Y. N. C.; Craig, G. S.; Schrock, R. R.; Cohen, R. E. *Chem. Mater.* **1992**, *4*, 885-894.

(5) Feast, W. J.; Gibson, V. C.; Khosravi, E.; Schrock, R. R. *Abstracts Of Papers Of The American Chemical Society 199* **1990**, 106.

(6) Risse, W.; Grubbs, R. H. *J. Mol. Catal.* **1991**, *65*, 211-217.

(7) Steltzer, F.; Grubbs, R. H.; Liesing, G. *Polymer* **1991**, *32*, 1851-1856.

(8) Hillmyer, M. H.; Laredo, W.; Grubbs, R. H. *Manuscript in preparation* **1994**,

(9) Hillmyer, M. A.; Grubbs, R. H. *Macromolecules* **1993**, 26, 872.

(10) Korshak, Y. V.; Korshak, V. V.; Kanischka, G.; Höcker, H. *Makromol. Chem., Rapid Commun.* **1985**, *6*, 685-692.

(11) Tlenkopachev, M. A.; Korshak, Y. V.; Orlov, A. V.; Korshak, V. V. *Doklad. Akad. Nauk, Eng. Transl.* **1987**, *291*, 1036-1040 (Original Russian article: pp. 409-413, 1986).

(12) Klavetter, F. L.; Grubbs, R. H. *J. Am. Chem. Soc.* **1988**, *110*, 7807-7813.

(13) Gorman, C. B.; Ginsburg, E. J.; Grubbs, R. H. *J. Am. Chem. Soc.* **1993**, *115*, 1397-1409.

(14) Herisson, J. L.; Chauvin, Y. *Makromol. Chem.* **1970**, *141*, 161.

(15) Landon, S. J.; Schulman, P. M.; Geoffroy, G. *J. Am. Chem. Soc.* **1985**, *107*, 6739.

(16) Toledano, C. A.; Rudler, H.; Daran, J. C.; Jeanan, Y. *J. Chem. SOc., Chem. Comm.* **1984**, , 574.

(17) Casey, C. P.; Vollendorf, N. W.; Haller, K. J. *J. Am. Chem. Soc.* **1984**, *106*, 3754.

(18) Katz, T. J.; McGinnis, J. *J. Am. Chem. Soc.* **1975**, *97*, 1592-1594.

(19) Katz, T. K.; Ho, T. H.; Shih, N. Y.; Ying, Y. C.; Stuart, W. I. W. *J. Am. Chem. Soc.* **1984**, *106*, 2659.

(20) Schrock, R. R.; Rocklage, S.; Wemgrovius, J.; Rupprecht, G.; Fellmann, J. *J. Mol. Catal.* **1980**, *8*, 73-83.

(21) Kress, J.; Wesolek, M.; Osborn, J. A. *J. Chem. Soc., Chem. Commun.* **1982**, ,514-516.

(22) Quignard, F.; Leconte, M.; Basset, J. M. *J. Chem. Soc., Chem. Comm.* **1985**, ,1816-1817.

(23) Schrock, R. R. *Abstracts Of Papers Of Am. Chem. Soc.* **1988**, 397-397.

(24) Freudenberger, J. H.; Schrock, R. R. *Organometallics* **1985**, *4*, 1937.

(25) Blosch, L. L.; Abboud, K.; Boncella, J. M. *J. Am. Chem. Soc.* **1991**, *113*, 7066.

(26) VanderLende, D. D.; Abboud, K. A.; Boncella, J. M. *Organometallics* **1994**, *13*, 3378.

(27) Boutarfa, D.; Paillet, C.; Leconte, M.; Basset, J. M. *J. Mole Cat.* **1991**, *69*, 157-169.

(28) Couturier, J. L.; Paillet, C.; Leconte, M.; Basset, J. M.; Weiss, K. *Angew. Chem.e Int. Ed. In English* **1992**, *31*, 628-631.

(29) Couturier, J. L.; Leconte, M.; Basset, J. M.; Ollivier, J. *Organomet. Chem.* **1993**, *451*, C 7-C 9.

(30) Couturier, J. L.; Tanaka, K.; Leconte, M.; Basset, J. M.; Ollivier, J. *Angew. Chem.e Int. Ed. In Englishh* **1993**, *32*, 112-115.

(31) Johnson, L., Ph.D. Thesis, **1992.**

(32) Johnson, L. K.; Grubbs, R. H.; Ziller, J. W. *J. Am. Chem. Soc.* **1993,** *115(18),* 8130.

(33) Binger, P.; Muller, P.; Benn, R.; Mynott, R. *Angew. Chem., Int. Ed. Engl.* **1989,** *28,* 610-611.

(34) Bazan, G.; Khosravi, E.; Schrock, R. R.; Feast, W. J.; Gibson, V. C.; O'Regan, R. B.; Thomas, J. K.; Davis, W. M. *J. Am. Chem. Soc.* **1990,** *112,* 8378.

(35) Bazan, G. C.; Schrock, R. R.; Cho, H. N.; Gibson, V. C. *Macromolecules* **1991,** *24,* 4495-4502.

(36) Wu, Z.; Wheeler, D. R.; Grubbs, R. H. *J. Am. Chem. Soc.* **1992,** *114,* 146-151.

(37) Gorman, C. B.; Ginsburg, E. J.; Marder, S. R.; Grubbs, R. H. *Angew. Chem. Adv. Mater.* **1989,** *101,* 1603-1606.

(38) Gorman, C.; Ginsburg, E.; Marder, S.; Grubbs, R. *Polym. Prepr.* **1990,** *31(1),* 386-7.

(39) Gorman, C. B.; Ginsburg, E. J.; Sailor, M. J.; Moore, J. S.; Jozefiak, T. H.; Lewis, N. S.; Grubbs, R. H.; Marder, S. R.; Perry, J. W. *Synth. Met.* **1991,** *41,* 1033-1038.

(40) Gorman, C., Ph.D. Thesis **1991.**

(41) Ginsburg, E. J.; Gorman, C. B.; Grubbs, R. H.; Klavetter, F. L.; Lewis, N. S.; Marder, S. R.; Perry, J. W.; Sailor, M. J. in *Conjugated Polymeric Materials: Opportunities in Electronics, Optoelectronics, and Molecular Electronics;* Bredas, J. L.; Chance, R. R. Eds.; Kluwer Academic Publishers: Dordrecht, The Netherlands, 1990; Vol. 182, pp. 65-81.

(42)Mata, J. D. l.; Fujimura, O. manuscript in preparation **1995.**

(43) Mata, J. D. l.; Grubbs, R. H. unpublished results.

(44) J. De la Mata has developped a large part of the synthesis of the oxo carbene **10**. An experimental procedure for its synthesis is described in reference 43. Improved synthesis is the object of researches by T. Wilhelm. Optimized procedure is to be described in a future publication.

(45) Chiu, K. W.; Lyons, D.; Wilkinson, G.; Thornton-Pett, M.; Hursthouse, M. B. *Polyhedron* **1983**, *2(8)*, 803. Carmona, E.; Sanchez, L.; Poveda, M. L.; Jones, R. A.; Hefner, J. G. *Polyhedron* **1983**, *2(8)*, 797.

(46) Butcher, A. V.; Chatt, J.; Leigh, G. J.; Richards, P. L. *J. Chem. Soc. Dalton Trans.* **1972**, 1064.

(47) Schmidbaur, H.; Jeong, J.; Schier, A.; Graf, W.; Wilkinson, D. *New. J. Chem.* **1989**, *13*, 341.

(48) Schmidbaur, H. *Acc. Chem. Res.* **1975**, *8*, 62.

(49) Asselt, A. V.; Burger, B. J.; Gibson, V. C.; Bercaw, J. E. *J. Am. Chem. Soc.* **1986**, *108*, 5347.

(50) Sharp, P. R.; Schrock, R. R. *J. Organomet. Chem.* **1979**, *171*, 43.

(51) Schwartz, J.; Gell, K. I. *J. Organomet. Chem.* **1980**, *184*, C1-C2.

(52) Oskam, J. H.; Schrock, R. R. *Journal Of The American Chemical Society* **1992**, *114*, 10680-10680.

(53) Oskam, J. H.; Schrock, R. R. *Journal Of The American Chemical Society* **1993**, *115*, 11831-11845.

(54) Gray, H. B., personal communication.

(55) Dr. S. Brown is acknowledged for suggesting this explanation.

(56) Fagan, P. J.; Mahoney, W. S.; Calabrese, J. C.; Williams, I. D. *Organometallics* **1990**, *9*, 1943-1852.

(57) Gagne, M. R.; Grubbs, R. H.; Feldman, J.; Ziller, J. W. *Organometallics* **1992**, *11(12)*, 3933-3935.

(58) Koelle, U.; Ruether, T.; Klaui, W. *J. Organomet. Chem.* **1992**, *426*, 99-103.

(59) Koelle, U.; Kossakowski, J. *J. Chem. Soc., Chem. Commun.* **1988**, 549.

(60) Hathaway, B. J. in *Comprehensive Coordination Chemistry;* Wilkinson, G.; Gillard, R. D.; McCleverty, J. A. Eds.; Pergamon Press: Oxford, 1987; Vol. 3, pp. 583.

(61) Schrock, R. R.; Depue, R. T.; Feldman, J.; Yap, K. B.; Yang, D. C.; Davis, W. M.; Park, L.; Dimare, M.; Schofield, M.; Anhaus, J.; Walborsky, E.; Evitt, E.; Kruger, C.; Betz, P. *Organometallics* **1990**, *9*, 2262-2275.

(62) Feast, W. G.; Gibson, V. C.; Marshall, E. L. *J. Chem. Soc. - Chem Comm* **1992**, *16*, 1157.

(63) This experiment has been gratefully provided by D. Elder

(64) Klavetter, F. L., Ph. D. Thesis, California Institute of Technology, 1989.

(65) Gold, L. *J. Chem. Phys.* **1958**, *28*, 91.

(66) Strazielle, C.; Benoit, H. *J. Chim. Phys.* **1965**, 986.

# CHAPTER 3

# REACTIVITY OF W CATALYSTS WITH ALCOHOLS

## I. Introduction

The accepted mechanism of metathesis is the cycloaddition of an olefin to a metal carbene, followed by retro 2+2 addition.[1] With the appearance of so-called well defined tungsten and molybdenum catalysts, it is assumed that the isolated form of the catalyst is actually the active species in the metathesis catalytic cycle.[1-9]

In this chapter, our interest will be mainly focused on catalysts **1** to **6** (Figure 1). For this class of catalysts $M(=CHR)(OR)_2(=X)L$ (M = Mo and W, X= NR or O, OR = tertiary alkoxide), it is usually accepted that ligand L dissociates before metathesis occurs. Two experimental facts support this conclusion: (1) metathesis in the presence of ligand L (catalysts **4** to **6**) is much slower than without any ligand (catalysts **1** and **2**), (2) chelating carbenes, such as **3**, initiate poorly.

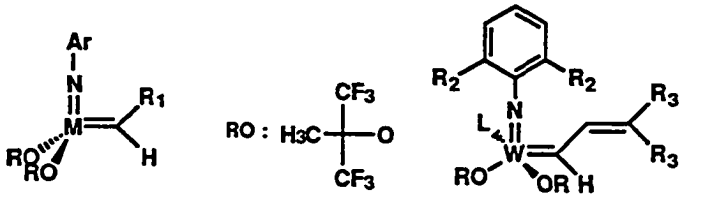


**1 : M = Mo, $R_1$ = $^t$Bu**
**2 : M = W, $R_1$ = $^t$Bu**
**3 : M = W, $R_1$ = o-MeOPh**
**Ar = 2,6-*i*-PrPh**

**4: $R_2$ = *i*-Pr, $R_3$ = Ph, L=P(OMe)**
**5: $R_2$ = *i*-Pr, $R_3$ = Ph, L =THF**
**6: $R_2$ = H, $R_3$ = Me, L = $PMePh_2$**

Figure 1. Catalysts **1** to **6**

A typical catalytic cycle is shown in Figure 2. This polymerization scheme, established by Schrock, was confirmed by isolation of the intermediate metallacyclobutane.[2, 7, 10]

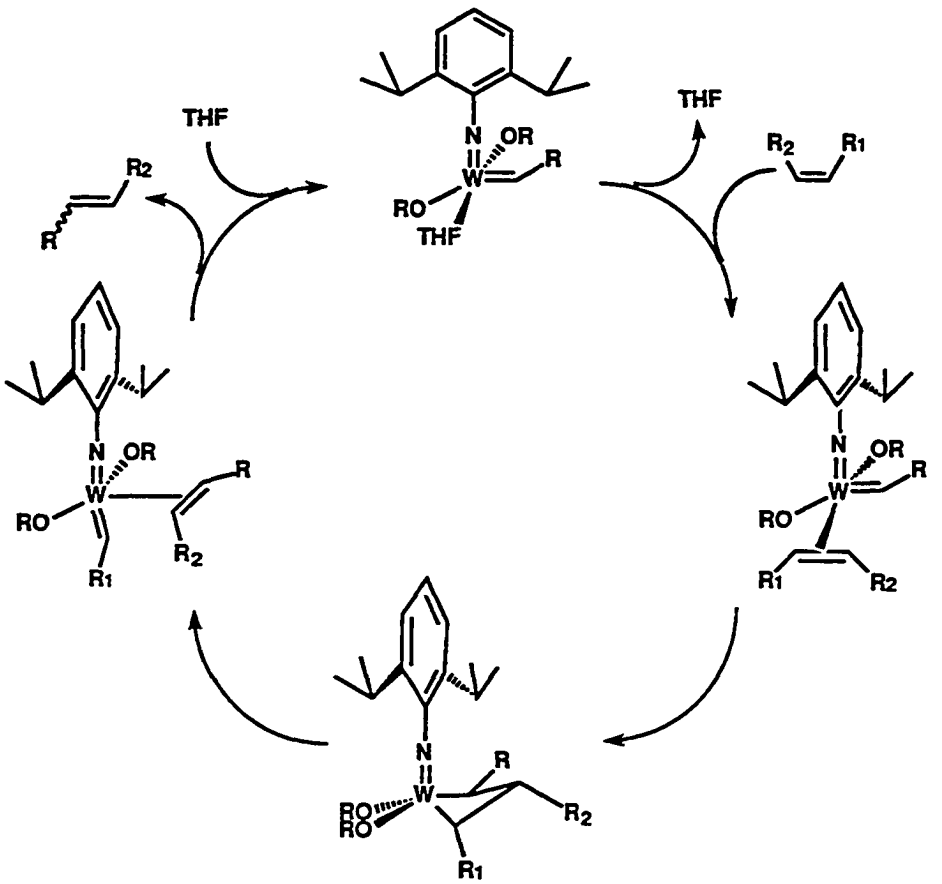


**Figure 2.** Mechanism of the metathesis reaction by catalysts of the type $M(=CHR)(OR)_2(=X)L$

Schrock[10-12] has demonstrated that syn and anti rotamers (see Figure 15, Chapter 2) have very different behaviors: the anti rotamer is much more reactive than the syn rotamer. The rate of syn/anti interconversion is therefore an important factor in the outcome of the polymerization. When the interconversion is very fast (faster than the polymerization rate), the anti rotamer, although in small amounts, effects the polymerization, and gives polymers with very high trans contents. Direct monomer insertion by the majoritary syn rotamer is not observed, but fast interconversion to the anti rotamer followed by monomer insertion is the usual pathway for

polymerization. This fast interconversion is observed for catalysts with electron rich alkoxides. When the interconversion is slow (highly electron withdrawing alkoxides), the syn rotamer is the only rotamer present (the anti rotamer, once consumed is not reformed), resulting in high cis polymers.

This theory, developed for neopentylidene carbenes (catalysts **1** and **2**), seems to be less accurate for vinyl alkylidenes (catalysts **4** to **6**): usually, both anti and syn starting or propagating rotamers are observed and are slowly interconverting, likely because of the coordinating Lewis base L (see previous chapter). High cis polymers are usually formed at first (that is to say before backbiting) with highly electron withdrawing alkoxides. The difference of reactivity between both rotamers is small, since both of them are observed.

In the most general conditions, Figure 2 shall be now corrected for the presence of the two different active sites (syn and anti), which can be interconverted.

In this chapter, the possibility of an even more complicated mechanism is raised. This assumption arises from the fortuitous discovery that metathesis catalysts are usually contaminated by trace amounts of alcohol. We will present first evidence for the presence of alcohol, as well as interesting reactivity implications. Then, these results will be interpreted in mechanistic terms. The effect of the alcohol on the microstructure of the polymer will also be described.

## II. Alcohol detection and exchange

We have found that tungsten and molybdenum metathesis catalysts **1** to **6**, containing hexafluoro-*tert*-butoxides ligands, are contaminated by a small amount of hexafluoro-*tert*-butanol (HFB). A small amount of hexafluoro-*tert*-butoxide lithium (HFBLi) is sometimes observed and originates from the incomplete separation of the alkoxide from the catalyst, during purification of these catalysts. The amount of HFB varies from batch to batch, and is typically on the order of 1% of the total alkoxides. During the following discussion, the HFB content will be reported as a percent fraction of the total amount of hexafluoro-*tert*-butyl, which can be in the form of alcohol (HFB), lithium alkoxide (HFBLi) or tungsten bound alkoxide.

### 1. Detection of HFB in catalysts

$^{19}F$ NMR allows easy detection and quantification of HFB and HFBLi. The resonances of the alcohol (-79.2 ppm) and HFBLi (- 80.8 ppm) are clearly separated from those of the metal alkoxides, which range from -76 to -79 in benzene (Table 1). In contrast, $^{1}H$ NMR does not always allow facile detection of HFB, because of the presence of many overlapping resonances in the region of interest. The chemical shift of the hydroxyl proton of HFB is highly dependent on the experimental conditions. In *rigorously dry* medium, this proton resonates at 1.46 ppm at 18 °C in benzene. However, the addition of a small amount of dry THF can shift this resonance downfield by as much as 5.5 ppm. The chemical shift of this proton is also highly dependent on temperature, as one could expect from the highly acidic nature of this alcohol (pKa = 9.93).

**Table 1.** Selected $^{19}F$ chemical shift of trifluoromethyl groups at room temperature in benzene.

| Compound | Chemical Shift |
|---|---|
| HFB | - 79.24 |
| 1[a,b] | - 77.93 |
| 2[a] | -77.85, -77.96 |
| 3[a] | - 77.67, - 77.92 |
| 4 syn | -76.10, -77.28, - 78.23, - 78.8 |
| 4 anti | -76.38, - 77.45, - 77.85, -77.5 |
| 5 syn + anti[b] | - 78.3 |
| 6 syn | -76.52, -77.53, -77.94, -78.06 |
| 6 anti | -76.8, - 77.41[c] |

a. Syn rotamer ( the catalyst is > 99% syn)
b. The alkoxide resonances coincide, but can be separated with variable temperature.
c. The two last resonances of the anti rotamer are overlapped with those of the syn rotamer

HFB is found not only in catalysts **1** to **6**, but in all catalysts containing hexafluoro ligands that we analyzed. In addition, we also found trifluoro-*tert*-butyl alcohol in M(=CH-*t*-Bu)(OC($CH_3$)$_2$($CF_3$))$_2$(=N-*i*-$Pr_2$-$C_6H_3$) (M = W, Mo) samples and the monoalcohol (TBECLiOH) in samples containing the ligand $TBECLi_2$ (see chapter 2, II. 2. b).

## 2. Origin of HFB

Compounds **1** to **6** are stored in the solid state under nitrogen in a freezer. In solid state, the amount of HFB in **1** to **6** is constant over extended periods of time and is typically less than 1%. In contrast, the HFB content of catalyst solutions slowly increases over time. For example, a 8.85 $10^{-3}$ mol/l solution of **2** in benzene shows 0.78 % of HFB immediately after dissolution. The amount of HFB increases to 4.8% or to 15.8% after 16 hours at room temperature or 60 °C respectively. Similarly, a 9.83 $10^{-3}$ mol/l solution of **4** in benzene initially has a HFB content of 6.6%, but this increases to 15.8% after 16 hours at room temperature and to 41.8 % after 16 hours at 40 °C. In this last case, considerable decomposition is observed by both $^1H$ and $^{19}F$

NMR. In view of these results, we believe that HFB is a product of the *thermal decomposition* of catalysts **1** to **6**. Interestingly, catalysts **1** to **3** (neopentylidene and benzylidene) seem to be more robust than **4** to **6** (vinyl alkylidenes) toward thermal decomposition. The thermal decomposition therefore correlates with the bulk of the carbene ligand. The mechanism of the decomposition is unknown at this time, but one can postulate that the carbenic proton is abstracted by the alkoxide to generate HFB and undetermined organometallic fragments.

In freshly synthesized, not recrystallized samples of **1**, **2**, **4** and **6**, large amounts of HFB were observed (up to 30%). This amount was decreased to less than 0.2% by two successive fast recrystallizations from ether or ether/pentane. We believe that in this case the HFB is created during the reaction of two equivalents of HFBLi with the dichlorocarbene precursor, by a mechanism still unraveled at this time. Notably, isolated yields of the chloride/alkoxide substitution never excesses 70% (see chapter 2), which seems to indicate that a competitive reaction is occurring.

Finally, it should be stated that it is not possible to discount the possibility that the presence of adventitious water[10] may be responsible for the presence of HFB during the synthesis, storage or characterization of theses catalysts. Reaction of water with catalysts **1** to **6** releases HFB as well as 1,3-diisopropylaniline and unidentified organometallic fragments. In our case, little to no aniline derivative could be observed along with HFB, which suggests that HFB is not created by reaction with water. Even if HFB formed during reaction with adventitious water, the origin of the acidic

---

[10] only 2 ppm of water in a deuterated solvent could account for the typical amount of HFB observed by NMR.

proton should be of little to no concern to the casual user of these catalysts. First, as we show below, HFB is completely *compatible* with the catalyst, and does not induce further decomposition. Secondly, from the results presented below, it is clear that HFB is *necessary* to allow optimal use of these catalysts. Nevertheless, in order to be able to reach such conclusions, we have devised a way to prepare catalysts **1** to **6** free of HFB.

### 3. Preparation of HFB free catalyst

It is possible to quench HFB in catalysts **1, 2, 3, 4,** and **6** by titrating it with a dilute solution of PhLi in benzene. Because of the very low solubility of PhLi in benzene, a drop of THF is added to homogenize the solution, however, this technique is not used for kinetic experiments, because of the THF coordination on tungsten complexes. After quenching, the resulting HFBLi is observed by NMR. This reaction occurs free of decomposition, unless an excess of PhLi is used. In this case, more HFBLi is created, the carbene is partially decomposed, and no new carbene complex is observed.

In the case of **5**, adding a dilute solution of PhLi induces partial decomposition of the catalyst, followed by release of additional HFB. When a large amount of PhLi is added, the solution turns green, and the color change is accompanied by massive catalyst decomposition. Eventually, the $CuCl.P(OMe)_3$ polymer (see previous chapter) releases free phosphite, which reacts with the remaining **5**, to give **4**. The attack of the $CuCl.P(OMe)_3$ polymer by PhLi to form a cuprate may explain these results.

Instead of quenching HFB, we can effectively decrease the acidity of the system by adding HFBLi. We found this technique to produce identical results in reactivity studies to the PhLi quenching, indicating that indeed, the phenomena observed are due to an acid/base process. Nevertheless, large

excess of HFBLi induces decomposition of the catalyst. The origin of this decomposition is unclear at that time.

4. Stability of the catalysts with alcohols

Finding HFB in the presence of tungsten and molybdenum carbenes is surprising, considering the high nucleophilicity of the metal carbene fragment. We additionally found that catalysts **1** to **6** are stable in the presence of large quantities of HFB. All these catalysts retain their catalytic activity (see below) in solution in HFB (with one drop of benzene, for solubility purpose). Additionally, no decomposition was observed in NMR spectra for any of these catalysts, when 40 equivalents of *dry* HFB were present. At the price of an alkoxide exchange, these catalysts are stable in the presence of other tertiary alcohols for prolonged periods of time at room temperature, and to secondary alcohols at low temperature (see Table 2).

In contrast, these catalysts decompose rapidly in the presence of phenol, primary alcohols, acetic acid and water. No decomposition is observed with acids possessing non-nucleophilic bases, such as $B(PhF_5)_3$, $Na_2HPO_4$ and $KHSO_4$. Therefore, these metathesis catalysts are not attacked by acidic protons unless the conjugate base is nucleophilic enough to displace the alkoxide.

The stability of tungsten and molybdenum carbenes to tertiary alcohols indicates that the degree of polarization of the metal carbon double bond is not as large as one could expect. A number of reactions, scattered through literature, seems to support this observation. For example, in early transition metals, alkyl-metal bonds are less prone to proton attack than a carbene (equation 1).[13] For molybdenum and tungsten, opposite reactivity is observed (equation 2).[14]

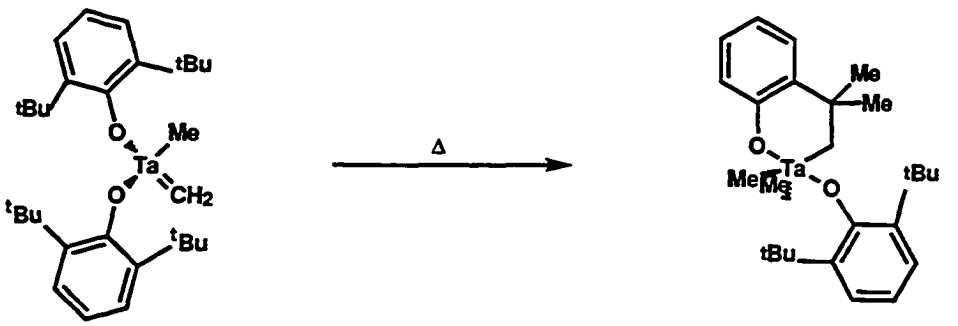


(1)

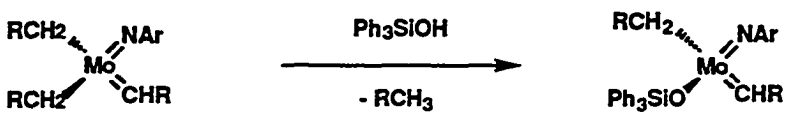


(2)

Similarly, in bis-imido carbenes, the second imido is more nucleophilic than the carbene substituent (Equation 3[15] and 4[14]).

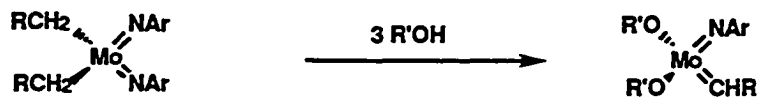


(3)

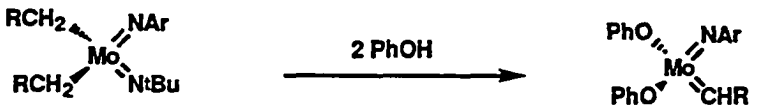


(4)

Equations 3 and 4 also indicate that, to a certain extent, molybdenum catalysts present some stability toward alcohols (although the fate of the phenoxide species in equation 4 is not detailed).

5. Exchange alkoxide-alcohol

Tertiary alcohols displace the hexafluoro alkoxide at room temperature (Table 2). The exchange is easy for *tert*-butanol (fast and quantitative) and is slower and incomplete for more acidic alcohols such as perfluoro-*tert*-butanol. The order of reactivity for the exchange reaction is:

$(CF_3)_3COH$ < $(CF_3)_2(CH_3)COH$ ~ $(CF_3)_2PhCOH$ < $(CF_3)(CH_3)_2COH$ < $(CH_3)_3COH$.

For example, 6 equivalents of perfluoro-*tert*-butanol displace less than 60% of hexafluoroalkoxide on catalyst **4**, after 12 hours of reaction. On the other hand, the exchange is instantaneous and quantitative with *tert*-butanol. Secondary alcohols readily displace the alkoxides at low temperature (see Table 2), but major decomposition is observed when the samples are warmed to room temperature. This indicates that the bulk of the alkoxide ligand is crucial to ensure stability of the complex. For primary alcohols, only decomposition is observed, even at - 60 °C. We suspect that a very fast displacement of the alkoxide occurs, which is then immediately followed by decomposition of the catalyst.

As expected, the order of reactivity of the alcohol roughly correlates with sterics: primary < secondary < tertiary. In addition, more basic alcohols reacts more readily than more acidic ones. Interestingly, the phenylhexafluoro-*tert*-butanol does not react further via orthometallation of the carbene. This contrasts with the observation by Schrock and coworkers, who described orthometallation by a tolyl alkoxide (equation 5).

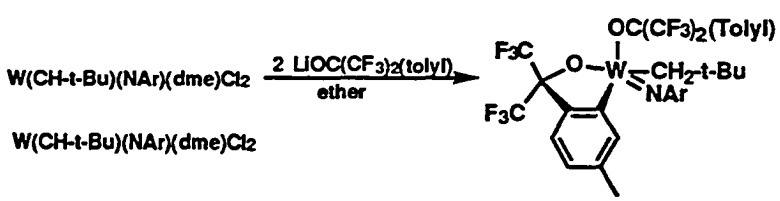

(5)

**Table 2.** $^1H$ NMR shift of the carbene protons of catalyst **2** and **5** after alkoxide exchange, in benzene at room temperature.

| RO | 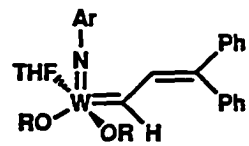 Syn | Anti | 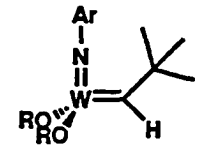 |
|---|---|---|---|
| $(CH_3)(C_2H_5)HCO$ [a] | 9.74 | 8.81 | 8.97 |
| $(CF_3)_2HCO$ [a] | 11.66 | 10.44 | 9.44 |
| $(CH_3)_3CO$ | 9.42 | 9.93 | 8.00 |
| $(CH_3)_2(CF_3)CO$ | - [b] | - [b] | 8.43 |
| $(CH_3)(CF_3)_2CO$ | 10.2 | 11.4 | 8.92 |
| $(CF_3)_2PhCO$ | 10.17 | 11.3 | 9.16 |
| $(CF_3)_3CO$ | 10.76 | - [c] | - [c] |

a. At -42 °C, in toluene d8
b. Not recorded
c. Rotamer not observed

III. Reactivity dependency on alcohol.

After identifying and characterizing the presence of HFB in metathesis catalysts, one should wonder if this alcohol plays any role. It was found that excess HFB could strongly activate catalysts. For example, at room temperature or 60 °C, catalysts **1** and **4** (with HFB content < 1%) do not catalyze the polymerization of *sec*-butylcyclooctatetraene (sBCOT) neat or in solution. When the polymerization is done in solution in HFB, the reaction is quantitative after 2 hours at room temperature. In view of these interesting

results, we have decided to more thoroughly investigate the catalyst activation by HFB.

## 1. Polymerization of 1,5-cyclooctadiene

**Table 3.** $k_p/k_i$ for COD polymerization by different catalysts, at room temperature.

| Catalyst | [MON] (mol/l) | [MON]/[CAT] | [HFB] (%) | [HFBLi] (%) | % initiation | $k_p/k_i$ |
|---|---|---|---|---|---|---|
| II | 0.13 | 13.8 | 740 | 0 | 7 | 5500 |
| II | 0.13 | 14.2 | 1.7 | 0 | 7 | 5500 |
| II | 0.12 | 12.3 | 0 | 20.4 | <1 | $> 2.10^5$ |
| 6a | 0.12 | 7.8 | 91 | 0 | 33 | 10 |
| 6a | 0.12 | 7.8 | 1.5 | 0 | 33 | 9 |
| 6a | 0.12 | 7.8 | 0 | 9.7 | 27 | 50 |

a. For catalysts VI, the $k_p/k_i$ is obtained by use of Gold equation, although the rate law is not first order in catalyst (because of phosphine inhibition). Nevertheless, the relative order of $k_p/k_i$ can be compared, because the experiments are done with similar monomer and catalyst concentrations.

Effects of alcohol on catalyst activity was investigated for the polymerization of COD. First, using Gold's equation, the ratio $k_p/k_i$ was measured for different amounts of alcohol and alkoxide: the initiation drastically improved when the amount of alcohol increased (Table 3). The presence of various amounts of alcohol did not have any repercussion on the microstructure of the COD polymer (see previous chapter, IV. 3.).

Because the study of the ratio $k_p/k_i$ did not distinguish between initiation and propagation rates, kinetics of initiation and propagation were studied separately in the presence of varying alcohols concentrations. Such a study requires a catalyst which initiates completely and which propagates slowly enough so kinetics can be followed at room temperature. Fast initiation is crucial, because propagation kinetics can only be followed under

the conditions of full initiation (number of chains constant). Catalyst **6** fulfills these two conditions and was used for this study. The rate of polymerization for catalyst **6** is :

$$\text{Rate} = k_p [\text{MON}] \frac{[\text{CAT}]}{\frac{[\text{P}]}{K_d} + \frac{[\text{MON}]}{K'}} \qquad (6)$$

where [P] is the concentration of free phosphine, $K_d$ is the dissociation constant of the phosphine from the propagating carbene and $k_p$ is an apparent polymerization rate which is dependent on the amount of alcohol. The kinetics of polymerization are presented in Figures 3 and 4.

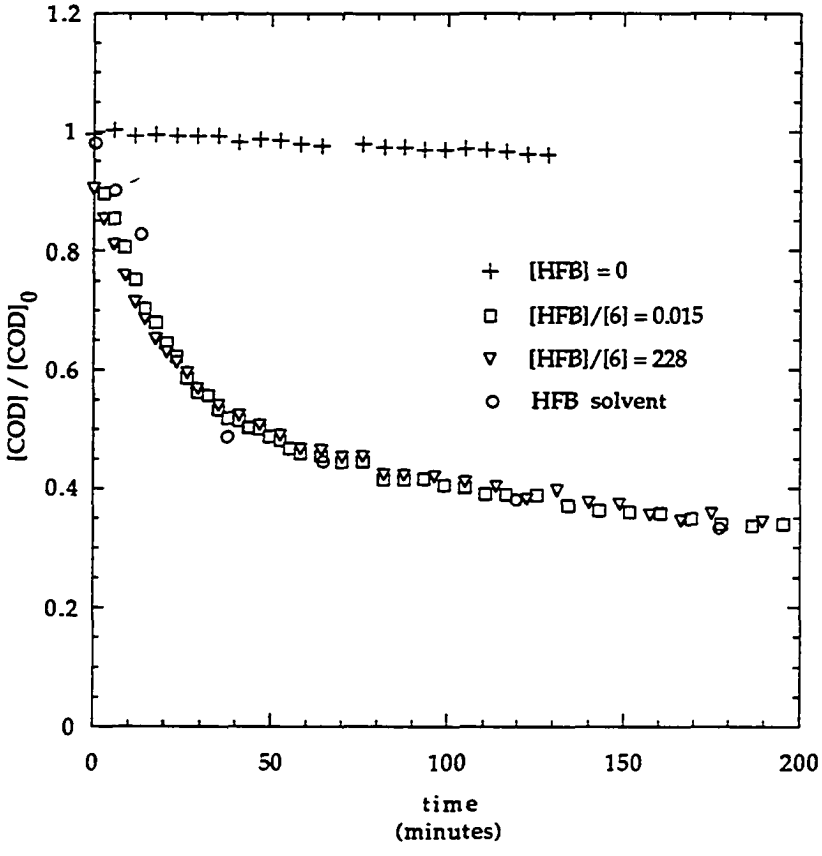


**Figure 3.** Kinetics of polymerization of COD by **6** with different alcohol concentrations. [COD] / [6] = 250, [6] = 4.53 $10^{-3}$ mol/l.

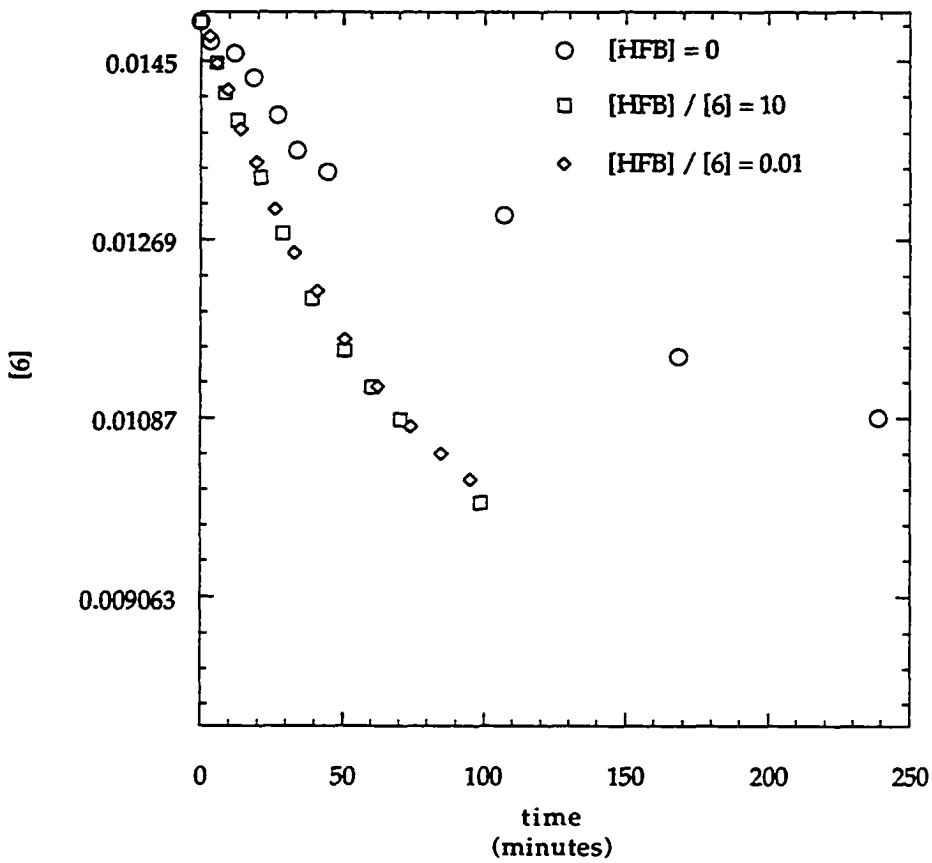


**Figure 4.** Kinetics of initiation of COD by **6** with different alcohol concentrations. [COD] / [6] = 7.6, [6] = 1.52 $10^{-2}$ mol/l.

In the absence of alcohol, the initiation as well as the propagation are very slow, but the addition of as little as 1% of alcohol to the catalyst is enough to speed up the reaction by two orders of magnitude (for the propagation). Addition of more alcohol does not change the kinetics of initiation or propagation. The behavior of HFB is typical of a Lewis or Bronsted acid activation : above a ceiling value, adding more HFB does not produce additional activation, because all the active sites are "saturated". It would be interesting to know if the lowest kinetic values found in the

absence of alcohol (Table 4) correspond to inherent rate of polymerization of **6** in purely aprotic medium, or if the rate is zero in the total absence of protons. However, with the exception of **4**, the least active of the catalysts **1** to **6**, COD polymerization always occurs, albeit at a slow rate, even in stringent aprotic conditions. Therefore, it can only be concluded that the rate of polymerization is slower than the HFB catalyzed rate.

**Table 4.** Apparent rate of propagation $k_p$ and of initiation $k_i$ of COD by **6**, for different amounts of HFB and HFBLi.

| process | [HFB]/[6] | [HFBLi]/[6] | k (l. $mol^{-1}min^{-1}$) |
|---|---|---|---|
| initiation | 0.011 | 0 | $4.1\ 10^{-2}$ |
| initiation | 0.91 | 0 | $3.9\ 10^{-2}$ |
| initiation | 0 | 0.096 | $1.6\ 10^{-2}$ |
| propagation | 0 | 0.082 | $2.9\ 10^{-4}$ |
| propagation | 0.015 | 0 | $2.1\ 10^{-2}$ |
| propagation | 228 | 0 | $2.3\ 10^{-2}$ |
| propagation | solvent | 0 | $2.2\ 10^{-2}$ |

2. Polymerization of sBCOT

Most of the work on the polymerization of sBCOT was done using catalysts **2** and **5**. Similar to COD, the polymerization is activated by the presence of HFB. For example, 13 equivalents of sBCOT (conc = 0.16 mol/l) polymerized completely in 13 hours when [HFB] / [**2**] = 6.1. The same mixture was only 15% polymerized in rigorously aprotic medium.

Careful examination of the kinetics of polymerization of sBCOT was not possible because of the poor initiation properties of **2**. Therefore, catalyst **5** was used (see previous chapter). In addition to monomer consumption, %bb, which is the fraction of consumed monomer incorporated in *sec-*

butylbenzene[11], was monitored. A typical observation is shown in Figure 5; in addition to a quasi-exponential decay of the monomer concentration, a flat curve for %bb is observed (note that %bb is not very clearly defined at the beginning of the polymerization, because very little polymer has appeared). A constant value for %bb indicates that the amount of *sec*-butylbenzene created at any time is proportional to the amount of monomer consumed. This implies that when all the monomer is consumed, the backbiting reaction stops. Indeed, such a trend is observed: after four hours, all monomer is consumed and samples present 15% to 25% %bb products. After 24 hours, this percentage remains unchanged. Yet, after 24 hours, the catalyst is still active and will polymerize COD. In addition, a purified sample of poly-*sec*-butylCOT in a 0.25 mol/l benzene solution containing catalyst 5 does *not* show appearance of backbiting products over time. These results may seem contradictory with the mechanism, one usually expects an increase in backbiting (Chapter II, Figure 4) and eventually depolymerization of the polymer to *sec*-butylbenzene.

Although backbiting of poly(*sec*-butylCOT) does stop with monomer depletion under "normal" conditions, backbiting increases slowly over time when large amounts of alcohol are added to the catalyst 5 (Figure 6). This build-up of backbiting product is also accompanied by a modest increase in the rate of polymerization, indicating that activation by HFB occurs (Table 5).

---

[11] %bb is the ratio of weight of *sec*-butylbenzene to the weight of polymer + *sec*-butyl benzene.

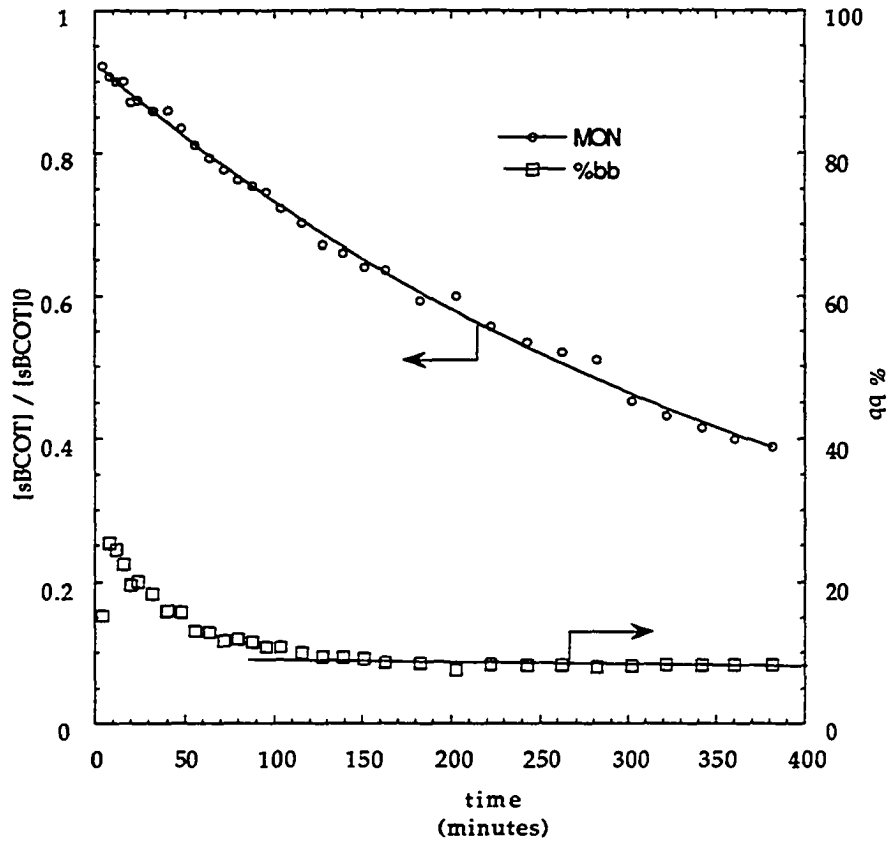


**Figure 5.** Monomer decay and %bb versus time for the polymerization of sBCOT by 5. $[sBCOT]_0$ = 0.47 mol/l, [MON] / [5] = 82. [THF] / [5] = 140, [HFB] / [5] = 0.03.

**Table 5.** Kinetics of polymerization of sBCOT by 5. All the polymerizations have been carried out in toluene-$d^8$.

| Temp (°C) | [sBCOT] (mol/l) | [THF] (mol/l) | [sBCOT] /[5] | %bb[a] | $k_p$ ($l.mol^{-1}.min^{-1}$) | [HFB][b] /[5] |
|---|---|---|---|---|---|---|
| 18 | 0.47 | 0.80 | 82 | 7 | 0.44 | 0.03 |
| 18 | 0.47 | 0.80 | 82 | 15[c] | 0.53 | 3.22 |
| 18 | 0.47 | 0.80 | 82 | 21[c] | 0.60 | 24 |

a. percentage of monomer converted in sec-butylbenzene.

b. amount of alcohol, as measured by $^{19}F$ NMR.

c. the amount of backbiting increases with time.

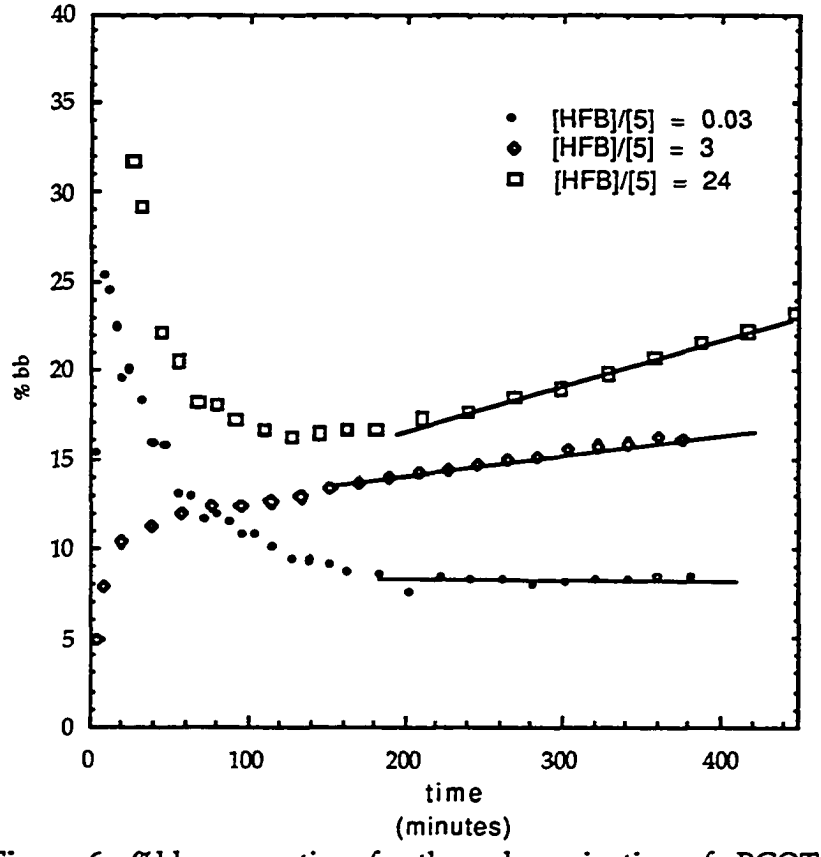


**Figure 6.** %bb versus time for the polymerization of sBCOT by 5 in the presence of different amounts of HFB. $[sBCOT]_0$ = 0.47 mol/l, [MON] / [5] = 82. [THF] / [5] = 140. %bb values are meaningless at small time, because of the very small amount of polymer created at that time.

In the absence of large amounts of HFB, the reactions of propagation and backbiting are simultaneous reactions: in average, for 100 monomer insertions, %bb backbiting steps occur. When the catalyst is activated by HFB, the %bb can grow (although modestly) even when the polymerization stops. A possible interpretation of this phenomenon can be offered in view of the nature of the conjugated carbene. The backbiting reaction will be easy when the incoming double bond is disubsituted (carbene A), and a lot harder or even impossible when the double bond is trisubstituted (carbene B) (Figure 7). Therefore, when no more monomer is present, backbiting reaction occurs until all carbenes are of type B. In this case, in the absence of HFB, the backbiting stops completely, whereas for activated catalyst, it is possible to imagine that metathesis with the triply bonded olefin occurs, although at a slow rate, explaining the slow increase of %bb after the end of the polymerization.

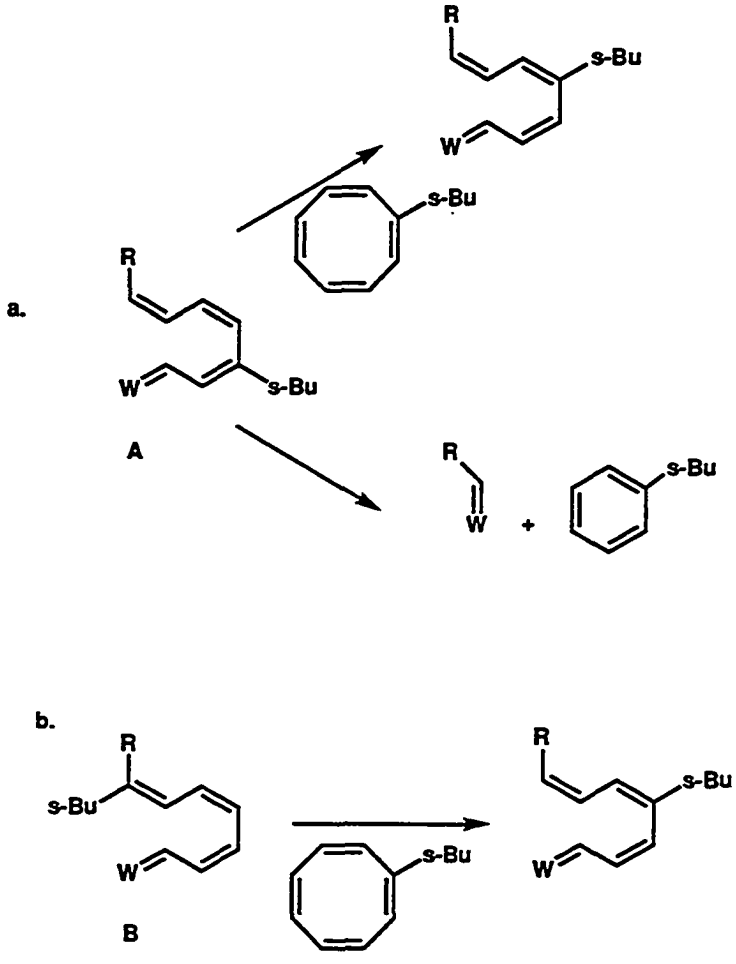


**Figure 7.** Possible mechanistic scheme explaining the kinetics of appearance of backbitten products.

## 3. Polymerization of NBE

### a. Kinetic aspects

Norbornene polymerization with catalysts **1** to **6** is extremely rapid, precluding the possibility of studying the rate of polymerization as a function of HFB amount. The rate of initiation relative to propagation can be evaluated using Gold's equation. In most cases, we observed a significant improvement of the initiation relative to the propagation, especially with

catalysts **1**, **2**, **4** and **6** (Table 6). Catalyst **3** possesses a chelating initiating carbene and $k_p/k_i$ is so high (no propagating carbene is observed) that it cannot be measured accurately. Catalyst **5** initiates the polymerization of norbornene so quickly so that no improvement is seen upon addition of HFB. Notably, as discussed above, the decrease of $k_p/k_i$ with increasing concentrations of HFB is not due to a poisoning of the catalyst by the alcohol.[12] If such was the case, the polymerization rate should be considerably decreased in pure alcohol (see for example the kinetics of cyclooctadiene polymerization above). Actually qualitative observations indicate that the rate of propagation increases with HFB.

HFB is not the only alcohol which effects the rates of initiation and propagation. For example, norbornene can be polymerized by W(=NAr)(O-*t*-Bu)$_2$(=CHCPhMe$_2$), in *t*-BuOH solvent (with one drop of benzene) to give a monodisperse polymer. In addition, for Mo(=NAr)(O-*t*-Bu)$_2$(=CHCPhMe$_2$), **7**, the initiation is improved by the addition of *t*-BuOH (Table 7).[16] However, the polymerization of NBE by **7** stops after a few monomer insertions. It is likely that major decomposition occurs, indicating a difference of behavior between **7** and its tungsten analogue and between *t*-BuOH and HFB. Therefore, cautiousness should be used to interpret the results of Table 7.

---

[12] Kinetics of 1,5-cyclooctadiene polymerization confirmed that no inhibition or regulation of the propagation occurs.

**Table 6.** $k_p/k_i$ for norbornene polymerization by different catalysts, at room temperature.

| Catalyst | [MON] (mol/l) | [MON]/[CAT] | [HFB] (%) | [HFBLi] (%) | % initiation | $k_p/k_i$ |
|---|---|---|---|---|---|---|
| **1** | 0.12 | 13 | 2.3 | 0 | 19 | 625 |
| **1** | 0.12 | 13 | 2.3 | 470 | 19 | 50000 |
| **1** | 0.12 | 13 | 3.8 | 6.5 | 14 | 1130 |
| **1** | 0.12 | 13 | 636 | 0 | 16 | 782 |
| **2** | 0.13 | 15.2 | 680 | 0 | 47 | 89 |
| **2** | 0.13 | 14.2 | 1.7 | 0 | 31 | 227 |
| **2** | 0.14 | 15.5 | 0 | 11.7 | 6 | 7900 |
| **2**[1] | 0.14 | 10.1 | 1.7 | 0 | 25 | 259 |
| **2**[2] | 0.13 | 7.4 | 4.6 | 0 | 34 | 91 |
| **4** | 0.14 | 13.3 | 0 | 5.2 | 21 | 16 |
| **4** | 0.14 | 13.3 | 1.6 | 0 | 46 | 54 |
| **4** | 0.14 | 13.3 | 240 | 0 | 72 | 268 |
| **5**[3] | 0.12 | 12.1 | 720 | 0 | 90 | 7 |
| **5**[3] | 0.12 | 12.1 | 10 | 0 | 84 | 9 |
| **6**[4] | 0.12 | 4 | 0 | 3.1 | 4 | 4800 |
| **6**[4] | 0.12 | 4 | 3.1 | 0 | 56 | 13 |
| **6**[4] | 0.12 | 4 | 412 | 0 | 57 | 12 |

1 With 5 equivalents of $B(C_6F_5)_3$

2 With $Na_2HPO_4$

3 With 60 equivalents of THF

4 For catalysts VI, the $k_p/k_i$ is obtained by use of Gold equation, although the rate law is not first order in catalyst (because of phosphine inhibition). Nevertheless, the relative order of $k_p/k_i$ can be compared, because the experiments are done with similar monomer and catalyst concentrations.

**Table 7.** $k_p/k_i$ for norbornene polymerization by **7**, at room temperature.The polymerization is not living and polymerization quickly stops when large amount of *t*-BuOH are present. (R = *t*-Bu)

| [MON] (mol/l) | [MON] /[CAT] | [ROH] (%) | [ROLi] (%) | % initiation | $k_p/k_i$ |
|---|---|---|---|---|---|
| 0.247 | 13.3 | 0 | 0 | 77 | 16 |
| 0.247 | 13.3 | 450 | 0 | 80 | 14 |
| 0.247 | 13.3 | 900 | 0 | 98 | 3.9 |
| 0.247 | 13.3 | 1350 | 0 | 100 | ≈1[a] |

a. $k_p/k_i$ can not be calculated exactly, because the Gold equation diverges for 100% initiation.

**b. Polymer morphology**

In a typical polynorbornene polymerization, there is apparent contamination of the polymer by a very high molecular weight fraction ($M_n$ ~ 500000 g/mol) , which appears as a shoulder in the GPC. In the past, studies conducted on the polymerization of norbornene by **2** concluded that this shoulder was due to a trace amount of a highly active impurity which contaminates **2**.[4] However, since the synthetic route for catalysts **1**, **2**, **5** and **6** are quite different, this explanation seems unlikely. It has also been more recently proposed that this high molecular weight shoulder in the GPC distribution originates from traces of adventitious oxygen.[17,18]

It was found that adding HFB reduces the size of the high molecular weight peak (Figure 8). For all catalysts except **5**, only the very high molecular weight peak is observed in aprotic conditions, whereas only the expected low molecular weight peak is observed when the polymerization is run in *neat* HFB. Typical dry-box conditions (HFB/CAT ≈ 1%) produce a polymer which is contaminated by 20% of high molecular weight product. The high-molecular weight polymer and low molecular weight polymer are both ROMP type polynorbornene. The high molecular weight fraction is up to 99% cis (Figure 9) and of very regular structure. The low molecular weight fraction is usually at least 95% cis. Although tacticity has never been assigned for ROMP polynorbornene, the extreme simplicity of the $^{13}C$ spectrum for both fractions seems to support the fact that the polymer is highly tactic. Using substituted norbornenes, it has always been found that catalysts **1** and **2** give highly syndiotactic polymers;[6,9] therefore it is likely that the polymer is highly syndiotactic. When the polymerization is run in dry HFB, the polymer does not present any high molecular weight shoulder,

and in this case, the molecular weight grows linearly with the ratio of the monomer to catalyst concentrations.

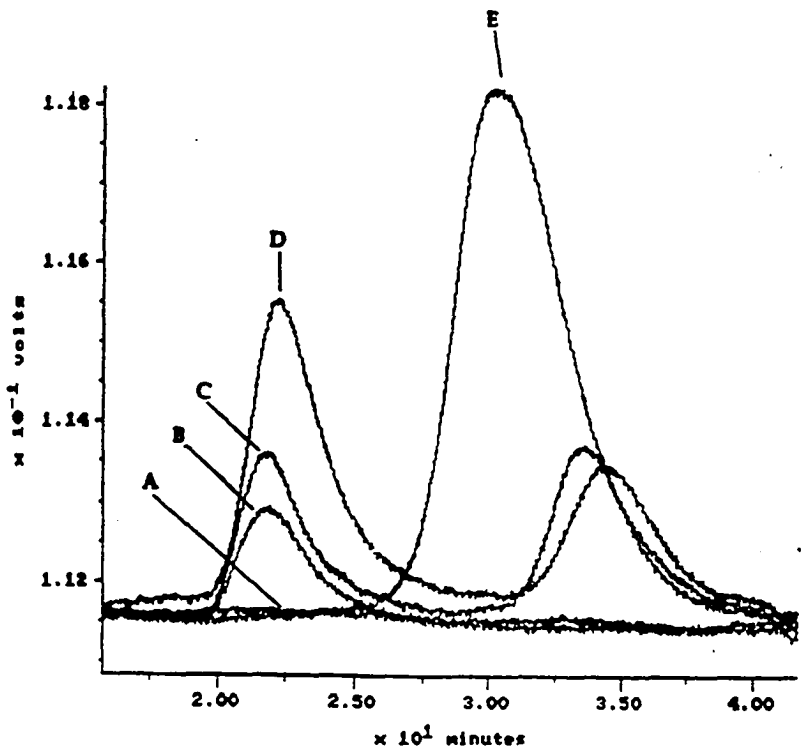


Figure 8. GPC trace of polynorbornenes made with different HFB amounts. Experimental conditions: [NBE] / [2] = 65, [NBE] = 0.58 mol/l A. Excess $Rf_6OLi$ (no polymerization) B. [Rf6OLi] / [2] = 2.0, [Rf6OH] / [2] = 0; C. [Rf6OLi] / [2] = 0.02, [Rf6OH] / [2] = 0; D. [Rf6OLi] / [2] = 0, [Rf6OH] / [2] = 21; E. [Rf6OLi] / [2] = 0.0, [Rf6OH] / [2] = 1160. Similar results are also obtained for catalysts **3**, **4** and **6**. The molybdenum catalyst **1** shows less pronounced effects. For catalyst **5**, a very high molecular weight peak is exclusively observed for large amounts of Rf6OH.

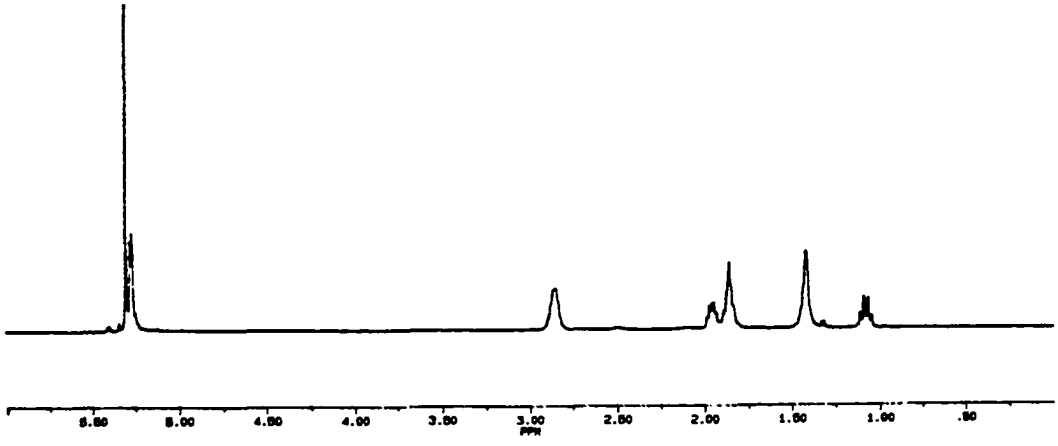


**Figure 9** $^{1}H$ (top) and $^{13}C$ (bottom) NMR of high molecular weight polynorbornene.

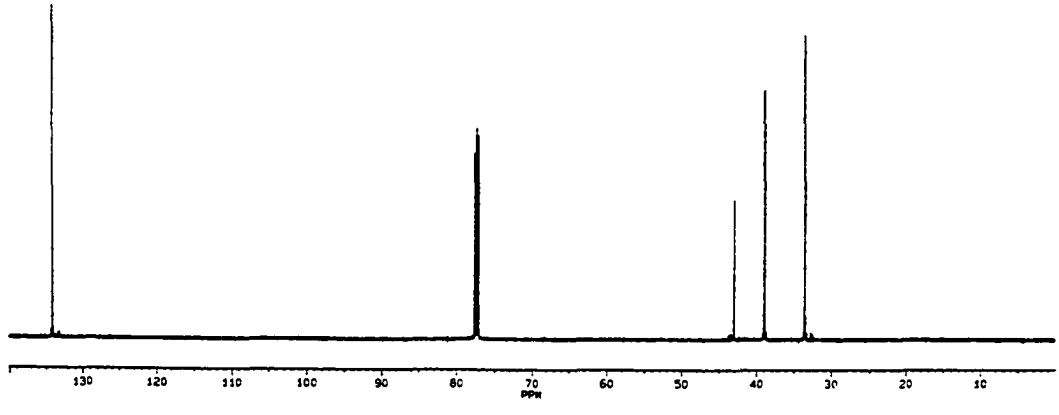

This set of experiments seems to support the existence of two active sites: one giving high molecular weight polymer, and the other one giving low molecular weight polymer. One possibility is that the low molecular weight polymer is produced by the living catalyst, whereas the high molecular weight polymer is created by a very active impurity. Interestingly, when the polymerization is run at very low temperature ( - 45 °C), only the very high molecular weight fraction is formed, despite the fact that a non negligible amount of propagating carbene (8%) is observed by NMR. Therefore, the origin of the high molecular weight fraction is possibly due to other factors. For example, Figure 10 features the GPC traces of a high molecular weight polynorbornene sample (A) which was sonicated (B), then heated to 120 °C under vacuum and slowly cooled[13] (C), then sonicated again (D): after each sonication the high molecular weight fraction disappeared, whereas after the annealing process it reappeared, although not quantitatively

Analogously, an exclusively low molecular weight polynorbornene (A) was annealed, and then showed a high molecular weight shoulder (B) (Figure 11). Such results indicate that the nature of the high molecular weight sample is physical and not chemical. Further evidence demonstrates the "physical" nature of this high molecular weight peak. For example, the $T_g$ of a high molecular weight sample is 59.6 °C[19] whereas the Tg of a typical polynorbornene is 38 °C.[20,21]

---

[13] Trace amounts of BHT were added to avoid crosslinking

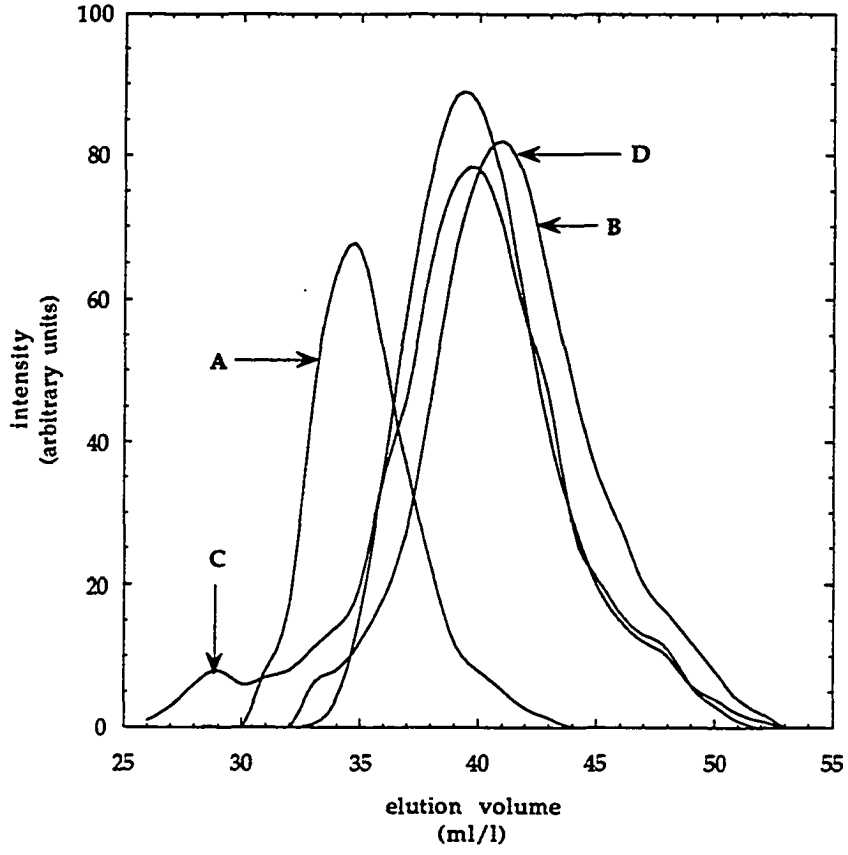


**Figure 10.** GPC trace of polynorbornene sample obtained from reaction of 370 equivalents of NBE with a 1.91 $10^{-2}$ mol/l solution of **2**. **A.** PNBE before sonication, $M_n$ = 150 $10^3$ g/mol, PDI = 2; **B.** PNBE after sonication, $M_n$ = 15 $10^3$ g/mol, PDI = 2.5; **C.** annealed sample, $M_n$ = 27 $10^3$ g/mol, PDI = 7 (high molecular weight shoulder $M_n$ = 1380 $10^3$ g/mol, PDI = 1.3); **D.** sonicated annealed sample, $M_n$ = 14 $10^3$ g/mol, PDI = 2.8.

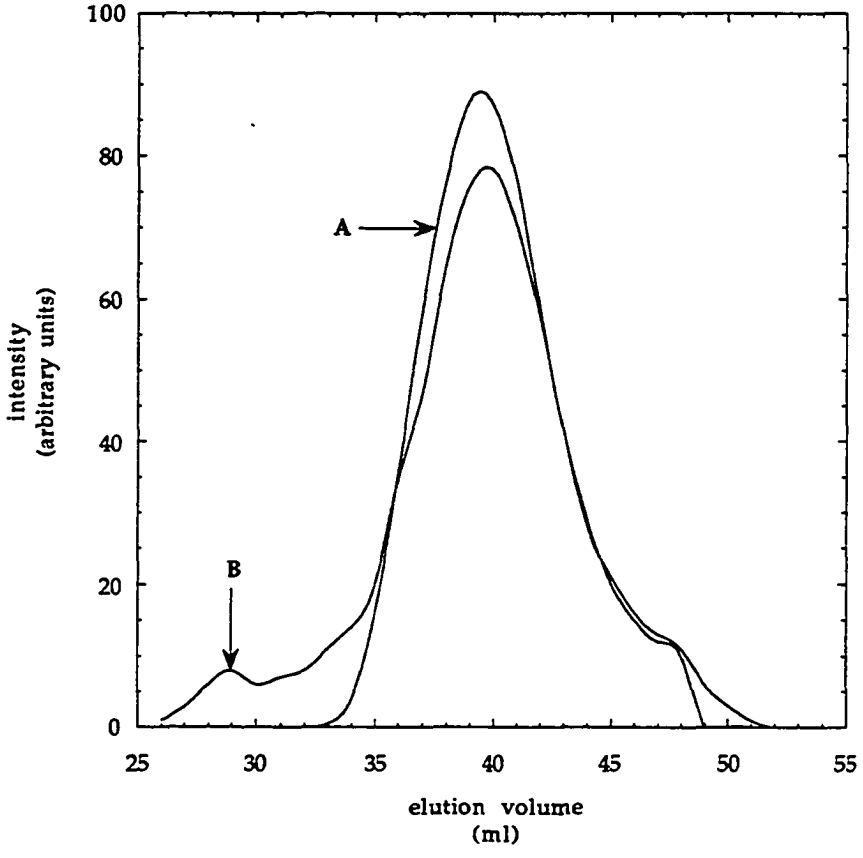


**Figure 11.** GPC trace of polynorbornene sample obtained from reaction of 360 equivalents of NBE with a 1.91 $10^{-2}$ mol/l solution of **2** in neat HFB. **A.** PNBE from polymerization, $M_n$ = 17 $10^3$ g/mol, PDI = 2; **B.** PNBE after annealing, $M_n$ = 26 $10^3$ g/mol, PDI= 3.5 (high molecular weight shoulder: $M_n$ = 1745 $10^3$ g/mol, PDI = 1.2)

To confirm this hypothesis, we have end-capped a short polynorbornene sample (equation 6) with benzaldehyde. The NMR of the purified and isolated polymer indicates that phenyl endgroups account for 1.3% of the number of units in the chain (Figure 12). Therefore, if we suppose a yield of end-capping of 100%, the average number molecular weight of the chains by NMR is 7300 g/mol.

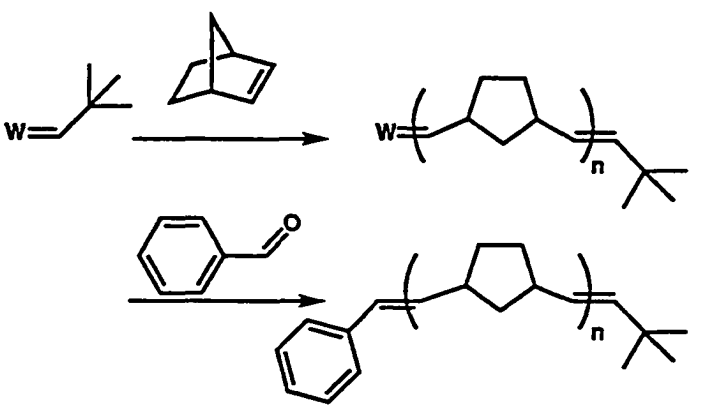


(6)

By GPC, the distribution of this oligomer is clearly bimodal: the short chains have a $M_n$ of 12000 g/mol (PDI = 1.2) (relative to polystyrene), whereas the long chains have a $M_n$ of 190000 g/mol (PDI = 2.1) (Figure 13). When corrected to PNBE standards,[22] the short chains have approximately a molecular weight of 6000 g/mol, which corresponds to the molecular weight calculated by $^1H$ NMR. Both these short and long polymers do absorb strongly in UV, indicating that they are end-capped by benzaldehyde.[23] The average number molecular weight for the average of the two distributions is 37000 g/mol (PDI = 8.5), which is in large excess of what is expected from NMR. This indicates that the chains which appear as very high molecular weight by GPC, are actually lower molecular weight chains.

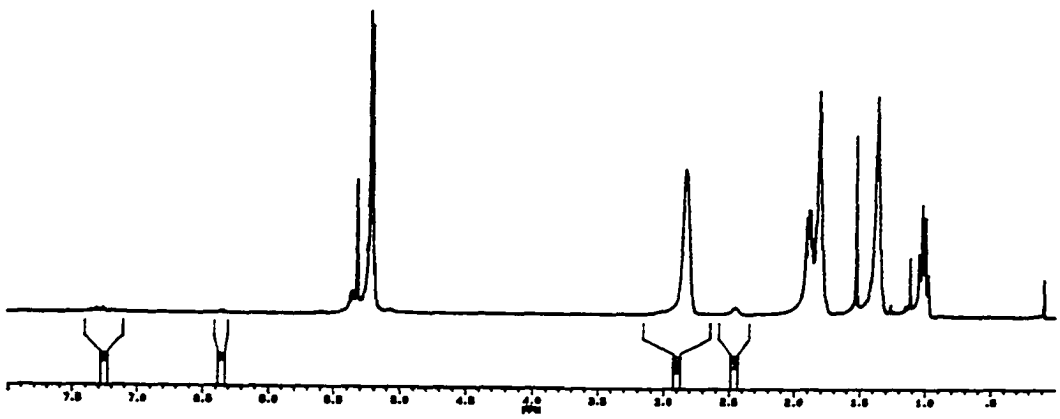

**Figure 12.** $^{1}H$ NMR of polynorbornene oligomer end-capped by benzaldehyde. The polymer has been done in 1.0 $10^{-2}$ mol/l solution of catalyst **2** in hexane, using 10.1 equivalents of NBE.

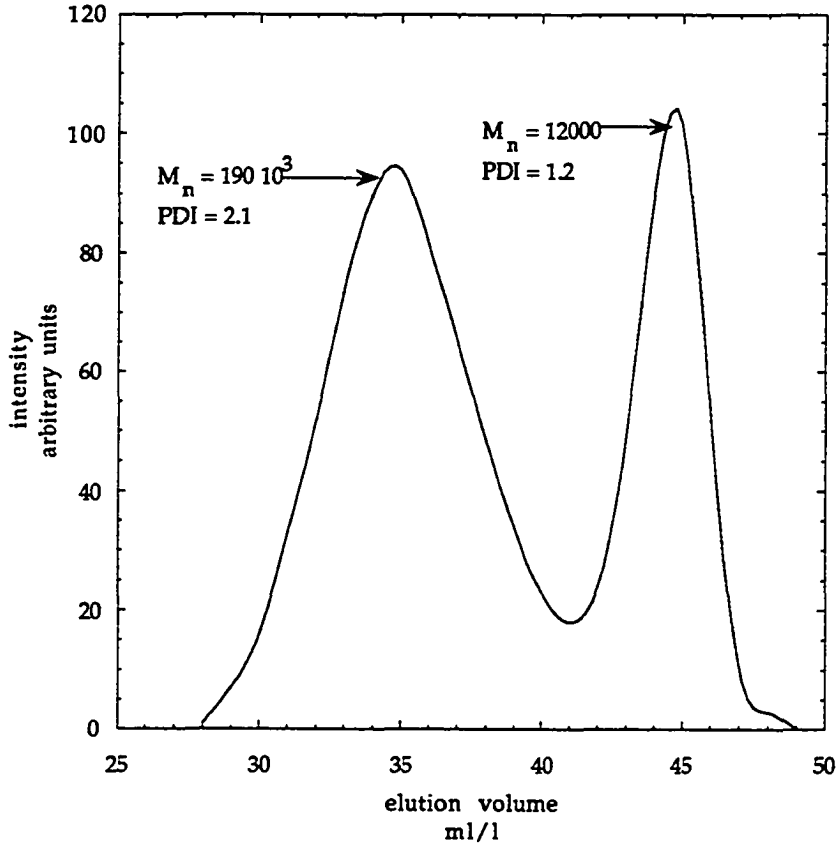


**Figure 13.** GPC trace of a polynorbornene sample end-capped with benzaldehyde obtained from reaction of 10.1 equivalents of NBE with a 1.0 $10^{-2}$ mol/l solution of **2** in hexane

c. Possible interpretation

At this stage, it is still too early to present a definitive interpretation of the results presented here. However, a possible explanation is given here. The PNBE samples prepared by catalysts **1** to **6** are highly tactic and are therefore likely to crystallize easily. During the synthesis of the polymer, if the rate of crystallization is comparable to the rate of propagation, the resulting polymer will include small clusters of polynorbornene chains (crystallites) which are held together by Van der Waals forces. The GPC of this type of samples indicates a very high molecular weight peak corresponding roughly to the weight of a crystallite.[14] Sonication breaks the crystallites to give a fully dissolved polymer. A similar phenomenon has been observed for poly(vinylchloride) : when the polymer has too a high degree of tacticity, GPC indicates a very high molecular weight, unless the sample is sonicated before hand.[24] Annealing an amorphous yet tactic sample will allow the chains to rearrange, to create crystallites, thus explaining the reversible presence of high molecular weight shoulder upon heating a low molecular weight polymer.

When the polymerization is done in the absence of any protic impurity, or at low temperature, the rate of polymerization may be slower than the rate of crystallization: therefore, during polymerization, the chains have time to rearrange, and form crystallites. In the presence of large excess of alcohol, the polymer is formed very rapidly (the reaction is also very

---

[14] GPC separates fractions by hydrodynamic volumes, not molecular weight, and high molecular weight fractions and crystallites will elute at similar time.

exothermic) and the polymer chains may entangle before formation of crystallites and yield samples without "high molecular weight" peak.

IV. Mechanistic implications

HFB increases the rate of polymerization for most monomers. This activation could have dramatic effects on the morphology and physical properties of the polymer. Nevertheless, at this time, the precise mechanism of activation is still unclear. In this part, preliminary results are presented : they do not allow the elucidation of the mechanism but do narrow down the number of possible mechanisms.

The role of HFB is not completely clear, but, it seems it acts as a proton source. Catalysts **1** to **6** are stable to Bronsted acids such as $KHSO_4$ and $Na_2HPO_4$, and seem to be slightly activated by them (entry 9 of Table 6). We also found that HCl reacts smoothly with catalyst **1** to give mainly untouched starting material as well as a new carbene, of unknown structure at this time.[30] Catalyst with HCl added rapidly polymerizes sBCOT, whereas the pristine catalyst does not. Strong Lewis acids such as $B(C_6F_5)_3$ seems to act as moderate activators (entry 8 of Table 6), whereas alkylaluminum compounds trigger the decomposition of the catalysts.

Three possible activation sites by a proton can be envisaged : on the carbene ligand, on the imido ligand and on an alkoxide (Figure 14).

Reversible addition of a proton on a carbene is conceivable since activation of titanium carbenes by chlorodialkylaluminum is readily observed.[25-27] If this reaction takes place, then addition of HFB deuterated in the hydroxyl position should generate a deuterated carbene by proton exchange. Such a result is not observed for any of the catalysts **1** to **6**.

The rate of carbene rotation (interconversion from anti to syn) should be affected if protonation occurs on the carbene. Table 8 summarizes the results about the rate of interconversion for various amounts of HFB.[12] In general, this experiment is practically difficult, so that it seems possible to conclude that within experimental errors, the rate of interconversion syn to anti is not affected by the presence of HFB.

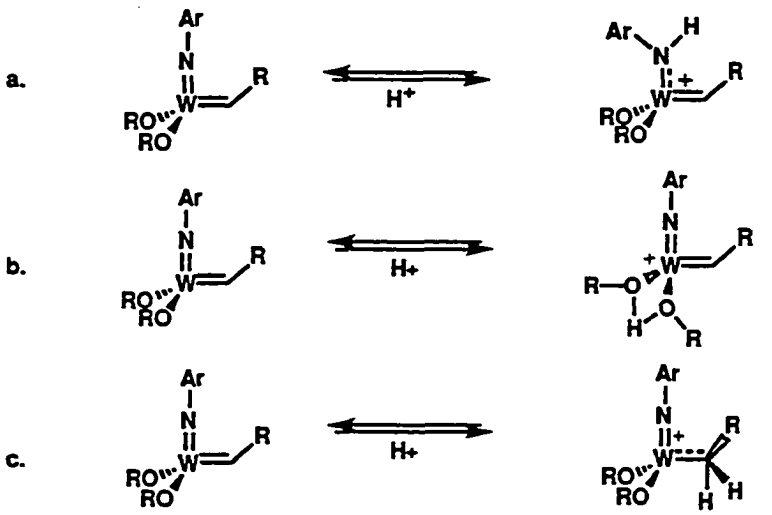


**Figure 14.** Sites of proton attack.

**Table 8.** Rate $k_{a/s}$ of rotation of the anti rotamer to the syn rotamer in toluene d8.[28]

| Catalyst | [HFB] / [CAT] | ka/s ($s^{-1}$) | T (K) |
|---|---|---|---|
| **1** | 0 | $0.95\ 10^{-4}$ | 248 |
| **1** | $1.5\ 10^{-2}$ | $0.64\ 10^{-4}$ | 248 |
| **1** | 2.37 | $2.67\ 10^{-4}$ | 248 |
| **2**[a] | 0.01 | $7.1\ 10^{-4}$ | 261 |
| **2**[a] | 3.2 | $26.1\ 10^{-4}$ | 261 |

a. The catalyst is contaminated by a trace amount of diethyl ether.

In order to assess if the acid attack occurs on the imido ligand, the rotation rate of the N-C bond was assessed using the degeneracy of the

methyl groups of the isopropyl groups of catalyst **1**.[29,12] At low temperature in THF $d^8$, each pair of methyl group is diastereotopic, and appears as two doublets. At high temperature, degeneracy (one doublet) is observed (T*coalescence* = - 10 °C). Using band shape analysis, it is found that the rate of rotation of the N-C bond is independent of the amount of HFB. Activation parameters for this process were found to be $\Delta H^{\ddagger}$ = - 20 kcal/mol and $\Delta S^{\ddagger}$ = 28 e.u. This experiment is therefore non-conclusive: if the rate of imido rotation was to be drastically changed by the amount of HFB, then it would be possible to conclude in imido attack by a proton, but attack of the proton on the imido ligand does not necessary entail a change in the imido rotation, for the reason that only a small amount of the catalyst may be activated at a given time.

Experiments to assess the rate of alkoxide exchange in the presence or absence of alcohol are underway.

## V. Conclusion

In this chapter, the presence of small amounts of alcohol was detected in samples of most well defined ROMP molybdenum and tungsten catalysts. The alcohol is the protonated form of the metal bound alkoxide of the corresponding catalyst, and originates from the thermal decomposition of the catalyst over time, and from incomplete purification during the synthesis of these catalysts.

These metathesis catalysts were found to be stable in the presence of large excesses of tertiary alcohol, an interesting feature considering the nucleophilicity of the carbene. It was also found that tertiary alcohol promotes exchange with the bound alkoxide, to generate a new catalyst. Therefore, tuning the activity of the catalyst is now possible by adding alcohol.

Alcohols, especially hexafluoro-*tert*-butanol act as a remarkable activator of the polymerization. This activation is attributed to the Bronsted acid character of the alcohol. We showed that rates of polymerization and initiation are increased by the presence of even a small amount of alcohol. Catalysts which do not polymerize sBCOT or COD by themselves, do polymerize it rapidly in the presence of alcohol. The residual activity of the catalyst without alcohol was not found, and it is not obvious that catalysts have any activity (except for norbornene polymerization) without the presence of protic compounds. Activation by an excess of alcohol can be detrimental to solution polymerization of sBCOT, because of the increase in backbiting.

In norbornene polymerization, the apparent molecular weight of the polymer depends on the amount of HFB present: in aprotic conditions, only a very high molecular weight sample is observed, whereas in neat alcohol, a

clean low molecular weight sample is obtained. Under other conditions, a bimodal distribution is observed. We *propose* (until confirmation) that the apparent molecular weight does not reflect the real molecular of the polymer chains, but the mere physical state of the polymer. The observed "very high molecular weight polymer" is only a crystallite, which can be dissolved upon sonication.

The origin of the alcohol activation has been partially investigated: at this time, it is clear that proton addition to the carbene ligand does not occur but method of activation remains unclear.

## VI. Experimental Part

General methods are described in the experimental section of Chapter 2.

**-Kinetics of decomposition.**

11.0 mg of freshly synthesized catalyst 4 were dissolved in 1.024 mg of benzene $d^6$. All the glassware necessary for this experiment was washed with concentrated $NH_4OH$ or a silanizing agent, and then dried at 150 °C for 6 hours. This solution was separated into two aliquots which were immediately analyzed by NMR. The amount of alcohol is calculated from the ratio of the integrals in $^{19}F$ NMR I(free alcohol) / [ I(free alcohol) + I(bound alkoxide) + I(free alkoxide)]. The first NMR tube was stored under anaerobic conditions for 16 hours, after which a NMR assay was taken. The second NMR tube was introduced in a large flask equipped with a Kontes valve, which was filled with enough toluene so that a third of the NMR tube was immersed in the liquid. The flask was then brought out of the dry box and heated at 40 °C for 16 hours. The NMR tubes were brought out of the flask just before NMR analysis.

**-Kinetics of COD polymerization by 6.**

**NMR analysis**

17.6 mg of 6 ($2.02\ 10^{-5}$ mol) were dissolved in 482.5 mg of toluene $d^8$ (c = $3.6\ 10^{-2}$ mol/l). This solution is used as stock solution for all kinetics experiments. 50 µl of the stock solution are added to 250 µl of benzene $d^6$ in an NMR tube. Just before inserting the tube in the NMR probe, 100 µl of COD are added, and the kinetics is followed by setting up a routine which accumµlates a spectrum every three minutes. If HFB is present, the amount

of benzene is reduced so that the total volume of the sample is exactly 400 µl. From the integration of the olefin peaks of the monomer and polymer, data are extracted, which are fitted to the rate law [MON] = a0 + b0 * exp ( - k t).

**GC analysis**

To 377 mg of HFB, are added 100 µl of monomer (COD) and 50 µl of the stock solution of catalyst as well as 20 µl of xylene (internal standard). The kinetics is followed at intervals of approximately 5 minutes. The polymer precipitates during the polymerization. Every aliquot withdrawn from the polymerization mixture is added to a large amount of benzaldehyde. The sample is brought out of the dry box, flushed with methanol and filtered. After injection on GC, the integrals of the signals of the monomer and internal standard are compared and kinetic data are henceforth extracted.

**Calcµlation of the ratio $k_p/k_i$ for different amounts of alcohol**

A stock solution of catalyst **2** is prepared ( c = 1.34 $10^{-2}$ mol/l in benzene d6). 3 NMR tubes are prepared containing the same amount of the catalytic solution. In tube 1, nothing is added: $^{19}F$ NMR indicates the presence of 1.7% of HFB. In tube 2 6 µl of a PhLi solution are added (obtained from 21.7 mg of PhLi in 408.6 mg of benzene $d^6$ and 88.6 mg of THF $d^8$). $^{19}F$ NMR indicates the presence of 18.7% of HFBLi
and no HFB. $^1H$ NMR indicates very slight decomposition of the catalyst due to adding excess of PhLi. In tube 3, 3.5 µl of HFB are added.

A norbornene solution (0.445 mol/l in benzene d6) is prepared in a vial endcapped with a screw cap and a septum. The vial is kept in a nitrogen filled glove-bag by the NMR spectrometer. In each tube, 200 µl of the norbornene solution is injected through syringe. The $^1H$ NMR is recorded

immediately after injection, so as the eventual decomposition of the propagating carbene is minimal. $k_p/k_i$ is obtained using Gold equation (see chapter 1). The propagating carbene can also be observed by 19F NMR: 6 peaks are visible at -76.68, -77.29, -77.73. -78.277 and -78.38 ppm.

**Polymerization of norbornene in pure HFB**

6.4 mg of of catalyst 2 ($7.98\ 10^{-6}$ mol), dissolved in 50 µl of benzene are added to 563 µl of HFB. 235 µl of a 3.41 mol/l solution of norbornene in benzene are added to the stirring yellow solution. Immediately, an exothermic reaction, inducing solvent boiling, is observed, and a clear white polymer precipitates out of the yellow solution. After 12 seconds, benzaldehyde is added, and the sample is exposed to air. The polymer is filtered off the liquid and washed with methanol. Addition of methanol to the liquid affords the precipitation of a very small amount of additional polymer. After drying in vacuo, 75 mg of polymer is collected (y = 99 %). GPC analysis (toluene, 60 °C) $M_n$ = 19220, PDI = 1.7.

**Polymerization of norbornene in aprotic conditions**

**Technique 1** A stock solution of catalyst **2** ($1.34\ 10^{-2}$ mol/l) is prepared. 250 µl of this solution are added to 3.3 mg of *freshly* sublimed HFBLi. The solution turns slightly darker after stirring. 98 µl of 3.41 mol/l solution of norbornene in benzene are added to the solution, and precipitation occurs immediately, giving an extremely viscous, unstirrable mixture. After 12 seconds, benzaldehyde is added, and the sample is exposed to air (longer exposition to catalyst will reduce the viscosity). GPC analysis (toluene, 60 °C) $M_n$ = 496964, PDI = 1.9 (additionnal small peak, Mn

= 12000, PDI = 1.5). Addition of large excesses of HFBLi results in catalyst decomposition.

**Technique 2** To a solution of benzene (5 ml), 6 mg of pure PhLi is added. The PhLi is allowed to settle, and 787.6 mg of clear benzene from the decanted suspension are withdrawn to be added to 102 mg of norbornene (187 equivalents). 4.6 mg of catalyst **2**, ($5.25\ 10^{-6}$ mol, 1 equivalent) are dissolved in 200 µl of the benzene withdrawn from the stock solution. Upon addition of norbornene solution to the catalyst, polymerization occurs immediately, to give an extremely viscous mixture. After 2 minutes, 100 µl of acetone are added to stop the polymerization and the mixture is stirred 10 minutes, after which the polymer is dissolved in $CH_2Cl_2$, and then precipitated from MeOH. Most of the sample (white pellet) can be collected from the solution, and the rest of the polymer is collected after centrifugation. After drying in vacuo overnight, 102 mg of polymer are obtained (y = 99%). GPC analysis ($CH_2Cl_2$, RT) : $M_n = 149\ 10^3$ g/mol, PDI =2.07. cis/trans = 97/3

$^1$H NMR ($CDCl_3$): cis: 5.22 (2, d, J = 6.1 Hz, CH=CH), 2.8, (2, $CHR_3$), 1.88 (1, dd, J = 6,7 Hz, J = 6.2 Hz $CHR_3$-CHH'-$CHR_3$), 1.8 (2, b, CHH'), 1.37 (2, b, CHH'), 1.03 (dd, J = 12.3 Hz, J = 10.1 Hz $CHR_3$-CHH'-$CHR_3$)

trans : 5.4 (b, 2), 2.4 (b, 2), 1.5 (b, 2), other resonances overlapped by cis polymer.

$^{13}$C NMR ($CDCl_3$): cis : 134.1, 42.96, 38.83, 33.45.

$T_g$ = 59.7 °C (by DSC)[19].

**Sonication and annealing**

The previous sample was dissolved in 25 ml of $CH_2Cl_2$ and sonicated for 13 hours in a pressure tube. Eventually, the temperature of the sonicating bath reaches 45 °C.

A clean purified low molecular weight sample (containing ca 1% BHT) is placed in a round bottom flask under vacuum. The flask is immersed in an oil bath which is slowly raised to 125 °C. After 4 hours at this temperature, heating is stopped, and the flask is cooled to room temperature over a period of two hours.

**Rate of interconversion ka/s**

A NMR tube containing 10.3 mg of **1** in toluene d8 and 10 µl of HFB is placed in a glass Dewar equipped with a filter window ($\lambda$cutoff = 364nm). The liquid of the NMR tube is placed just against the filter window, and the Dewar is cooled at -85 °C (heptane cold bath). Irradiation is carried out for 24 hours at this temperature, with a medium pressure 250W Hannovia mercury lamp. The NMR tube is then frozen in liquid nitrogen, and allowed to thaw to -25°C in the NMR probe. The decay of the anti carbene (13 % maximum) and the recovery of the syn carbene follows first order kinetics.

**Rate of C-N bond rotation and band shape analysis[29,12]**

21.4 mg of **1** are dissolved in 484.2 mg of THF $d^8$. NMR spectrum are recorded at different temperatures ( - 60 °C, -50 °C , -40 °C, -30 °C, -20 °C, -10 °C, 0 °C, 10 °C, 20 °C and 30 °C). Methyl resonances of the isopropyl group appears as two doublets at low temperature, and one doublet at high temperature. The rate of rotation (in $s^{-1}$) is calculated from $k = \pi \delta\nu / 2^{1/2}$ at coalescence temperature (-10 °C). $\delta\nu$ is the separation (in Hertz) between the two doublets at very low temperature ($\delta\nu$ = 110.98 Hz at - 60 °C). The rate of

rotation above coalescence temperature is calculated as $\pi \delta\nu^2 / 2 (W^* - Wo)$ where Wo is the half width of one of the doublet peaks at high temperature (Wo (30 °C) = 2.4 Hz) and W* is the half width of one of the doublet at the temperature considered. If, at this temperature, the 2 peaks of the doublets overlap, then W* = half width of the non resolved doublet - J (J = 6.72 Hz). The results for C-N bond rotation in the presence of 2.4 equivalents of HFB are listed in Table 9.

**Table 9.** $^1H$ line shape analysis forC-N rotation in catalyst **1** in the presence of 2.4 equivalents of HFB. The activation parameters, as given by an Eyring plot, are $\Delta H^{\ddagger} = -20$ kCal/mol and $\Delta S^{\ddagger} = 28$ e.u.

| T ( °C) | W* - Wo (Hz) | k ($s^{-1}$) |
|---|---|---|
| - 10 | coalescence | 246 |
| 0 | 12.2 | 1146 |
| 10 | 4.9 | 3343 |
| 20 | 1.2 | 13743 |

## VII. References

(1) (a) Ivin, K. J. *Olefin Metathesis*; Academic: London, 1983. (b) Katz, T. J.; McGinnis, J. *J. Am. Chem. Soc.* **1975**, *97*, 1592-1594. (c) Herisson, J. L.; Chauvin, Y. *Makromol. Chem.* **1970**, *141*, 161. (d) Grubbs, R. H. *Prog. Inorg. Chem.* **1978**, *24*, 1. (e) Calderon, N; Ofstead, E. A.; Ward, J. P.; Judy, W. A.; Scott, K. W. *J. Am. Chem. Soc.* **1968**, 4133, 90. (f) Mol, J. C.; Moulijn, J. A.; Boelhouwer, C. *J. Chem. Soc., Chem. Comm.* **1968**, 633. (g) Dall'Asta, G; Motroni, G. *Eur. Polym. J.* **1971**, *7*, 707. (h) Bradshaw, C. P. C, Howman, E. J.; Turner, L. *J. Catal* **1967**, 269, 7. (i) Grubbs, R. H. in *Comprehensive Organometallic Chemistry*; Wilkinson, G.; Stone, F. G. A.; Abel, E. W. Eds.; Pergamon Press: New York, 1982; Vol. 8, pp. 499-551. (j) Ivin, K. J. *Olefin Metathesis*; Academic Press: London, 1983. (k) Dragutan, V.; Dimonie, M. *Olefin Metathesis and Ring-Opening Polymerization of Cyclo-Olefins*; Wiley: New York, 1985. (l) Feldman, J.; Schrock, R. R. in *Progress in Inorganic Chemistry*; Lippard, S. J. Eds.; Wiley: New York, 1991; Vol. 39, pp. 1-74. (m) Schrock, R. R. *Acc. Chem. Res.* **1990**, *23*, 158-165. (n) Aguero, A.; Osborn, J. A. *New J. Chem.* **1988**, 12, 2.

(2) Schrock, R. R.; DePue, R. T.; Feldman, J.; Schaverien, C. J.; Dewan, J. C.; Liu, A. H. *J. Am. Chem. Soc.* **1988**, *110(5)*, 1423-1435.

(3) Schrock, R. R. *Abstracts Of Papers Of The American Chemical Society 195* **1988**, 21.

(4) Schrock, R. R.; Feldman, J.; Cannizzo, L. F.; Grubbs, R. H. *Macromolecules* **1987**, *20*, 1169-1172.

(5) Schrock, R. R.; Murdzek, J. S.; Bazan, G. C.; Robbins, J.; Di-Mare, M.; O'Regan, M. *J. Am. Chem. Soc.* **1990**, *112*, 3875.

(6) Schrock, R. R. *Accounts Of Chemical Research 23* **1990**, 158-165.

(7) Schrock, R. R.; Murdzek, J. S.; Bazan, G. C.; Robbins, J.; Dimare, M.; Oregan, M. *J. Am. Chem. Soc. 112* **1990**, , 3875-3886.

(8) Schrock, R. R. *Abstracts Of Papers Of The American Chemical Society 199* **1990**, , 476.

(9) Schrock, R. R.; Mcconville, D.; Oskam, J.; Odell, R.; Hofmeister, G. *Abstracts Of Papers Of The American Chemical Society* **1994**, *207*, 58-INOR.

(10) Schrock, R. R. *Organometallics* **1990**, 9, 2850-2850.

(11) Oskam, J. H.; Schrock, R. R. *J. Am. Chem. Soc.* **1992**, *114*, 10680-10680.

(12) Oskam, J. H.; Schrock, R. R. *J. Am. Chem. Soc.* **1993**, *115*, 11831-11845.

(13) Chamberlain, L. R.; Rothwell, I. P.; Huffman, J. C. *J. Am. Chem. Soc.* **1986**, *108*, 1502.

(14) Ehrenfeld, D.; Kress, J.; Moore, B. D.; Osborn, J. A.; Schoettel, G. *J. Chem. Soc., Chem. Comm.* **1987**, 1062.

(15) Bell, A.; Clegg, W.; Dyer, P. W.; Elsegood, M. R. J.; Gibson, V. C.; Marshall, E. L. *J. Chem. Soc. Chem. Comm.* **1994**, , 2547.

(16) Thanks to A. Pangborn for providing this set of values.

(17) Feast, W. J.; Gibson, V. C.; Kosravi, E.; Marshall, E. L.; Mitchell, J. P. *Polymer* **1992**, *33(4)*, 872.

(18) Perrott, M. G.; Novak, B. M. *Abs. Pap. Am. Chem. Soc.* **1993**, *206*, 187-Poly.

(19) Dr G. Coates is gratefully ackowledged for providing these values

(20) Stelzer, F.; Grubbs, R. H.; Leising, G. *Polymer* **1991**, 32, 1851-1856.

(21) Stelzer, F.; Leitner, O.; Pressl, K.; Leising, G.; Grubbs, R. H. *Synthetic Metals* **1991**, *41*, 991-994.

(22) Novak, B. M., Ph. D. Thesis, California Institute of Technology, 1989.

(23) Canizzo, L., Ph.D. Thesis, California Institute of Technology, 1989.

(24) Abdel-Alim, A. H.; Hamielec, A. E. *J. Applied. Pol. Sci.* **1972**, 16, 1093. Abdel-Alim, A. H.; Hamielec, A. E. *J. Applied. Pol. Sci.* **1973**, 17, 3033.

(25) Anslyn, E. V.; Grubbs, R. H. *J. Am. Chem. Soc.* **1987**, *109*, 4880-4890.

(26) Grubbs, R. H. in *Comprehensive Organometallic Chemistry*; Wilkinson, G.; Stone, F. G. A.; Abel, E. W. Eds.; Pergamon Press: New York, 1982; Vol. 8, pp. 499-551.

(27 Grubbs, R. H.; Tumas, W. *Science* **1989**, *243*, 907-915.

(28) D. Elder is gratefully acknowledged for the important participation he took in this experiment.

(29) Sandström, J. *Dynamic NMR Spectroscopy*; Academic Press: San Diego, **1982**.

(30) Similar results have also been observed by A. Pangborn. A. Pangborn is gratefully acknowledged for sharing her observations and results.